MicroRNA Profiling of Human Hepatocytes Induced by HBx in Hepatocarcinogenesis

YIP, Wing Kit

A Thesis Submitted in Partial Fulfilment
of the Requirements for the Degree of
Master of Philosophy
in
Medical Sciences

The Chinese University of Hong Kong

August 2009

Abstract

Background and Aim: Hepatitis B virus (HBV) infection is associated with an increased risk of hepatocellular carcinoma (HCC). The virus encodes a hepatitis B virus X protein (HBx) which plays an important trans-activation role in HCC development. Recent studies showed that COOH-terminal truncated HBx was frequently observed in liver tumors but not in their adjacent liver tissues, suggesting that the truncated HBx mutants may play an important role in hepatocarcinogenesis. The aims of this project are to investigate the biological effects of COOH-terminal truncated HBx on cell proliferation, cell cycle analysis and cell apoptosis; and to identify miRNAs that were induced by full-length HBx and COOH-terminal truncated HBx in human hepatocyte. Results: PCR amplification of HBx showed that COOH-terminal truncated HBx was detected in 50% of HCC tissues, but not in the adjacent non-tumor tissues. Immunochemical staining of the tissue sections confirmed their expression. To investigate the biological effects of the COOH-truncated HBx mutants, lentivirus expressing full-length HBx, HBxΔ14 and HBxΔ35 (14 and 35 amino acids deletion at the COOH-terminus) were generated to transduce a human non-tumorigenic liver cell line, MIHA. In comparison with a mock-infected control, HBxΔ35 stimulated cell proliferation, whereas full-length HBx inhibited cell growth. Cell cycle analysis revealed that HBxΔ35 promoted S phase progression, but full-length HBx attenuated cells at G0/G1 phase and blocked G1/S phase transition. However, HBx and its truncated mutants had no effect on cell apoptosis. To identify the differentially expressed miRNA in full-length HBx and HBxΔ35-infected cells, miRNA profiling was conducted using Agilent Human miRNA Microarray kit (V2) (v. 10.1). A total of 23 miRNAs were deregulated by full-length HBx and/or HBxΔ35 by at least 2-fold. Subsequent validation by

real-time PCR analysis confirmed that 2 miRNAs were commonly down-regulated, whereas 4 miRNAs were commonly up-regulated by the two versions of HBx. Importantly, miR-146a, miR190 and miR-29c were differentially expressed in full-length HBx and HBxΔ35- infected cells, and were significant down-regulated in liver tissues. In summary, we showed the importance of COOH-terminal truncated HBx in HCC and explored the possible linkage between miRNAs and truncated HBx-induced hepatocarcinogenesis. Our findings might provide biological insight on the mechanism of HBV-induced HCC.

摘要

研究背景與目的：乙型肝炎病毒感染增加患肝細胞型肝癌的風險。該病毒編碼一乙型肝炎病毒 X 蛋白，該蛋白在肝細胞型肝癌的發展過程中發揮重要作用。新近研究表明短縮了羧基末端的乙型肝炎病毒 X 蛋白高頻出現於肝腫瘤中，但在鄰近肝組織中卻沒有發現該蛋白。這表明乙型肝炎病毒 X 蛋白的變異體在肝癌的發生發展過程中起重要作用。我們實驗計畫的目的是研究短縮了羧基末端的乙型肝炎病毒 X 蛋白在細胞增殖，細胞週期，細胞凋亡中的作用，並識別人類肝細胞中由全長乙型肝炎病毒 X 蛋白及短縮了羧基末端的乙型肝炎病毒 X 蛋白誘導產生的微小核糖核酸 (miRNA)。

實驗結果：聚合酶鏈反應擴增實驗表明編碼短縮了羧基末端的乙型肝炎病毒 X 蛋白的基因在 50%的肝細胞型肝癌組織中測出，在鄰近非腫瘤組織中卻沒有測出。該組織的免疫化學染色證實了短縮了羧基末端的乙型肝炎病毒 X 蛋白的表達。以慢病毒屬表達型作爲載體的全長乙型肝炎病毒 X 蛋白及短縮了羧基末端 14 個氨基酸和 35 個氨基酸的乙型肝炎病毒 X 蛋白被構建並轉染人類非致瘤的肝細胞系 MIHA，用於研究短縮了羧基末端的乙型肝炎病毒 X 蛋白變異體的生物學效應。與轉染了對照載體的肝細胞系比較，短縮了羧基末端 35 個氨基酸的乙型肝炎病毒 X 蛋白刺激細胞增殖，而全長乙型肝炎病毒 X 蛋白抑制細胞生長。細胞週期分析表明短縮了羧基末端 35 個氨基酸的乙型肝炎病毒 X 蛋白促進細胞分裂 S 期，而全長乙型肝炎病毒 X 蛋白削弱細胞的 G0/G1 期並阻斷 G1/S 期轉換。然而，乙型肝炎病毒 X 蛋白及它的末端短縮變異體對細胞凋亡效應不明顯。以 Agilent Human miRNA Microarray Kit (V2) (v. 10.1) 的微小核糖核酸分析，用於識別受全長乙型肝炎病毒 X 蛋白及短縮了羧基末端 35 個氨基酸的乙型肝炎病毒 X 蛋白轉染的細胞中微小核糖核酸的不同表達。共有 23 個 miRNAs 被全長乙型肝炎病毒 X 蛋白或短縮了羧基末端 35 個氨基酸的乙型肝炎病毒 X 蛋

白下調至少 2 倍表達。隨後的即時聚合酶鏈反應分析證實了 2 個 miRNAs 同時被全長乙型肝炎病毒 X 蛋白和短縮了羧基末端 35 個氨基酸的乙型肝炎病毒 X 蛋白下調表達，而 4 個 miRNAs 同時被全長乙型肝炎病毒 X 蛋白和短縮了羧基末端 35 個氨基酸的乙型肝炎病毒 X 蛋白上調表達。重要的是，miR-146a，-190 和 -29c 在受全長乙型肝炎病毒 X 蛋白及短縮了羧基末端 35 個氨基酸的乙型肝炎病毒 X 蛋白轉染的細胞中的表達不同。

歸納起來，我們表明短縮了羧基末端的乙型肝炎病毒 X 蛋白在肝細胞型肝癌中起重要作用，並研究 miRNAs 與短縮了羧基末端的乙型肝炎病毒 X 蛋白在肝癌發生發展中的相互聯繫。我們的發現爲乙型肝炎病毒誘導的肝細胞型肝癌的發生機制提供了生物學基礎之一。

ACKNOWLEDGEMENTS

I would like to express my heartfelt gratitude to my supervisor, Professor Henry Chan, for his sincere as well as patient guidance, thoughtful discussion and tremendous support during the course of my study. I am also motivated by his enthusiasm and deeply influenced by his profound inspirations.

I am grateful to my co-supervisor, Prof. Alfred Cheng, for his patient guidance, helpful discussion and invaluable advice. Without his critical comments and encouragement, my thesis would not be completed. I am also deeply impressed by his enthusiasm towards medical research.

Special thanks must be devoted to Prof. Enders Ng for introducing me to the amazing field of microRNA research.

Thanks must be expressed to Prof. Yang Chow Chan for his assistant in lentivirus generation. In particular many thanks go to Mr. Victor Wong, Mr. James Chow, Miss Olivia Hui, Mr. Vincent Shek and Mr. Kent So for their assistant in immnohistochemical staining and scoring. Thanks also go to Prof. Paul Lai for providing precious clinical specimens.

I am thankful to the team members of the Institute of Digestive Disease, Dr Hongchuan Jin, Dr Julia Li, Dr Martin Chan, Dr Paul Cheung, Miss Suki Lau, Miss May Li, Miss Michelle Liu and Miss Emily Liu for their immense support and countless technical assistance. Thanks also go to Miss Denise Chan and Dr. Arthur Ching for their excellent technical support on flow cytometry.

Finally, I herewith dedicate my whole-hearted gratitude to the colleagues on 4/F Cancer Center and in Room 701, Li Ka Shing Medical Science Building who have given me kind advice, thoughtful assistance and most importantly, the precious friendship during the years of my study.

TABLE OF CONTENTS

LIST OF TABLES

LIST OF FIGURES

LIST OF ABBREVIATIONS

7-AAD	7-Amino-actinomycin D
aa	Amino acid
BSA	Bovine serum albumin
cDNA	Complementary DNA
CO_2	Carbon dioxide
CMV	Human cytomegalovirus
CIP	Calf Intestine Alkaline Phosphatase
Cy3-pCp	Cyanine3-pCp
cPPT	HIV-1 central polypurine tract
DMEM	Dulbecco's modified Eagle's medium
DMSO	Dimethyl sulfoxide
DNA	Deoxyribonucleic acid
DNMT	DNA methyltransferases
dNTP	Deoxynucleotide triphosphates
E. coli	Escherichia coli
EGFP	Enhanced green fluorescent protein
FBS	Fetal bovine serum
HBcAg	Hepatitis B virus core protein
HBeAg	Hepatitis B virus e antigen
HBsAg	Hepatitis B virus surface portein
HBV	Hepatitis B virus
HBx	Hepatitis B virus X protein
HBxΔ14	Hepatitis B virus X protein (14-aa deleted)
HBxΔ35	Hepatitis B virus X protein (35-aa deleted)

HCC	Hepatocellular carcinoma
HCV	Hepatitis C virus
HEK	Human embryonic kidney cells
IRES	The internal ribosome entry site of the encephalomyocarditis virus
kb	Kilo base pair
LB	Luria Broth
LTR (ΔU3)	Deletion in the HIV-1 LTR U3 sequence
min	Minute(s)
miRNA	MicroRNA
mRNA	Messager RNA
N	Normal tissue
NT	Adjacnt non-tumor tissue
PBS	Phosphate buffered saline
PBST	Phosphate buffered saline Tween-20
PCR	Polymerase chain reaction
PE	Phycoerthrin
PI	Propidium Iodide
PRE	Human hepatitis virus posttranscriptional regulatory element
Pre-miRNA	MicroRNA precusor
Pri-miRNA	MicroRNA primary transcript
PTEN	Phosphatase and tensin homolog
s	Second(s)
REE	HIV Rev response element
RISC	RNA-induced silencing complex
rRNA	Ribosomal ribonucleic acid

RNA	Ribonucleic acid
RSV	Rous sarcoma virus and HIV chimeric long terminal repeat
RT-PCR	Reverse transcription-PCR
SDS	Sodium dodecylsulfate
TBE	Tris-boric acid-EDTA
TSS	Transcription start site
UTR	Untranslational region

Chapter 1 INTRODUCTION

1.1 Hepatocellular Carcinoma

1.1.1 Epidemiology

Liver cancer is the sixth most common cancer worldwide and the third most common cause of cancer mortality (Parkin *et al.*, 2005). Hepatocellular carcinoma (HCC) accounted for around 90% of liver cancers, while cholangiocarcinoma and hepatoblastoma contributed to the remaining 10%. The incidence of HCC distributed geographically, mainly in Africa, eastern and southeastern Asian. China alone accounted for 55% of the global cases. In addition, HCC showed male predominance with male to female ratio ranging from 2:1 to 4:1 in most regions, but different age distribution varied by sex, geographic region and etiology (Parkin, 2002).

1.1.2 Etiology

A number of risk factors had been associated with HCC, including viral hepatitis, heavy alcohol consumption (Donato *et al.*, 2002), aflatoxin diet intake (Soini *et al.*, 1996), excessive vinyl chloride exposure (Mastrangelo *et al.*, 2004) and use of contraceptive (Maheshwari *et al.*, 2007). Furthermore, HCC was also associated with certain disease states, for instance nonalcoholic fatty liver disease (Bugianesi *et al.*, 2002), obesity, diabetes mellitus (Regimbeau *et al.*, 2004) and hereditary hemochromatosis (Hellerbrand *et al.*, 2003). In some cases, two or more risk factors co-existed and exerted synergistic effects on HCC development (Marrero *et al.*, 2005).

Among various risk factors, chronic infection with hepatitis B virus (HBV) or hepatitis C virus (HCV) contributed to more than 80% of HCC cases worldwide, and it was more prevalence in developing countries than developed countries (Parkin, 2006). Except Japan, the prevalence of HBV was much higher than HCV in most Asian countries (Merican *et al*., 2000). In addition, the risk of HCC in HBV-positive individuals was 100-fold higher than uninfected individuals (Beasley, *et al*, 1981). Altogether, the epidemiological data suggests an urgent need in conducting researches in HBV-related HCC.

1.2 Hepatitis B Virus

1.2.1 The Epidemiology of Hepatitis B Virus Infection

Two billion people worldwide have been infected with HBV, which caused acute and chronic liver disease. The symptom of acute infection might be mild and most adults would eventually recover, but approximately 5 to 10%, corresponding to 350 million people, were unable to clear the virus and became chronically infected (Liang. 2009). In addition to HCC, chronic HBV infection could progress to worsening disease condition, including compensated cirrhosis, decompensated cirrhosis and liver failure. The prevalence of chronic HBV infection imposed a huge health and economic burden to the society (Zhiqiang *et al.*, 2004; Yang *et al.*, 2004). Nevertheless, the population of HBV carriers could be effectively minimized by promoting public awareness of the diseases and adopting vaccination at birth (Poovorawan *et al.*, 2009).

Body serum, semen and saliva are the sources of infectious HBV, but this virus could also survive outside the body and remained infectious for at least 7 days (Bancroft et al., 1977; Alter et al., 1997; Bond *et al.*, 1981). It was transmitted by percutaneous or mucosal exposure to blood or body fluids of infected patients, but the mode of transmission varied in different regions. In developing countries, people were usually infected at young age through mother-to-child and child-to-child route. On the contrary, perinatal transmission through blood transfusion and sexual behavior were prevalent in developed countries (CDC. 2005; Frenette *et al.*, 2009). Childhood infection was often resulted in chronic hepatitis, while most adults could recover from acute infection and developed efficient adaptive immune responses

(Fisicaro *et al.*, 2009).

1.2.2 The Morphology and Genome of Hepatitis B Virus

HBV belongs to a family of DNA virus, called the hepadnaviruses. The viron is a 42-nm sphere that consists of an outer lipid envelope and an inner core or nucleocapid, encompassing HBV genome and the polymerase (Figure 1.1). The viral envelope is composed of large, middle and small surface proteins, which are synthesized differentially on a single open reading frame containing three in-frame start codons. Viral infection is initiated by the interaction between an intact pre-S domain of the large envelop protein and a hepatic surface receptor, the glycoaminoglycan (GAG) side chains of cell-surface associated heparin sulfate proteoglycans (Schulze *et al.*, 2007; Leistner *et al.*, 2008). Being detectable in most chronic hepatitis B patients, the viral surface proteins (HBsAg) could be used as a marker to monitor the disease progression and to predict the clinical outcomes (Arase *et al.*, 2006; Yuen *et al.*, 2008).

HBV consists of a partially double-stranded DNA of 3.2 kb in size, containing four overlapping open reading frames that encode S, the surface or envelop gene; P, the polymerase gene; C, the core gene; and X, the X gene (Lee, 1997) (Figure 1.2). DNA virus replicates through an RNA intermediate by the reverse transcriptase function of HBV polymerase, which is covalently attached at the 5' end of the minus stand (Gerlich *et al.*, 1980). A number of licensed antiviral drugs, including lamivudine (Dienstag *et al.*, 1999), entacavir (Chang *et al.*, 2006), telbivudine (Lai *et al.*, 2007), adefovir dipivoxil and tenofovir disoproxil fumarate (Marcellin *et al.*, 2008), inhibit viral replication by acting as nucleoside analogs that block the catalytic

function of HBV polymerase.

The core protein, also called HBcAg, has the intrinsic property to self-assemble into a capid-like structure that encloses viral DNA during replication. Translation from another in-frame start codon of the core gene yields a secretary antigen, HBeAg, which is not required for replication or acute infection *in vivo* (Chang *et al.*, 1987). In contrast, this antigen may serve as an immunoregulatory protein that promotes chronicity in nature infection or a target for the inflammatory immune response (Maruyama *et al.*, 1993; Chen *et al.*, 2004).

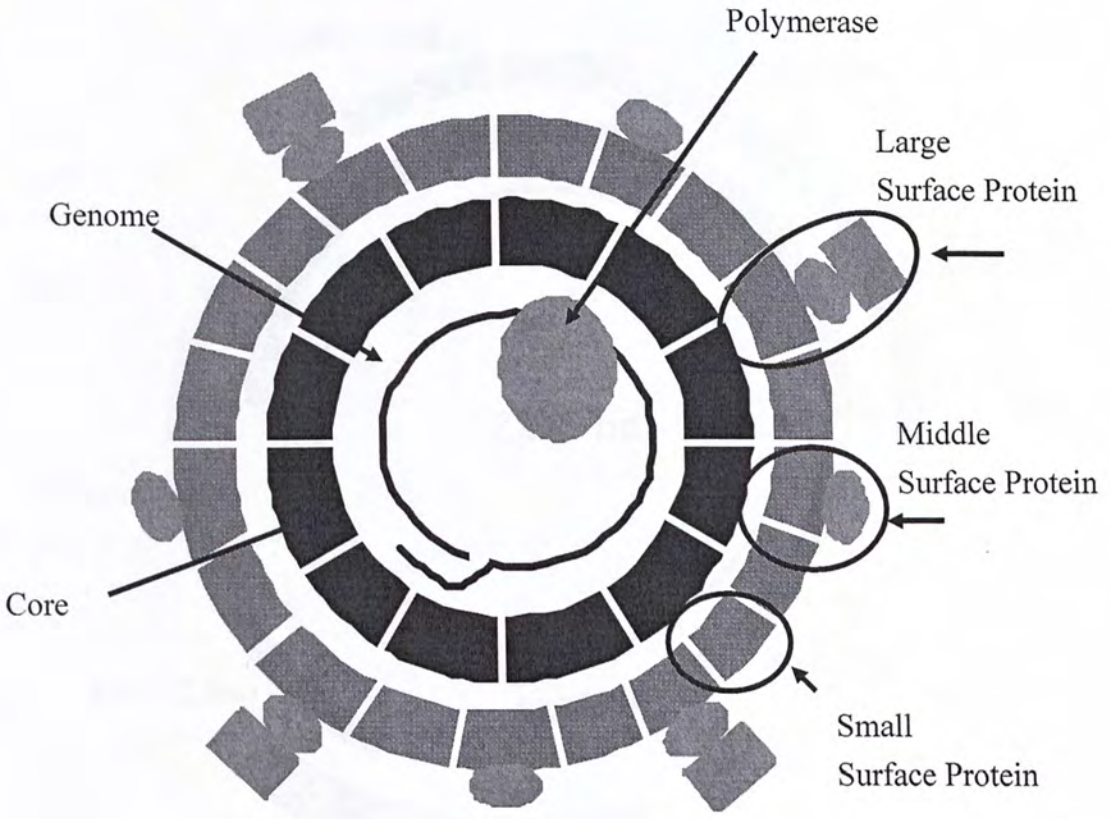

Figure 1.1 The schematic structure of hepatitis B virus. HBV is a double-shelled viral particle of 42-nm in diameter. The outer envelope is composed of large, middle and small surface protein, while the inner core encompassing the viral genome and polymerase.

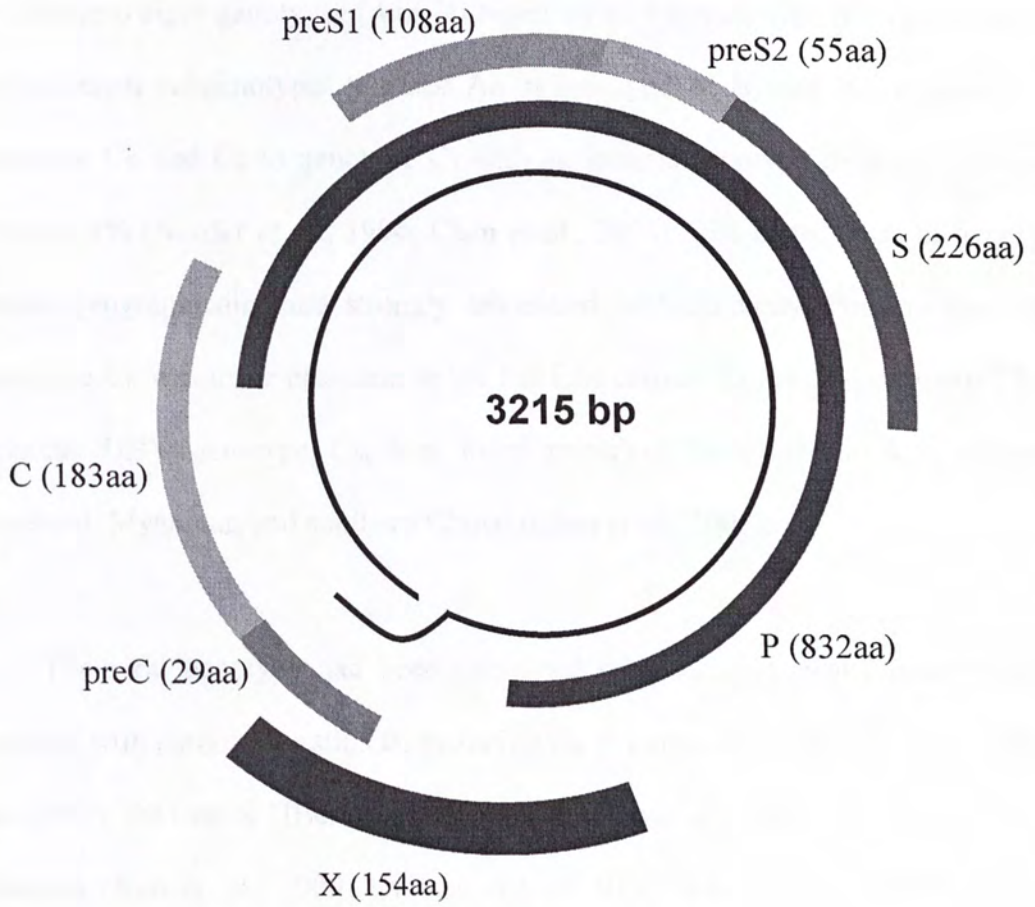

Figure 1.2 The genomic structure of HBV. HBV is a partially double-stranded DNA virus having four overlapping open reading frames, which encodes X gene, preC/C gene, P gene and the preS1/preS2/S gene.

1.2.3 HBV Genotypes and Their Significance

According to the phylogenic analysis of complete viral sequences, HBV can be divided into eight genotypes (A to H) based on an intergenotype divergence of ≥8% and different subgenotypes (Ae and Aa in genotype A; Bj and Ba in genotype B; genotype Ce and Cs in genotype C) with an intersubgenotype divergence between 4% and 8% (Norder *et al.*, 1994; Chan *et al.*, 2005). The distribution of genotypes varied geographically and strongly associated with eth nicity. For instance, HBV genotype Ce was more prevalent in the Far East (Japan, Korea, and northern China), whereas HBV genotype Cs, was more prevalent in Southeast Asia (Vietnam, Thailand, Myanmar, and southern China) (Chan *et al.*, 2005).

The viral genotype had been correlated with some clinical characteristics in patients with chronic hepatitis B, including the response to interferon therapy (Wai *et al.*, 2002), the rate of HBeAg seroconversion (Chu *et al.*, 2002), the severity of liver diseases (Kao *et al.*, 2000) and the risk of HCC (Chan *et al.*, .2004). In a 769 HBV-positive cohort, patients infected with hepatitis B subgenotype Ce had higher risk of HCC when compared to another viral subgenotype Cs and genotype B (Chan *et al.*, 2008). Furthermore, a large scale HBV whole genomic sequencing revealed a number of genotype-specific hot-spot mutations associated with HCC, for instance C1165T, A1762T and G1764A, T2712C/A/G, and A/T2525C in HBV genotype B; T31C, T53C, and A1499G in HBV subgenotype Ce; and G1613A, G1899A, T2170C/G, and T2441C mutation in HBV subgenotype Cs (Sung *et al.*, 2008). However, the functional significance of these HCC-associated hot-spot mutations is still unknown.

1.3 Hepatitis B Virus X Protein

HBx acted as a transcriptional transactivator that had been implicated in HCC. It is a 154-amino acid protein, with a molecular mass of 17kDa, detectable in both HCC tissues and adjacent non-tumor tissues. Depending on its intracellular expression level, the subcellular localization of HBx varied differently in the cytoplasmic and the nuclear compartment (Doria *et al.*, 1995; Henkler *et al.*, 2001).

No known DNA binding domain was identified in the HBx protein. However, this viral protein could transactivate gene expression through altering different signaling transduction pathways, epigenetic modifications and associating with a number of transcription factors. Certain oncogenes and tumor suppressor genes were frequently deregulated through these mechanisms, suggesting that HBx might be an important player in HBV-related HCC. A solid support of this notion was provided by an *in vivo* study demonstrating liver cancer development in transgenic mice over-expressing the X protein (Kim *et al*, 1991).

The subcellular localization of HBx governs its function as a potent transactivator (Majano *et al.*, 2001). At low expression level, HBx was predominantly localized in the nucleus, but it shifted to cytoplasm at elevated level (Henkler *et al.*, 2001). Nuclear localization signal tagged HBx (NLS-HBx) targeted to the nucleus and failed to activate AP-1 or NFκB dependent transcription, whereas the native HBx stimulated AP-1 and NFκB dependent transcription. These effects were mediated through the Ras-Raf-MAP kinase signaling pathway in the cytoplasm, showing the functional importance of HBx subcellular localization (Doria *et al.*, 1995).

1.3.1 HBx Alters Various Signal Transduction Pathways

HBx is well-characterized for its ability to activate various signal transduction pathways, including Ras/MAPK (Benn *et al.*, 1994), Jak-Stat (Lee *et al.,* 1998), SAPK/JNK (Diao *et al.*, 2001), PI-3K/Akt (Chung *et al.*, 2004), NF-kappaB, and FAK (Bouchard *et al.*, 2006). Deregulation of these pathways might cause cellular transformation and tumor development (Kim *et al.*, 2001). Furthermore, HBx also played a role in promoting HBV replication by activating calcium signaling pathways involving Pyk2 and Src tyrosine kinases (Bouchard *et al.*, 2001). Although the cytoplasmic compartmentation of HBx was required to activate a fraction of the pathways, the mechanism is still unclear (Doria *et al.*, 1995) (Figure 1.3).

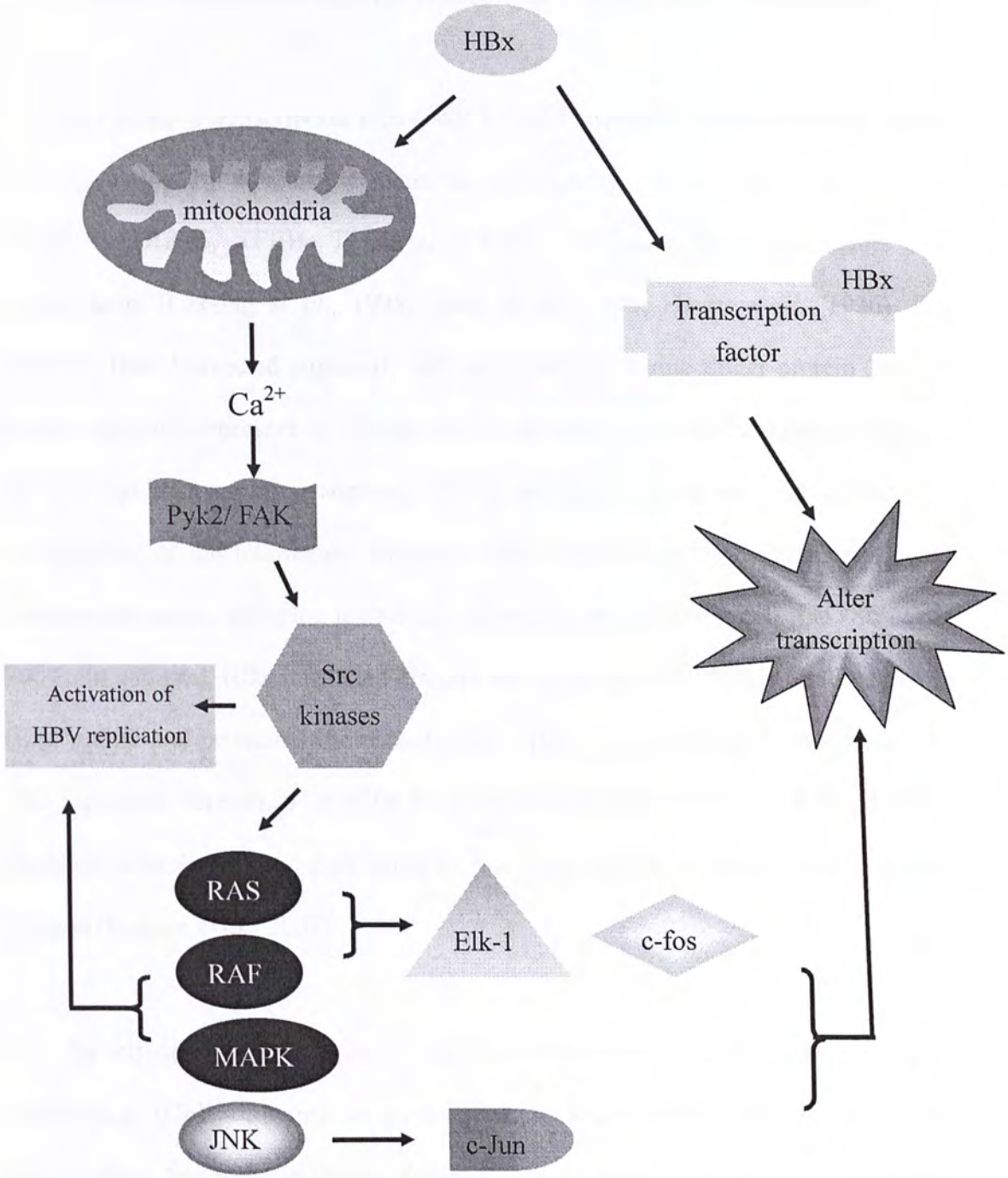

Figure 1.3 A network of HBx-mediated transactivation. HBx exerted its functions by transactivating a number of signal transduction pathways, including calcium signaling pathway, Ras-Raf-MAPK-JNK pathway etc. HBV replication was enhanced and gene transcription was altered by HBx.

1.3.2 HBx Interacts with Various Transcription Factors and Co-activators

HBx is not a transcription factor, but it could alter endogenous gene regulation and expression by associating with the components of the basal transcription machinery (RPB5, TFIIB, TFIIH and TBP), various transcription factors and co-activators (Cheong *et al.*, 1995; Qadri *et al.*, 1995; Haviv *et al.*, 1996). For instance, HBx interacted physically with myc-associated zinc finger protein (MAZ), a transcriptional repressor of human telomerase, and enhanced the binding efficacy of MAZ to its consensus sequence of the telomerase promoter. By acting as a co-repressor of the telomerase promoter, HBx down-regulated the transcription of human telomerase, inducing telomerase shortening in hepatoma cell line (Su *et al.*, 2007). In addition, HBx interacted directly with a co-activator CREB-binding protein (CBP)/p300 and promoted the recruitment of p300 to CREB-responsive promoters. The increased occupancy of p300 to promoter regions carrying CREB-responsive elements stimulated gene expression of interleukin 8 and proliferating cell nuclear antigen (Cougot *et al.*, 2007).

By utilizing the state-of-the-art chromatin immunoprecipitation with microarray technology (ChIP-on-chip), a gene network regulated directly by a specific transcription factor or indirectly through a transcription factor can be elucidated (Cheng *et al.*, 2006). This approach has been employed to identify the potential transcription factors interacting with HBx and the gene network regulated by HBx. A recent study has identified 184 direct transcriptional targets of HBx and 144 transcription factors potentially interacting with HBx were predicted. Of these, SMAD4, E2F1 and YY1 were validated as the putative transcription factors that interacted with HBx (Sung *et al.*, 2009). The integrative approach allows better

understanding of the combinatorial transcription regulated by HBx and a variety of transcription factors.

1.3.3 HBx Induces Epigenetic Alterations

DNA methylation of promoter CpG islands leads to gene silencing, an epigenetic modification mediated by DNA methyltransferases (DNMT). HBx engaged in this epigenetic network by interacting with DNMT3A or histone deacetylase 1 (HDAC1) directly, and transactivating a number of DMNTs, including DNMT1, DNMT3A1 and DNMT3A2 (Park *et al.*, 2007; Zheng *et al.*, 2009). A complex regulatory circuit seemed to regulate DNMT1, but not the other DNMTs, through the $p16^{INK4A}$-Cyclin D1-CDK4/6-pRb-E2F1 pathway (Jung *et al.*, 2007).

Of the genes regulated by HBx-mediated promoter methylation, interleukin-4 receptor (IL4R), metallothionetin-1F (MT1F), insulin-like growth factor-3 (IGFBP-3) and Cadherin 6 type 2 (CDH6) were studied in details. Epigenetic regulation mediated by HBx was a two-way strategy, one involved the direct interaction of HBx with DNMT3A, and silenced their transcription by recruiting DNMT3A to the promoter of IL4R or MT1F, whereas the other stimulated the transcription of IGFBP-3 or CDH6 by associating with DNMT3A and depriving DNMT3A from their promoters (Zheng *et al.*, 2009).

However, the HBx-mediated epigenetic modifications might be interfered by other factors, including the viral genotype and the cell line used in the studies, leading to an opposite effect of HBx on IGFBP-3 promoter methylation and gene transcription (Park *et al.*, 2007; Shon *et al.*, 2009).

1.3.4 Identification of COOH-terminal Truncated HBx in Liver Tumors

Carboxyl (COOH)-terminal truncated HBx, instead of full-length HBx, was found in a number of primary liver tumor tissues (Tu *et al.*, 2001; Ma *et al.*, 2008). The number of amino acids deleted from the C-terminals varied from patients to patients. However, no conserved site of HBx truncation was observed and the exact mechanism leading to the formation of truncated HBx is still unknown.

One proposed mechanism involved human APOBEC3 (apolipoprotein B mRNA editing enzyme, catalytic polypeptide 3) cytidine deaminases, which inhibited mammary virus replication. It preferentially mediated G-to A hypermutations in the HBx region of HBV DNA, causing the formation of a 119 aa C-terminal truncated HBx protein (35-aa deleted) by generating a premature stop-codon (TAA) at nucleotide position 359 and 360 (TGG to TAA). Sequencing of HBx in primary liver tissues further supported the occurrence of this event (Xu *et al.*, 2007).

Another possible mechanism leading to COOH-terminal truncated HBx is the integration of HBV DNA into the host genome, a frequent event observed in liver tissues of chronic hepatitis patients and HCC patients (Shafritz *et al.*, 1981; Murakami *et al.*, 2005). In this regard, HBV integration generated the hybrid virus-cell transcripts containing sequences of viral surface gene, the viral enhancer and different truncated forms of HBx (Wei *et al.*, 1995). By using Alu-PCR, a natural mutant of 27-aa deletion in HBx was identified in the liver tumor (Zhang *et al.*, 2008).

The full-length and COOH-terminal truncated HBx showed distinct biological

effects on liver cell culture systems, although they shared a large portion of the N-terminal domain. Functional mapping of various COOH-terminal deleted HBx suggested that the last 14-aa was corresponded to be a growth suppressive domain (Tu *et al.*, 2001). By deleting at least 14-aa from the COOH-terminal, the growth suppressive effect induced by the full-length HBx was abrogated, or in some reports, it even enhanced cell proliferation. In addition, the apoptotic effect induced by full-length HBx was also abolished in COOH-terminal HBx deletion mutants (Ma *et al.*, 2008). However, the deletion might interfere with the transactivation domain, leading to decrease in transactivation efficacy of HBx deletion mutants (Tu *et al.*, 2001). Altogether, the biological effects of COOH-terminal truncated HBx seemed to be more consistent with the role of HBx in hepatocarcinogenesis.

1.4 MicroRNAs

Since the discovery of miRNA (lin-4) in *C. elegans*, the research in this field grew exponentially in recent years (Lee *et al.*, 1993). MiRNAs are 21- 25 nt non-coding small RNAs, which have been found in vertebrates, plants, viruses, insects, etc. Until 2009, the sequences of 706 human mature miRNAs were delineated and over 9000 mature miRNA products were uncovered in 103 species in a miRNA registry, miRBase (v. 13.0) (http://microrna.sanger.ac.uk/) (Griffiths-Jones *et al.*, 2008).

MiRNA acts as a posttranscriptional regulator that fine-tunes endogenous gene expression. A single miRNA could repress the production of hundreds of proteins, but the level of down-regulation was mostly mild (Selbach *et al.*, 2008). These tiny molecules could be induced by various environmental stimuli, including temperature (Johnston *et al.*, 2009), hypoxia (Fasanaro *et al.*, 2008) and ethanol exposure (Wang *et al.*, 2009b). Besides, they had been implicated in various developmental processes, cellular differentiation, transformation and cancer development. In embryonic stem cells, up-regulation of miR-145 was shown to regulate SOX2, OCT4 and KLF4, a core network of transcription factors that maintain self-renewal and pluripotency (Xu *et al.*, 2009).

1.4.1 Transcriptional Regulation and Biogenesis of MicroRNAs

Little is known about the promoter regions, regulatory elements and the transcription start sites (TSS) that are essential for miRNA synthesis and regulation. MiRNA promoters are usually located several hundred base pairs upstream the TSS, and are essential for the regulation of their endogenous mature miRNA levels. Some miRNAs process their own promoters, whereas the others share the same promoters and co-transcript with nearby genes (Ozsolak *et al.*, 2008). One of the most extensively studied promoters, miR-21, is located within an intron of a coding gene, TMEM49, but they are regulated independently. *In silico* analysis revealed the binding sites of AP-1, p53, STAT3, EST/PU1 and E2-box in the enhancer and promoter region, and activated AP-1, STAT3 or E2-box have been shown to stimulate the transcription of miR-21 (Du *et al.*, 2009; Fujita *et al.*, 2008; Loffler *et al.*, 2007).

RNA polymerase II or III is responsible for transcribing miRNA primary transcripts (Pri-miRNA), which are cleaved to liberate a stem-loop miRNA precursor (Pre-miRNA) by an RNase III endonuclease called Drosha (Borchert *et al.*, 2006; Lee *et al.*, 2004). The resulting precursor transcript is actively exported out of the nucleus by Ran-GTP and the nuclear export receptor, Exportin-5. In the cytoplasm, another RNase III endonuclease, Dicer, further cleaves the 60-70 nt pre-miRNA at the loop sites, resulting in the formation of a short, double-stranded RNA molecule (miRNA::miRNA*). This duplex RNA molecule is composed of a guide strand and a passenger strand. The passenger strand is degraded rapidly while the guide strand associates with the RNA-induced silencing complex (RISC) to carry out the posttranscriptional regulation of its target genes (Figure 1.4) (Bartel, 2004).

Acting as a post-transcriptional regulator, miRNA mediates its effects through inhibiting translation or inducing degradation of target mRNAs (Selbach *et al.*, 2008). The expression level of its target proteins drops with or without an accompany reduction in the mRNA levels. Analysis of miRNA-mRNA interaction revealed that the miRNA seed region (nucleotide 2- 8) seemed to play a critical role in governing its mRNA targets (Lewis *et al.*, 2005). These tiny RNA molecules regulated gene expression by partial complementary to the 3' untranslational region (3'UTR), and in some reports, to the coding sequences of the target mRNA transcripts (Forman *et al.*, 2008; Tay *et al.*, 2008).

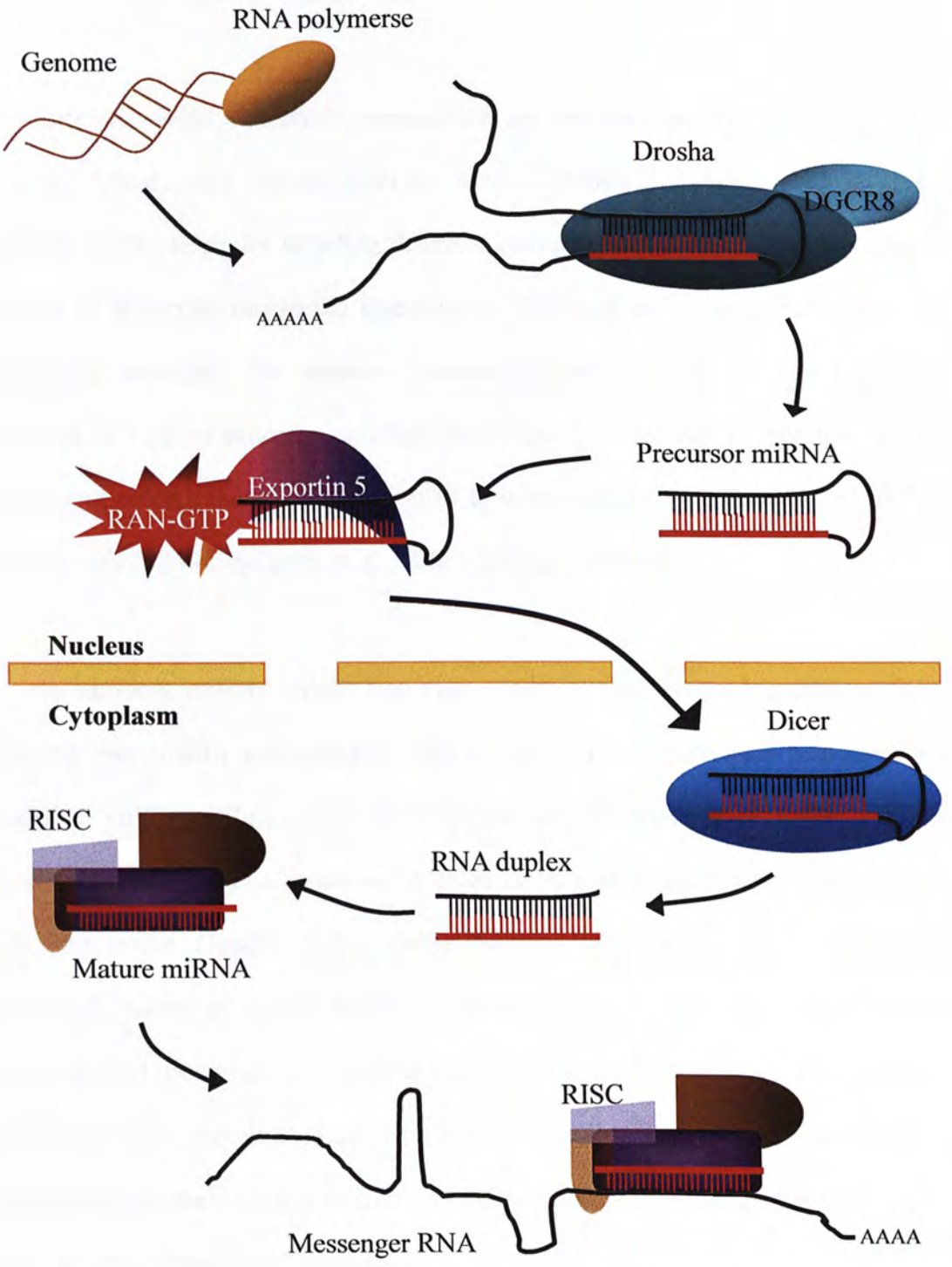

Figure 1.4 Biogenesis of miRNA. Transcription of miRNA is initated by RNA polymerase II or III to form a primary miRNA transcript. The transcript is processed by Drosha and Dicer to generate the mature miRNA. The functional miRNA stranded is selected by RISC and represses translation by interacting with the 3'UTR of target messenger RNAs.

1.4.2 MicroRNAs and Cancer

MiRNAs were frequently deregulated in various cancers, including lung, prostate, breast, liver cancer (Dalmay *et al.*, 2006). The deregulated miRNAs mediated their effects by targeting different oncogenes or tumor suppressor genes, leading to abnormal oncogenic phenotypes, including increased proliferation and metastastic potential. For instance, down-regulation of miR-145 was frequently observed in various cancers, including lung cancer, breast cancer, prostate cancer, gastric and colon cancer, and contributed to tumorigenesis by affecting cell growth (Dalmay *et al.*, 2006; Schetter *et al.*, 2008; Takagi *et al.*, 2009).

In addition, miRNA might also play a role in virus-associated cancers. Viral infection was usually accompanied with a cascade of host immune responses that prevented viral spreading and assist viral clearance (Koyama *et al.*, 2008). Cellular stress response was also arisen on infected cells, and deregulated the endogenous gene expression (Jindal *et al.*, 1992). Some viral infected cells differentially expressed a subset of cellular miRNAs, which modulated the host immune response and enhanced potential for carcinogenesis (Table 1.1). However, the host-virus interaction was complicated as viruses could utilize the cellular machinery to replicate and express over ten different viral proteins, while the viral proteins might alter the endogenous gene expression.

Like HBV, Human Papillomavirus (HPV), Epstein-Barr Virus (EBV), Kaposi's sarcoma-associated herpesvirus (KSHV) and Human T-lymphotropic virus Type I (HTLV-1) were strongly associated with higher incident rates of certain types of cancers (Table 1.3) (Parkin, 2006). The virus-related oncogenic transformation might

be mediated through the expression of viral oncoproteins that modulated cellular miRNA expression. For instance, HPV oncoprotein E6 suppressed miR-34a transcription, causing cell proliferation (Wang *et al.*, 2009c) Besides, EBV oncoprotein LMP1 and HTLV-1 oncoprotein Tax up-regulated miR-146a to modulate the host immune response (Pichler *et al.*, 2008; Cameron *et al.*, 2008).

Table 1.1 A list of cellular miRNAs deregulated by viral infection.

Virus	Infected cells	Cellular miRNAs altered	References
Human Papillomavirus (HPV)	HPV-16 positive vs HPV-negative cell lines	↑miR-193b, miR-200c, miR-203, miR-31, miR-34a, , miR-210 ↓miR-218	Wang *et al.*, 2009c
SL3-3 murine leukemia virus (Provirus)	Murine leukemia cell lines	↑miR-17-92 cistron	Wang *et al.*, 2006
Human T-lymphotropic virus Type I (HTLV-1)	Primary peripheral blood mononuclear cells	↑miR-93, miR-130b	Yueng *et al.*, 2008

Table 1.2 A list of cellular miRNAs deregulated by viral oncoproteins. The differentially expressed cellular miRNAs may contribute to viral infection associated cancer development by altering cell growth, cell cycle, migration or invasion.

Virus	Infection-associated cancer	Viral Oncoprotein	Cellular miRNAs altered	Pathway involved	References
Human Papillomavirus (HPV)	Cervical cancer	E6	↑miR-34a	Growth retardation, cell cycle arrest	Wang *et al.*, 2009c
Epstein-Barr Virus (EBV)	Burkitt's lymphoma, Hodgkin's lymphoma, nasopharyngeal carcinoma	LMP1	↑miR-146, ↑miR-155	-	Motsch *et al.*, 2007; Cameron *et al.*, 2008; Gatto *et al.*, 2008
Kaposi's sarcoma-associated herpesvirus (KSHV)	Kaposi's sarcoma	M type K15 protein	↑miR-21, ↑miR-31	Cell migration and invasion	Tsai *et al.*, 2009
Human T-lymphotropic virus Type I (HTLV-1)	T-cell lymphoma	Tax	↑miR-146	-	Pichler *et al.*, 2008

1.4.3 MicroRNAs and HCC

MicroRNA microarray and PCR-based TaqMan© MicroRNA Array were commonly used to examine miRNA expression profiles. A panel of deregulated miRNAs were identified by comparing the miRNA profiles between liver tumor tissues (T) and their matched adjacent nontumor tissues (NT) or normal tissues (N) (Table 1.3). A set of distinct miRNAs, including miR-21, miR-182, miR-221, miR-222, miR-224 were often up-regulated, while miR-122a and miR-145 were down-regulated in HCC (Murakami *et al.*, 2006; Meng *et al.*, 2007; Wong *et al.*, 2008a; Wang *et al.*, 2008b). Instead of identifying deregulated miRNAs in HCC, a great deal of useful information could be inferred from the profiling data. For instance, HCC tumors and the adjacent nontumor livers could be differentiated from each other by the expression levels of mir-222 and miR-223 alone (Wong *et al.*, 2008a). Besides, a set of 19 miRNA significantly correlated the disease outcomes, and distinguished patients with good survival from those with poor survival (Jiang *et al.*, 2008). Deregulation of certain miRNAs was also associated with various risk factors and oncogene or tumor suppressor gene mutations in HCC (Ladeiro *et al.*, 2008).

Though a number of deregulated miRNAs has been identified in profiling studies, their biological functions and roles in hepatocarcinogenesis remain largely unclear. Identification of miRNA targets remains one of the top challenges in microRNA researches. A number of computer programmes, including TargetScan, PicTar and MiRanda, were established to predict miRNA targets, but only a few miRNAs implicated in HCC development have been thoroughly studied. For instance: up-regulation of miR-21 in HCC tissues enhanced tumor cell proliferation,

migration and invasion. Phosphatase and tensin homolog (PTEN) was identified to be a direct target of miR-21 and mediated the effect of cell invasion (Meng *et al.*, 2007). On the other hand, down-regulation of miR-223 was common in HCC tissues. Re-expression of miR-223 suppressed cell viability, and possibly, through one of its downstream targets Stathmin 1 (STMN1) (Wong *et al.*, 2008a).

Furthermore, the role of miRNAs in the issue of high male to female HCC incident rate was proposed. MiRNA profiles of male and female HCC tissues were compared and a number of gender-specific miRNAs were implicated in contributing to higher HCC incident rate in male. Mir-18a was frequently up-regulated in female than male HCC tissues. Functional studies revealed that miR-18a targeted estrogen receptor 1 gene (ESR1) and stimulated the proliferation of hepatoma cells (Liu *et al.*, 2009). As the gene product, estrogen receptor α, was essential for mediating the effects of cellular estrogen, and up-regulation of miR-18a might play a role in abolishing the protective effects of estrogen in female leading to HCC development.

Patients diagnosed with HCC usually had poor prognosis, as most of them were identified at advanced stages. The 5-year disease-free survival rate was only 27% (Fan *et al.*, 1999), which was attributable to the high recurrent rates in the form of intrahepatic metastasis and multicentric occurrence and the poor response to chemotherapeutic drugs (Zhu *et al.*, 2006). Poor understanding of the molecular mechanism governing tumor metastasis hampers the design of potent chemotherapeutic agents.

In HCC, a set of 20-miRNAs signature that could discriminate the metastasis from non-metastasis cases was identified and associated with patient survival. Of

these, miR-219-1, miR-207, miR-338 were up-regulated, while miR-34a, miR-30c-1 and miR-148 were most down-regulated in metastasis cases (Budhu *et al.*, 2008). The metastasis-related miRNAs are different from the HCC deregulated miRNAs, suggesting that tumor metastasis may take different molecular pathways.

An independent study validated that miR-122, a liver-specific miRNA, was frequently down-regulated in liver cancers with intrahepatic metastasis. MiR-122 inhibited cell migration, invasion and tumor independent growth *in vitro*, while suppressed tumorigenesis and angiogenesis *in vivo*, and exerted its functions partly through one of its downstream target ADAM17, a disintegrin and metaloprotease 17 (Tsai *et al.*, 2009).

Table 1.3 Deregulated miRNAs in HCC profiling studies and validation studies. The column of "target genes" only listed some miRNA downstream targets that were validated experimentally in liver studies.

MicroRNAs	Target Genes	Biological Role of miRNA/ Target Genes	References
Up-regulation			
miR-10b	-	-	Wang *et al.*, 2008b
miR-18a	ESR1	Cell proliferation	Liu *et al.*, 2009
miR-101	FOS	Cell migration and invasion	Li *et al.*, 2009
miR-182	-	-	Wang *et al.*, 2008b; Wong *et al.*, 2008a
miR-183	-	-	Wang *et al.*, 2008b; Wong *et al.*, 2008a
miR-21	PTEN	Cell invasion	Meng *et al.*, 2007; Wong *et al.*, 2008a
miR-221	CDKN1B/p27, CDKN1C/p57	Cell cycle	Fornari *et al.*, 2008
miR-222	-	-	Wang *et al.*, 2008b; Wong *et al.*, 2008a
miR-224	API-5	Apoptosis	Wang *et al.*, 2008b
miR-31	-	-	Wong *et al.*, 2008a
Down-regulation			
miR-122a	Bcl-w	Apoptosis	Wong *et al.*, 2008a; Lin *et al.*, 2008
miR-126	-	-	Wong *et al.*, 2008a
miR-143	-	-	Wong *et al.*, 2008a
miR-145	-	-	Wang *et al.*, 2008b; Wong *et al.*, 2008a
miR-195	Cyclin D1, CDK6, E2F3	Cell cycle	Xu *et al.*, 2009
miR-223	STMN1	Cell growth	Wong *et al.*, 2008a

1.5 Hypothesis and Aims of the Study

Since previous studies have established the pivotal role of microRNAs in HCC, we hypothesize that COOH-terminal truncated HBx mediates its oncogenic effects through deregulating cellular miRNAs. The objectives of this study are (1) to detect full-length and COOH-terminal truncated HBx in HCC tissues; (2) to investigate the biological effects of full-length and COOH-terminal truncated HBx on cell proliferation, cell cycle progression and apoptosis; and (3) to identify and validate miRNAs that are regulated by different forms of HBx.

Chapter 2 MATERIALS AND METHODS

2.1 Patients

Twenty pairs of liver tumors and the matched nontumor adjacent tissues were collected from patients diagnosed with HCC during the curative surgery between 2004 and 2006 at the Prince of Wales Hospital in Hong Kong. All patients were HBV-positive. Fifteen patients had liver cirrhosis while the remaining five patients did not. The availability of tissue slides, tissue DNA and RNA for study were indicated in Table 2.1. Two viral DNA samples, extracted from the serum of patients, CH230 and BC265, were taken for the PCR amplification of HBx gene for molecular cloning.

2.2 Cell Lines

An immortalized non-tumorigenic human liver cell line, MIHA (described in Brown *et al.*, 2000) and 293T human embryonic kidney (HEK) cells (obtained from American Type Culture Collection) were cultured in Dulbecco's modified Eagle's medium (DMEM) (Gibco) supplemented with 10% Fetal Bovine Serum (FBS) (Thermo Scientific HyClone). The cell lines were maintained at 37°C in a humidified incubator with 5% CO_2.

Table 2.1 Demographic information of 20 patients diagnosed with HCC. The availability of clinical samples, including tissue slides, tissue DNA and RNA was marked as "+", present and "-", absent.

Case no.	Sex	Age	HBV	Cirrhosis	Availability of Tissue Slides	Availability of Tissue RNA	Availability of Tissue DNA
508	F	46	+	+	+	+	+
512	M	48	+	+	+	-	-
513	F	39	+	+	+	+	+
515	M	60	+	+	+	+	+
519	M	52	+	+	+	+	+
522	F	42	+	+	+	+	+
527	M	59	+	+	+	+	+
531	M	68	+	-	+	+	+
532	M	71	+	+	+	+	+
546	M	48	+	-	+	-	-
547	M	59	+	-	+	+	+
548	M	56	+	+	+	-	-
550	M	67	+	-	+	+	+
551	M	65	+	+	+	+	+
552	M	58	+	+	+	+	+
553	M	65	+	+	+	-	-
554	F	62	+	+	+	+	+
557	M	64	+	+	+	+	+
558	F	55	+	+	+	+	+
559	M	53	+	-	+	+	+

2.3 Cloning of Various HBx Constructs

2.3.1 PCR Amplification of HBx Fragments

DNA fragments of full-length HBx were amplified by polymerase chain reaction (PCR) using the viral DNA extracted from the serum of patients, CH230 or BC265, or a plasmid pBR-HBadr4 (Araki *et al.*, 1990), while COOH-terminal truncated HBx fragments was amplified using viral DNA of CH230 as template. PCR was carried out by flanking the HBx template with a forward primer, with a Kozak consensus sequence (GCCACC) preceding the start codon (ATG) and a flag-tag DNA sequence (GATTACAAGGATGACGATGACAAG) at the N-terminal of the HBx sequence, and reverse primers with an artificial stop codon (TAA) at different HBx deletion sites (Table 2.2) (Knappik and Pluckthun, 1994). The present of a Kozak sequence (GCCA/GCCAUGG) preceding the start codon enhances the efficiency of translation initiation in eukaryotic cells (Kozak, 1987; Nakagawa *et al.*, 2008).

PCR amplification of various HBx fragments was carried out in two 25-µl reactions, including 2.5 µl of GeneAmp® 10X PCR Gold Buffer, 2 µl of $MgCl_2$ solution, 0.5µl of 10 mM dNTP (MBI Fermentas), 0.5 µl of 10 µM Forward primer, 0.5 µl of 10 µM Reverse primer, 0.125 µl of AmpliTaq Gold® DNA Polymerase (Applied Biosystems), 2 µl of viral DNA (CH230) and 16.875 µl of nuclease-free water, and incubated in the GeneAmp® PCR System 2700 Thermal Cycler (Applied Biosystems) at 95°C for 10 min, 35 cycles of 95°C for 30 s, 52°C for 30 s and 72°C for 1 min, and 72°C for 7 min. The PCR products were resolved by electrophoresis on a 1.5% (w/v) agarose gel stained with 2 µl of GelRed Nucleic Acid Stain (Biotium)

in 1 × TBE buffer (89 mM Tris-base, 98 mM boric acid, 2 mM EDTA) and visualized with GelDoc XR (Bio-Rad Laboratories, Inc.). Targeted fragments were extracted using the Gel Extraction Kit (Qiagen) and eluted with 30 µl of sterile water.

2.3.2 Cloning of HBx Fragments into TA-vectors

Cloning of PCR products was performed using the TOPO TA Cloning Kit (Invitrogen). A 6-µl reaction, containing 4 µl of PCR products, 1 µl of salt solution (1.2 M NaCl, 0.06 M $MgCl_2$) and 0.5 µl of pCR2.1-TOPO or pcDNA™3.1/V5-His TOPO (10 ng/µl), were prepared and incubated at room temperature for 15 min. pCR2.1-X, pCR2.1-XΔ14, pCR2.1-XΔ35, TOPO3.1-X, TOPO3.1-XADR and TOPO3.1-X265 were generated.

2.3.3 Heat Shock Transformation

Transformation was performed by adding all ligation products to a vial of *E. coli* competent cells, TOP 10. After incubating on ice for 15 min, the cells were heat shock at 42°C for 1 min, and then kept on ice immediately. The cells were recovered by 250 µl of S.O.C. medium (Invitrogen) and incubated at a 37°C shaker for 1 hour. Cells from each transformation were allowed to growth on a LB agar plate [1 % tryptone, 0.5 % yeast extract, 1% NaCl, 15% agar (pH7.0)] containing 0.1 mg/ml ampicillin, at 37 °C overnight.

Colonies were allowed to grow in 3 ml of LB medium [1 % tryptone, 0.5 % yeast extract, 1% NaCl] containing 0.1 mg/ml ampicillin at 37 °C overnight. Plasmid DNA was extracted by QIAprep Spin Miniprep Kit (Qiagen) and eluted by 50 µl of

nuclease-free water. Nucleotide sequences and the orientation of the inserts were confirmed by DNA sequencing using BigDye® Terminator v3.1 Cycle Sequencing Kits (Applied Biosystems) and ABI PRISM® 3100 Genetic Analyzer.

2.3.4 Sub-cloning of HBx Fragments into Lentiviral Vectors

Various versions of HBx were sub-cloned to the *EcoR*I and *Sal*I restriction sites of a lentiviral vector, pRRL-cPPT-CMV-X-IRES-EGFP-PRE-SIN (A gift from Prof. Chen) (Figure 2.1). Restriction digestion was carried out in a 30-µl reaction, including 1X NEBuffer 3, 1X bovine serum albumin (BSA) (10 µg/ml), 10 units of *Sal*I restriction endonuclease (New England BioLabs Inc.), 12 units of *EcoR*I restriction endonuclease (Promega Biotech Co., Ltd), 4 µg of plasmid DNA (pCR2.1-X, pCR2.1-XΔ14 or pCR2.1-XΔ35) and nuclease-free water, for 4 hours in a 37°C incubator. The digested fragments were resolved in a 1.5% (w/v) agarose gel, and extracted using the Gel Extraction Kit (Qiagen) and eluted with 25 µl of sterile water.

Ligation of the digested products and the lentiviral vector was carried out in a 20-µl reaction mixture, containing 1 X T4 DNA Ligase Reaction Buffer, 400 units of T4 DNA Ligase (New England BioLabs Inc.), 100 ng of digested lentiviral vectors and 16 µl of gel purified DNA fragments. The ligation reaction was carried out at 16°C overnight. Please refer to 2.3.3 Heat Shock Transformation.

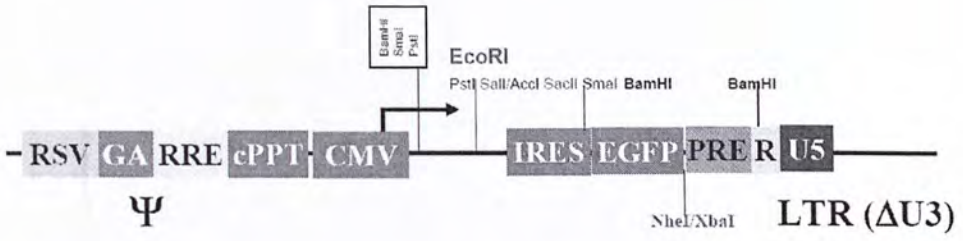

Figure 2.1 A schematic diagram of a lentivirus Vector, pRRL-cPPT-CMV-X-IRES-EGFP-PRE-SIN. Lentivirus transduction is characterized by its high infection efficiency, broad tropism and its ability to infect non-dividing cells or primary cell culture (Naldini *et al.*, 1996). A DNA copy of the viral RNA genome, the viral backbone with the insert, will integrate into the host cellular genome upon infection (Marshall *et al.*, 2007). The third-generation lentivirus vector encodes a self-inactivating construct in the 3'LTR to inactivate any production of wild-type lentivirus. Various versions of HBx fragments were PCR amplified and cloned into the *EcoR*I and *Sal*I restriction sites of the lentivirus vector. Transcription of the target genes was driven by the CMV promoter. The IRES element permits the translation of the gene of interest and the EGFP gene from a single bicistronic mRNA. The transduction efficiency can be estimated by the percentage of EGFP-positive cells under a fluorescent microscope or by flow cytometry.

Abbreviations: RSV, Rous sarcoma virus and HIV chimeric long terminal repeat; RRE, HIV Rev response element; cPPT, HIV-1 central polypurine tract; CMV, human cytomegalovirus; IRES, the internal ribosome entry site of the encephalomyocarditis virus; EGFP, enhanced green fluorescent protein; PRE, human hepatitis virus posttranscriptional regulatory element, LTR (ΔU3), deletion in the HIV-1 LTR U3 sequence (Barry *et al.*, 2001; Chen *et al.*, 2007).

Table 2.2 Primers. Underlined: restriction site sequence; bold: start or stop codon.

Primers for molecular cloning		
CH230Flag_F	Forward	5'-GCCACC**ATG**GATTACAAGGATGACGATGACAAGGCTGCTAGGATGTGCT-3'
ADRFLAG_F	Forward	5'-GCCACC**ATG**GATTACAAGGATGACGATGACAAGGCTGCTAGGGTGTGCTG-3'
BC265Flag_F	Forward	5'-GCCACC**ATG**GATTACAAGGATGACGATGACAAGGCTGCTAGGCTGTGCT-3'
XRCH230	Reverse	5'- TAGGGCGTCGAC**TTA**GGCAGAGGTGAAAAAGTTG -3'
X14RCH230	Reverse	5'- TAGGGCGTCGAC**TTA**TTTATGCCTACAGCCTCCTAG -3'
X35RCH230	Reverse	5'- TAG GGCGTCGAC**TTA**GTCTTTAAACACACAGTCTTTGA -3'

Primers for RT-PCR			**Tm**
XF (nt1286-1305)	Forward	5'-CAGCTTGTTTTGCTCGCAGC-3'	62°C
XR1 (nt1551-1570)	Reverse	5'-GCAGATGAGAAGGCACAGAC-3'	
XR2 (nt1691-1710)	Reverse	5'-TGAAGTATGCCTCAAGGTCG-3'	
XR3 (nt1713-1734)	Reverse	5'-CCCAGTCTTTAAACAAACAGTC-3'	
XR4 (nt1780-1800)	Reverse	5'-AGACCAATTTATGCCTACAGC-3'	
XR5 (nt1816-1835)	Reverse	5'-GGCAGAGGTGAAAAAGTTGC-3'	
β-actin	Forward	5'-TTCTTTGCAGCTCCTTCGTTGCCG-3	58°C
	Reverse	5'-TGGATGGCTACGTACATGGCTGGG-3	

2.4 Generation of Lentivirus

Packaging of lentivirus was performed by transient transfection of 293T human embryonic kidney cells with the lentivirus transfer vectors and three packaging vectors, pMDL/pRRE, pRSV-REV and pCMV-VSVG. The day prior to transfection, confluent 10-cm plates of 293T cells were split 1:5 and maintained in DMEM supplemented with 10% FBS at a 37°C incubator. A mixture of plasmids, including 10 μg of transfer vectors, 6.6 μg of pMDL/pRRE, 3.5 μg of pCMV-VSVG and 2.5 μg of pRSV-REV, was transfected to 293T cells by calcium phosphate method. Culture medium was removed a day after transfection. For an additional 24 hours, culture medium was harvested and the viral particles were concentrated by ultracentrifugation at 700000 x g for 2 hours at 20°C. The viral pellets were resuspended in 100 μl of 1 x HBSS and stored at -80°C (Tiscornia et al, 2006).

2.4.1 Lentivirus Infection

One day prior to infection, 2 x 10^4 of cells were seeded in wells of a 24-well plate and incubated in a 37°C incubator with 5% CO_2. The medium was removed and replaced with 400 μl of fresh medium (DMEM supplemented with 10% FBS) with 8 μg/ml polybrene (Sigma-Aldrich, Inc.) and lentivirus. Cells were transduced for 48 hours, and the virus-containing medium was discarded, and washed twice with PBS to remove any residual virus. The transduction efficiency was monitored by a fluorescent microscope. The amount of virus used for each transduction was determined by the percentage of EGFP-positive cells by flow cytometry at day 3 post-infection. Three viral levels were tested. To ensure linearity, the percentage of EGFP-positive cells was compared only for the infection rate between 5 – 20%.

2.5 RNA Extraction

Total RNA containing small RNA molecules was extracted using miRNeasy Mini Kit (Qiagen, Valencia, CA, USA) according to the standard protocol. In brief, cells were completely lysed by 1.4 ml of QIAzol, before mixing with 280 µl of chloroform. The homogenate was then centrifuged for 15 min at 12000 × *g* at 4°C to obtain the aqueous layer. Ethanol precipitation was carried out by mixing 750 µl of aqueous layer with 1.05 ml of 100% ethanol. The mixture was transferred into an RNeasy Mini spin column, and centrifuge at 8000 × *g* for 30 s to drain off the flow-through. The RNA binding membrane was then washed with 350 µl Buffer RWT, incubated with DNase I (Qiagen, Valencia, CA, USA), and washed by 350 µl Buffer RWT again and followed by 500 µl Buffer RPE twice. Buffer RWT contained guanidine thiocyanate as the chaotrophic agent and ethanol as the organic solvent, which allowed efficient binding of RNA to the silica membrane of the spin column. Substances that bound non-specifically to the silica membrane could be washed away by ethanol without disturbing the RNA-membrane interaction. Thus, RNA of high yield and purity could be obtained after elution. Total RNA was recovered by eluting with 50 µl of RNA-free water. The purity and concentration of RNA were determined by NanoDrop 1000 spectrophotometer (Thermo Fisher Scientific Inc.). The RNA was stored at -80°C before use.

2.6 Western Blot Analysis

Fifty micrograms of protein were resolved on a 15% SDS-PAGE. A PVDF membrane (Amersham Biosciences), 2 filter papers and the SDS-PAGE were equilibrated in a transfer buffer (39 mM glycine, 48 mM Tris-HCl, 0.037% SDS, 20% methanol, pH 8.3) before assembly in the Trans-Blot Semi-Dry Electrophoretic Transfer Cell (Bio-Rad Laboratories, Inc.).

After blotting, the membrane was blocked in 5 ml of blocking buffer [PBST with 5% (w/v) non-fat dried milk powder] at room temperature for 15 min. The membrane was probed with Hepatitis B Virus X antigen antibody [X36C] (ab2741) (Abcam plc) (1:2000) or anti-beta actin antibody (Santa Cruz Biotechnology, Inc.) (1:5000) at 4°C overnight, and then with anti-mouse antibodies conjugated with horseradish peroxidase (1:5000) (Santa Cruz Biotechnology, Inc.) at room temperature for 1 hour. The membrane was washed by 15 ml of PBST for 3 times. The blot was visualized with Western Lightning Chemiluminescence Reagent Plus (Amersham Biosciences) by exposing to the FUJI Medical X-Ray Film (FUJI) in a dark room. The film was processed by the developer and fixer.

2.7 MiRNA Microarray

Agilent Human miRNA Microarray Kit (V2) (Agilent Technology) was used for miRNA profiling of various HBx-expressing MIHA cell lines and a mock-infected control. One hundred nanograms of total RNA, including small RNA, were taken for miRNA profiling. The concentration and purity of total RNA were determined by NanoDrop 1000 spectrophotometer (Thermo Fisher Scientific Inc.) and the RNA integrity was determined by Agilent 2100 Bioanalyzer (Agilent Technology).

2.7.1 Cyanine3-pCp Labeling of RNA Samples

The input RNA was dephosphorylated by Calf Intestine Alkaline Phosphatase (CIP) in a 7-μl reaction mixture, containing 0.7 μl of 10X CIP buffer, 0.7 μl of CIP (16 U/ μl) (GE Healthcare), 4 μl of total RNA (25 ng/ μl) and 1.6 μl of nuclease free water, by incubating at 37°C for 30 min. The reaction mixture was further incubated with 5 μl of 100% dimethyl sulphoxide (DMSO) at 100°C for 8 min, and kept on an ice-water bath for a further 3 min.

Labeling of Cy-3 fluorescent dyes to 3' ends of miRNAs was carried out by mixing the 12 μl of dephosphorylated RNA with a 8-μl ligation master mix, including 2 μl of 10X T4 RNA Ligase Buffer, 2 μl of 0.1% BSA, 3 μl of Cyanine3-pCp (Cy3-pCp) and 1 μl of T4 RNA Ligase (15 U/μl) (GE Healthcare). The resultant ligation mixture was incubated at 16°C for 2 hours. Micro Bio-Spin 6 column (Bio-Rad Laboratories, Inc.) was used to purify the labeled RNA, by loading a mixture of the 20-μl RNA sample and 30 μl of RNase-Free water onto the gel bed of the column. The purified sample was obtained as the flow-through by centrifuging the column for 4 min at 100 x *g*.

2.7.2 Sample Hybridization

The purified sample was dried completely using a speed-vac at 45°C, and was resuspended with 18 µl of nuclease-free water, followed by 4.5 µl of the 10X GE Blocking Agent and 22.5 µl of 2X Hi-RPM Hybridization Buffer. The sample mixture was kept at 100°C for 5 min, and then on ice for a further 5 min. The hybridization sample was slowly dispensed onto the gasket well in a "drag and dispense" manner, and covered with a SureHyb chamber. The assembled slide chamber was installed in a hybridization oven with the rotor speed at 20 rpm at 55°C for 20 hours

2.7.3 Microarray Wash

The microarray wash procedure was carried out according to the conditions in Table 2.3. The Gene Expression Wash Buffer 2 was pre-warmed to 37°C the night before washing the arrays.

2.7.4 Array Slide Scanning and Data Processing

The microarray slide was scanned using an Agilent Microarray Scanner, and data was extracted using the Agilent Feature Extraction Software. Data analysis was performed on GeneSpring software (Agilent Technologies). Non-expression probes were filtered and data was normalized by 75% percentile shift method.

Table 2.3 W ash Conditions

Dish	Wash	Buffer	Temperature	Time
Disassembly	1	GE Wash Buffer 1	Room Temperature	
1st wash	2	GE Wash Buffer 1	Room Temperature	5 min
2nd wash	3	GE Wash Buffer 2	Elevated temperature	5 min
Acetonitrile Wash	4	Acetonitrile	Room Temperature	1 min
3rd wash	5	Stabilization and Drying Solution	Room Temperature	30 s

2.8 Detection of HBx Gene Deletion by PCR

HBx gene deletion was detected by PCR using a universal forward primer (XF) and five different reverse primers (R1, R2, R3, R4 and R5) flanking the full length and different lengths of HBx gene as stated by Ma *et al.* (Table 2.1). One hundred nanogram (100ng) of DNA extracted from liver tumors and the matched non-tumor adjacent tissues was taken as templates for the amplification of various versions of HBx gene. PCR of human β-actin gene was used as a loading control. A total volume of 25-µl reaction mix was prepared according to the standard protocol of Promega GoTaq Fexi DNA polymerase [5 µl of 5X Green GoTaq Fexi Buffer, 2 µl of 25 mM $MgCl_2$, 0.5 µl of 10 mM dNTP (Fermentas), 0.5 µl of 10 µM Forward primer, 0.5 µl of 10 µM Reverse primer, 0.125 µl of GoTaq DNA Polymerase (5U/µl), 100 ng of DNA template and nuclease-free water].

PCR was carried out in the GeneAmp® PCR System 2700 Thermal Cycler (Applied Biosystems) at 95°C for 2 min, 36 cycles of 95°C for 1 min, 62°C for 1 min and 72°C for 1 min, and 72°C for 7 min for the amplification of HBx genes, or 95°C for 2 min, 28 cycles of 95°C for 30 s, 58°C for 30 s and 72°C for 30 s, and 72°C for 7 min for the amplification of β-actin gene. The PCR products were then analyzed by electrophoresis on a 1.5% agarose gel stained with GelRed Nucleic Acid Stain (Biotium) and visualized by GelDoc XR (Bio-Rad Laboratories, Inc.).

2.9 Immunohistochemistry

Immunohistochemistry analysis was performed on 20 pairs of formalin-fixed and paraffin-embedded liver tissue sections, and 1 negative control section. Tissue sections were deparaffinized in Histolemon for 2 x 10 min and rehydrated through a graded alcohol series (100%, 95%,70%, H_2O) for 5 min. The slides were left at room temperature for 20 min, and then washed once in water. They were further incubated in 3% H_2O_2 for 5 min at room temperature for quenching of endogenous peroxidases, and washed twice in 1X TBS. Non-specific bindings were blocked with 10% normal rabbit serum for 10 min. The endogenous HBx protein was stained by anti-Hepatitis B Virus, X-Protein, (MAB8429) a.a. 50-88, clone 146 (Minipore, Chemicon) (1:100 dilution) by incubating the slides at 4°C overnight. The slides were incubated with goat-anti-mouse antibody for 30 min at 37°C (1:100 dilution) and washed twice in 1X TBS. The slides were incubated in peroxidase substrate solution for 5 min at room temperature. The reaction was blocked in water. The slides were counterstain with Hematoxilin for 15 s and were dehydrated through a graded alcohol series and mount with Eukitt (Ma *et al.*, 2008).

2.10 Quantitative Real-time PCR

The level of mature microRNAs was quantified by TaqMan MicroRNA Assays (Applied Biosystems) (Table 2.4). Input total RNA was first diluted to 2ng/μl by nuclease-free water. Five nanograms (5ng) of total RNA were converted to cDNA by TaqMan MicroRNA Reverse Transcription Kit (Applied Biosystems) in a 7.5 μl reaction volume. Five microlilter of reaction mix [0.075 μl of 100 mM dNTPs, 0.5 μl MultiScribe Reverse Transcriptase (50U/μl), 0.75 μl of 10X Reverse Transcription Buffer, 0.095 μl of RNase Inhibitor (20U/μl), 2.08 μl of nuclease-free water and 1.5 μl of miRNA-specific RT primer] together with 2.5 μl of total RNA (5ng) were prepared and incubated in the GeneAmp® PCR System 2700 Thermal Cycler (Applied Biosystems) at 16°C for 30 min, 42°C for 30 min and 85°C for 5 min.

The quantitative PCR was carried out in a 384-well plate by Applied Biosystems 7900HT Fast Real-Time PCR System. The 7.5 μl of reverse transcribed cDNA was diluted to 30 μl by adding 22.5 μl of nuclease-free water, and 2 μl of the diluted product was taken as the input cDNA. A total volume of 10-μl reaction mix [5 μl of TaqMan 2X Universal PCR Master Mix (No AmpErase UNG), 1 μl of TaqMan MicroRNA Assay (20X), 2 μl of diluted Reverse transcription product and 3 μl of nuclease-free water] was prepared and PCR amplification was done at 95°C for 10 min, 40 cycles of 95°C for 10 s and 60°C for 1 min. Data was normalized by U6 small RNA (RNU6B) and the fold change was determined by the comparative Ct method. All reactions were carried out in triplicate and blank controls were also included in every reaction.

Table 2.4 TaqMan MicroRNA Assays (Applied Biosystems) used for the validation of miRNA microarray results. The miRNA sequences were also included for reference. RNU6B, a small RNA, was used for normalization of miRNA real-time PCR results.

Assay Name	Part Number	Target Sequence
hsa-miR-125a-5p	4395309	UCCCUGAGACCCUUUAACCUGUGA
hsa-miR-146a	4373132	UGAGAACUGAAUUCCAUGGGUU
hsa-miR-193b	4395478	AACUGGCCCUCAAAGUCCCGCU
hsa-miR-19a	4373099	UGUGCAAAUCUAUGCAAAACUGA
hsa-miR-19b	4373098	UGUGCAAAUCCAUGCAAAACUGA
hsa-miR-23a	4373074	AUCACAUUGCCAGGGAUUUCC
hsa-miR-27a	4373287	UUCACAGUGGCUAAGUUCCGC
hsa-miR-190	4373110	UGAUAUGUUUGAUAUAUUAGGU
hsa-miR-29c	4395171	UAGCACCAUUUGAAAUCGGUUA
hsa-miR-365	4373194	UAAUGCCCCUAAAAAUCCUUAU
hsa-miR-99b	4373007	CACCCGUAGAACCGACCUUGCG
RNU6B	4373381	CGCAAGGAUGACACGCAAAUUCGUGAAGCGUUCCAUAUUUUU

2.11 Proliferation Assay

Cell viability was assessed by a colorimetric method using CellTiter 96® AQ_{ueous} One Solution Cell Proliferation Assay (MTS) (Promega Biotech Co., Ltd) for 5 consecutive days. Two-thousand of cells were seeded to the wells of a 96-well plate in 100 µl of DMEM supplemented with 10% FBS in sextuplicate. The plate was kept in a 37°C humidified incubator before carrying out the MTS assay. Culture medium was discarded, and replaced with a 120-µl of MTS mixture, including 100 µl of fresh culture medium (DMEM with 10% FBS) and 20 µl of MTS solution. The plate was light-protected by covering with an aluminium foil and kept in a 37°C humidified incubator for 1 hour. The absorbance of the colorimetric products formed was measured at 490 nm by µQuant Microplate Spectrophotometer (BioTek Instruments, Inc.). The background absorbance was subtracted from the wells of zero cells.

2.12 Cell Cycle Analysis

Flow cytometry was employed to analyze the cellular DNA content. Approximately, 1 x 10^6 of cells were harvested by trypsinization and washed twice by PBS. After centrifugation, supernatant was discarded and cells were resuspended by 0.5 ml of cold PBS. For detecting GFP-containing cells, cellular proteins were cross-linked by mixing a further 500 µl of cold PBS buffered with 2% formaldehyde solution. A final cell suspension containing 1% formaldehyde was kept at 4°C for 1 hour. After cross-linking, the formaldehyde-containing solution was removed by centrifugation, and the cell pellet was resuspended by 1 ml of PBS at room temperature. Ethanol permeablization of cells was carried out by adding 4 ml of ice-cold 70% ethanol to the cell suspension drop-by-drop while vortexing. The cell suspension was kept at 4°C for at least 12 hours before proceeding to propidium iodide (PI) staining. Staining buffer [PBS with 2% FBS] was used to wash the cell pellet after discarding the ethanol. The sample was resuspended by 1 ml staining buffer, and incubated with 500ug/ml of ribonuclease A (RNase A) (Invitrogen) at 37°C for 30 min to eliminate cellular RNA. Sample DNA was stained with 10 µl/ml of PI (BD Pharmingen) at room temperature for an additional 30 min in the dark.

Cellular DNA content was analyzed by BD FACSAria™ Flow Cytometer within 24 hours post-staining. Modfit LT 3.0 (Verity Software House) was used to conduct open-ends modeling of flow cytometry histograms, defining the position and the percentage of G_0G_1 phases, S phases, and G_2/M phases of cellular samples.

2.13 Annexin V Apoptosis Assay

Cell apoptosis was assessed by flow cytometry using a PE Annexin V Apoptosis Detection Kit I (BD Pharmingen). The detection ultilized two fluorescent dyes, 7-Amino-actinomycin D (7-AAD) and phycoerthrin (PE)-conjugated Annexin V, to differentiate viable cells from cells that underwent apoptotic or necrotic cell death. 7-AAD was used to discriminate viable cells from non-viable cells, while phycoerthrin (PE)-conjugated Annexin V bound to the externalized membrane phospholipid phosphatidylserin (PS) that differentiate apoptotic or necrotic cells from viable cells (van Engeland *et al.*, 1996; Zhang *et al.*, 1997).

One to two days before Annexin V-PE and 7-AAD staining, 1 x 10^5 of cells were seeded on a six-well plate. Culture medium was collected, and cells were harvested by trypsinization. The cells were washed twice by cold PBS, and resuspended with 100 µl of 1X Annexin V Binding Buffer. The sample was incubated with 5 µl of Annexoin V-PE and 5 µl of 7-AAD for 15 min at room temperature in the dark. An unstained control, a 7-AAD stained control, an Annexin V-PE stained control and a PE Annexin V and 7-AAD stained control were also set up to define the quadrants corresponding to viable cells, apoptotic and non-viable cells. EGFP-positive cells were gated for analysis.

2.14 Colony Formation Assay

One day before transfection, 4 x 10^5 cells were seeded on a 6-well plate. Transfection mix included 94 µl of serum-free DMEM, 6 µl of FuGENE6 Transfection Reagent (Roche) and 2 µg of plasmid DNA (TOPO3.1-X, TOPO3.1-XADR, TOPO3.1-X265 and a control vector) was incubated for 20 min at room temperature and added drop-by-drop to the wells. Geneticin G418 (Invitrogen) (1000 µg/ml) were added to select transfected cells 48 hours after transfection. Fresh medium with 1000 µg/ml of G418 was replaced twice a week for a total of 14 to 18 days. The colonies were stained with crystal violet (0.5% w/v) in methanol for 5 to 10 min at room temperature.

2.15 Statistical Analysis

Statistical analysis was performed by GraphPad Prism (GraphPad Software). Fisher's exact test was used to test the association between truncated HBx and HCC (Section 3.1). Mann Whitney U test was used to analyse the immunochemical scores (Section 3.2). Kappa analysis was used to assess the inter-observer agreement of the results of immunostaining (Section 3.2). Student's t test was used to analyse colony formation assay (Section 3.3), cell proliferation (Section 3.4.3) and cell cycle analysis (Section 3.4.4). Wilcoxon signed rank test was used to compare the levels of HBx-deregulated miRNAs in clinical tissues (Section 3.5.3). P value < 0.05 was considered as statistically significant. Graphs were generated by SPSS (SPSS Inc.) or GraphPad Prism (GraphPad Software).

Chapter 3 RESULTS

3.1 Detection of Full-length and COOH-terminal Truncated HBx in HCC Tissues

To address whether the COOH-terminal deleted HBx was implicated in HBV-associated HCC, PCR amplification of various lengths of HBx was carried out in 16 pairs of HCC tissues and the matched adjacent nontumor tissues. Five pairs of primers, a universal forward primer (XF) and five different reverse primers (R1, R2, R3, R4 and R5), encompassing the full length and various lengths of HBx gene were used as described (Ma *et al.*, 2008) (Figure 3.1a). Equal quantity of DNA was taken for PCR amplification of HBx gene, and for the detection of relevant PCR bands (Figure 3.1b). For full-length HBx, it was detected in all adjacent non-tumor tissues (16/16) and 50% (8/16) of HCC tissues. For COOH-terminal truncated HBx, it was present exclusively in HCC tissues. It suggested that COOH-terminal truncated HBx was more associated with HCC than adjacent non-tumor tissues ($p = 0.0024$) (Table 3.1).

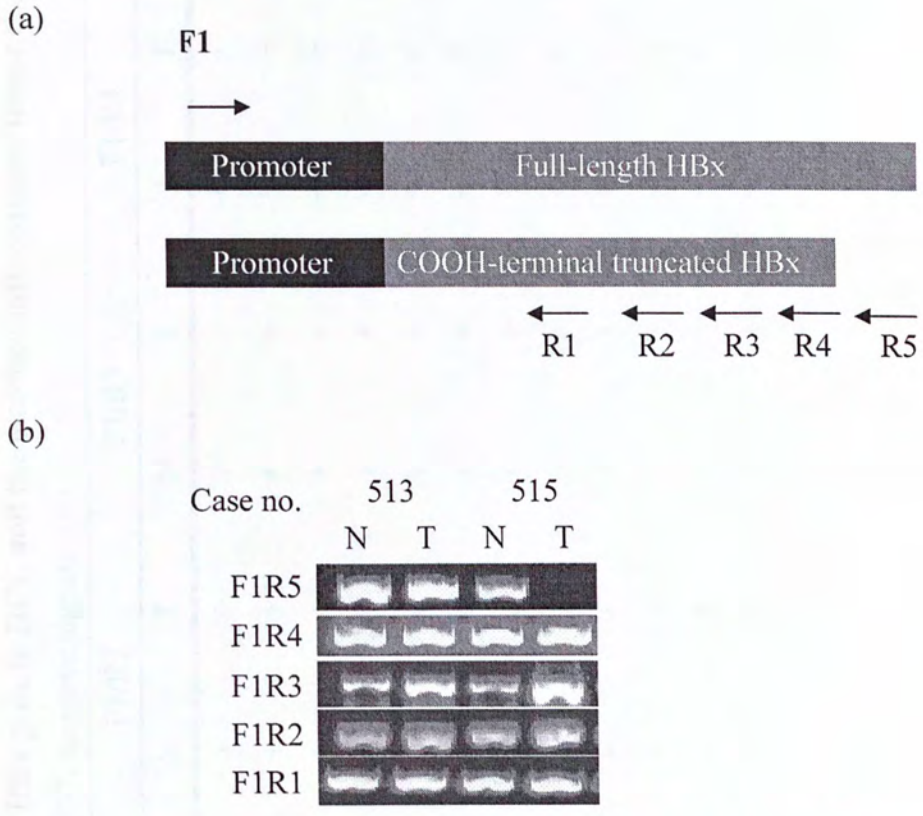

Figure 3.1 PCR amplification of HBx genes in tissue samples. (a) PCR analysis of COOH-terminal deletion in HBx gene. The forward primer XF encompassed the promoter region of HBx and the 5 different reverse primers at the C-terminal regions of HBx. (b) Representative figures of the PCR amplification of full-length HBx and truncated HBx by primer F1R1, F1R2, F1R3, F1R4 and F1R5 were shown. "N", adjacent non-tumor tissue; "T", HCC tissue.

Table 3.1 A summary of the PCR amplification of HBx gene in HCC and the matched adjacent non-tumor tissues. N, adjacent non-tumor tissue; T, tumor tissue. "+", positive signal; "-", negative signal.

	Immnostaining		F1/R1		F1/R2		F1/R3		F1/R4		F1/R5	
Case no.	N	T	N	T	N	T	N	T	N	T	N	T
508	+	+	+	+	+	+	+	+	+	+	+	-
513	+	+	+	+	+	+	+	+	+	+	+	+
515	+	+	+	+	+	+	+	+	+	+	+	-
519	+	+	+	+	+	+	+	+	+	+	+	-
522	+	+	+	+	+	+	+	+	+	+	+	+
527	+	+	+	+	+	+	+	+	+	+	+	-
531	+	+	+	+	+	+	+	+	+	+	+	-
532	+	+	+	+	+	+	+	+	+	+	+	+
547	+	+	+	+	+	+	+	+	+	+	+	+
550	+	+	+	+	+	+	+	+	+	+	+	+
551	+	+	+	+	+	+	+	+	+	+	+	-
552	+	+	+	+	+	+	+	+	+	-	+	-
554	+	+	+	+	+	+	+	+	+	+	+	+
557	+	+	+	+	+	+	+	+	+	+	+	+
558	+	+	+	+	+	+	+	+	+	+	+	+
559	+	+	+	+	+	+	+	-	+	-	+	-

3.2 Confirmation of HBx Expression in HCC Tissues

The expression of HBx protein was confirmed by the immunohistochemical staining using a monoclonal anti-HBx antibody (Millipore, Chemicon, MAB8429) targeting the 50 – 88 aa of HBx domain. By recognizing the central domain, the anti-HBx antibody could interact with full-length and various forms of truncated HBx. In this regard, the intensity of HBx staining reflected the total amount of full-length and various forms of truncated HBx and could not differentiate their expression. A HBV-negative liver tissue was included as a negative control (Figure 3.2).

The immunostaining results were scored by three independent observers based on (a) the percentage of staining area, which was defined as grade 2 for 5 - 30% coverage, grade 3 for 30 - 60% coverage and grade 4 for ≥ 60% coverage, (b) and the intensity of the staining signal, which was defined as weak (grade 1), moderate (grade 2) and strong (grade 3) (Figure 3.3). A moderate agreement was achieved among the three independent observers (Table 3.3). Interestingly, both of the staining area and staining intensity in HCC tissue sections were significantly smaller and weaker than the tumor adjacent tissues ($n = 20$, $p < 0.05$) (Table 3.2). In addition, the two scoring parameters were not differed between the group of full-length HBx and COOH-terminal truncated HBx samples (Table 3.4). The difference in the staining area and signal intensity could not be attributable to the binding affinity of the anti-HBx antibody to the HBxAg, as no observable gene deletion was detected on the 50 – 88 aa of HBx domain. The results suggested that the expression level of HBx in HCC was lower than the adjacent non-tumor tissues.

(A)

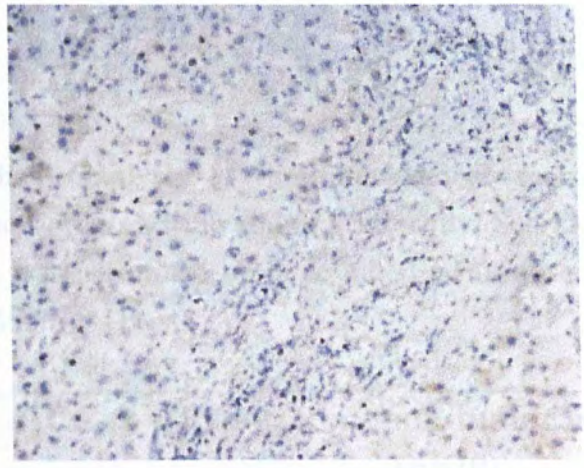

(B)

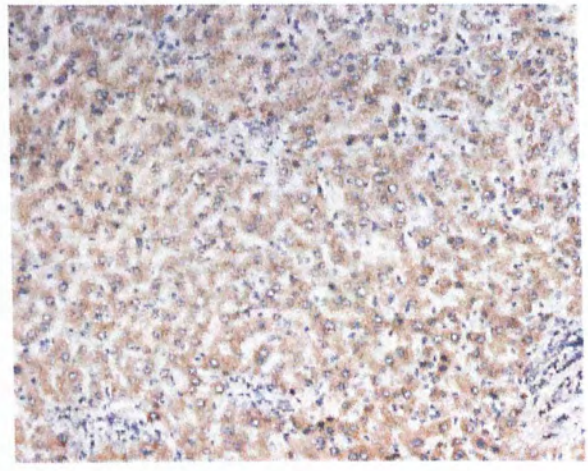

Figure 3.2 Immunohistochemical staining of liver tissue sections. The tissue sections were stained with anti-HBx antibody. (A) Negative Control, tissue section of a HBV-negative patient; (B) Positive control, tissue section of a HBx-positive patient.

Table 3.2 Statistical analysis of immunochemical scoring based on the percentage of stained area and the staining intensity. Scoring of the 20 pairs of liver tissue sections was performed by three independent observers (A, B and C). (*p*-value, by Mann Whitney U test)

	HCC (n=20)	Adjacent non-tumor tissues (n=20)	*p*
Median score (range)			
Area	3 (2-4)	4 (2-4)	0.047
Intensity	1 (1-3)	2 (1-3)	0.045

Table 3.3 Inter-observer agreement (Kappa analysis). Moderate agreement on the immunochemical scoring was achieved between three independent observers (A, B and C). Indicated were the kappa values (0 – 1).

	A vs B	A vs C	B vs C
Area	0.65	0.70	0.48
Intensity	0.65	0.69	0.72

Table 3.4 Comparison of the staining area and staining intensity between the full-length HBx tissues and the truncated HBx samples. (*p*-value, by Mann Whitney U test)

	Truncated HBx (n=8)	**Full length HBx (n=24)**	***p***
Median score (range)			
Area	3 (2-4)	4 (2-4)	0.322
Intensity	2 (1-3)	1 (1-3)	0.855

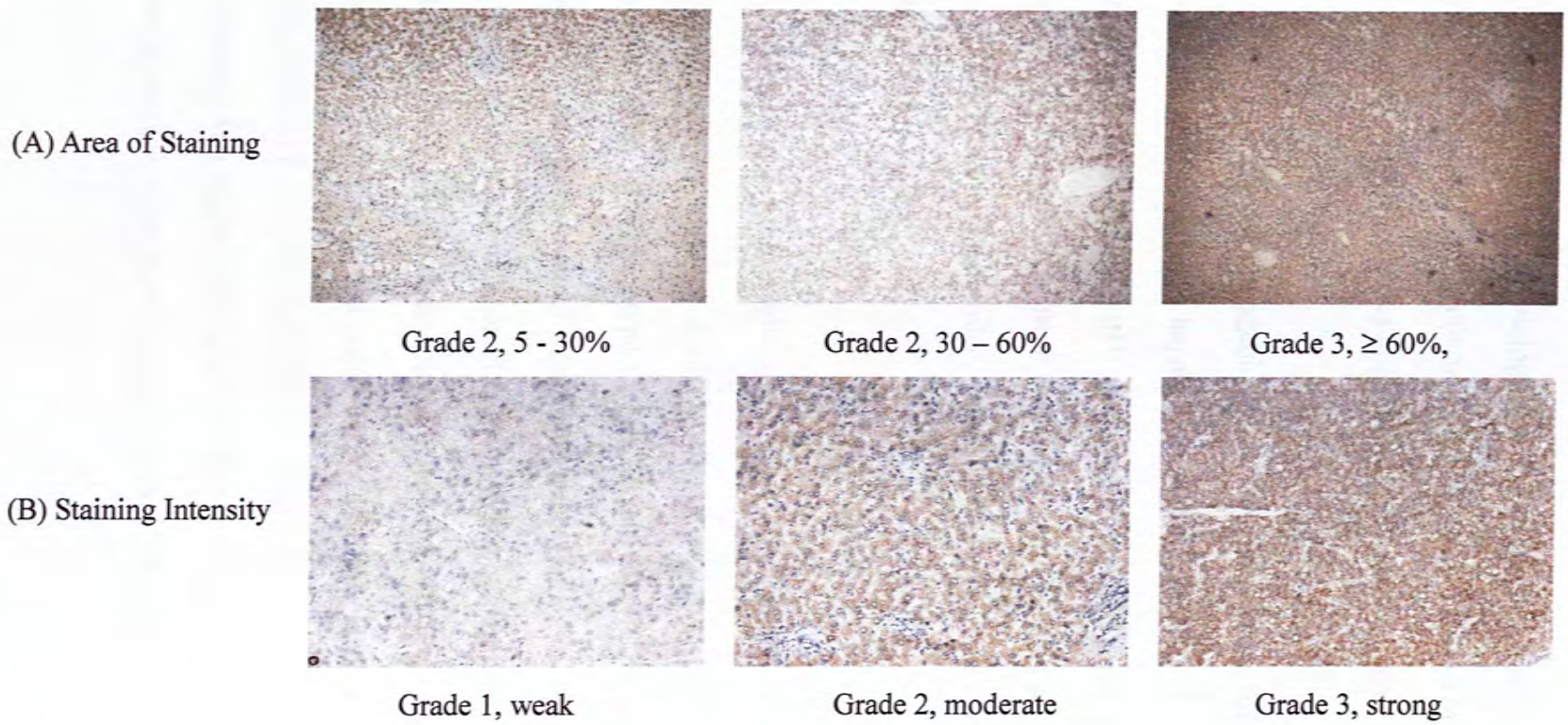

Figure 3.3 Representative pictures for immunochemical scoring of HBx-stained tissue sections. The figures were shown as references for immnostaining score, based on two criteria (A) percentage of stained area, Grade 2, 5 - 30%; Grade 2, 30 – 60%; Grade 3, ≥ 60% coverage; (B) Staining intensity, Grade 1, week; Grade 2, moderate; Grade 3, strong. Scoring was performed by 3 different people, and a moderate agreement was achieved among the three observers (Table 3.3).

3.3 Comparsion of HBx from Different HBV Strains

As COOH-terminal truncated HBx was often detected in liver tumors, we next aimed to investigate its biological significance in hepatocarcinogenesis. HBx from two viral strains, HBV genotype B and genotype C, were first compared, as sequence variation on the HBx genes might show different oncogenic potential.

To estimate the oncogenic effects of HBx, colony formation assay was carried out on a non-tumorgenic hepatocyte cell line, MIHA, by transfecting HBx derived from two viral strains, HBV genotype B (BC265) and genotype C (CH230). In addition, HBx obtained from HBVADR, which had been demonstrated to induce HCC in HBx-transgenic mice, was served as a reference (Araki *et al.*, 1990; Kim *et al.*, 1991).

Consistent to previous reports, all HBx-transfected cells had lower colony forming ability than the control cells ($p < 0.01$) (Figure 3.4a). Moreover, HBx derived from HBV genotype C, CH230 and HBVADR, had higher colony forming ability than HBx obtained from HBV genotype B, BC265 ($p < 0.05$) (Figure 3.4b). However, the mean number of colonies was not significantly different between HBx derived from CH230 and HBVADR ($p = 0.49$). Phylogenic analysis of the HBV sequence confirmed that both HBVADR and CH230 were belonged to HBV subgenotype Ce, which had been implicated in higher risk of HCC (Chan *et al.*, 2008) (Figure 3.5). Overall, HBx gene of HBV genotype Ce (CH230) might show stronger oncogenic potential and was chosen for the following studies.

(a)

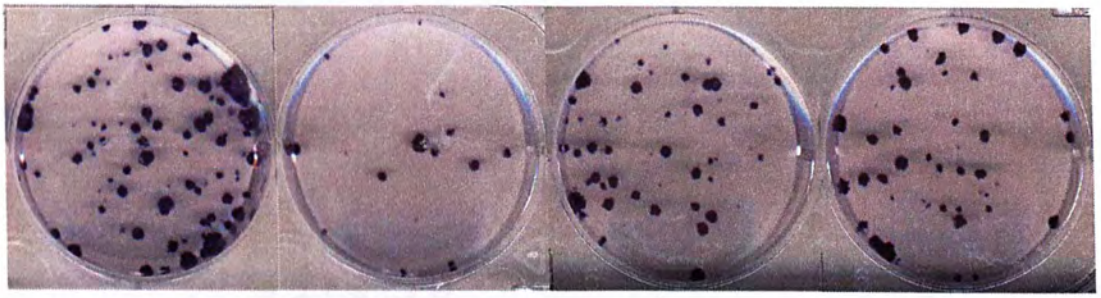

Empty vector control | HBxBC265 | HBxCH230 | HBxADR

(b)

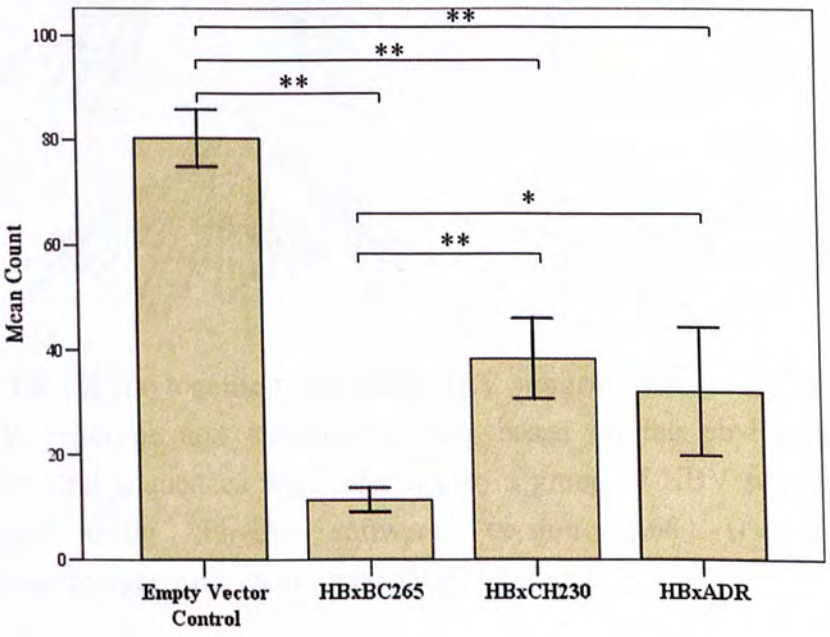

Figure 3.4 Colony Formation Assay. Full-length HBx derived from HBV genotype B, BC265, and HBV genotype C, CH230 and ADR, were compared on their ability to form colonies. (a) Pictures from a representative set of experiment. The colonies were stained by crystal-violet in methanol. (b) Experiment was performed in three replicates and the results were presented by the mean and SD. "*" indicated $p < 0.05$, and "**" indicated $p < 0.01$

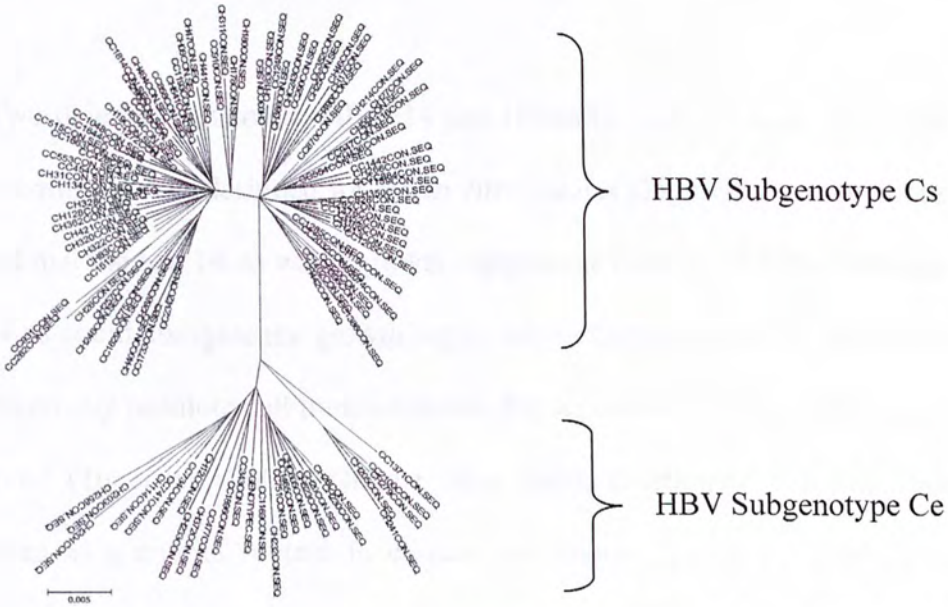

Figure 3.5 A phylogenic tree of two HBV subgroups, Cs and Ce. Classification of HBV genotype and subgenotype was based on the phylogenic analysis of complete viral sequences with reference to a group of HBV sequences of known genotypes using Phylip software version 3.68 (Felsenstein, 2008). http://evolution.genetics.washington.edu/phylip.html

3.4 Functional Characterization of COOH-terminal Truncated HBx

3.4.1 Selection of COOH-terminal Truncated HBx

As mentioned in the introduction, no truncation hot-spot was identified so far and the mechanism of C-terminal deletion is still unclear. HBx truncation might be a random event, and the extend of truncation seemed to vary among samples.

Two deletion constructs, HBxΔ14 and HBxΔ35, with 14-aa or 35-aa less from the C-terminus were designed for the *in vitro* studies (Figure 3.6). A previous study showed that the last 14-aa was a growth suppressive domain of HBx. Deletion of the last 14-aa could abrogate the growth suppressive effects induced by full-length HBx and effectively promote cell transformation, but its transactivition capability was still preserved (Tu *et al.*, 2001). On the other hand, deletion of the last 35-aa was identified as a natural mutant in clinical specimens (Xu *et al.*, 2007). For these reasons, a full-length HBx, two C-terminal truncated HBx constructs, HBxΔ14 and HBxΔ35, were constructed from HBV genotype C, and their biological effects were compared with an empty vector control (Figure 3.6).

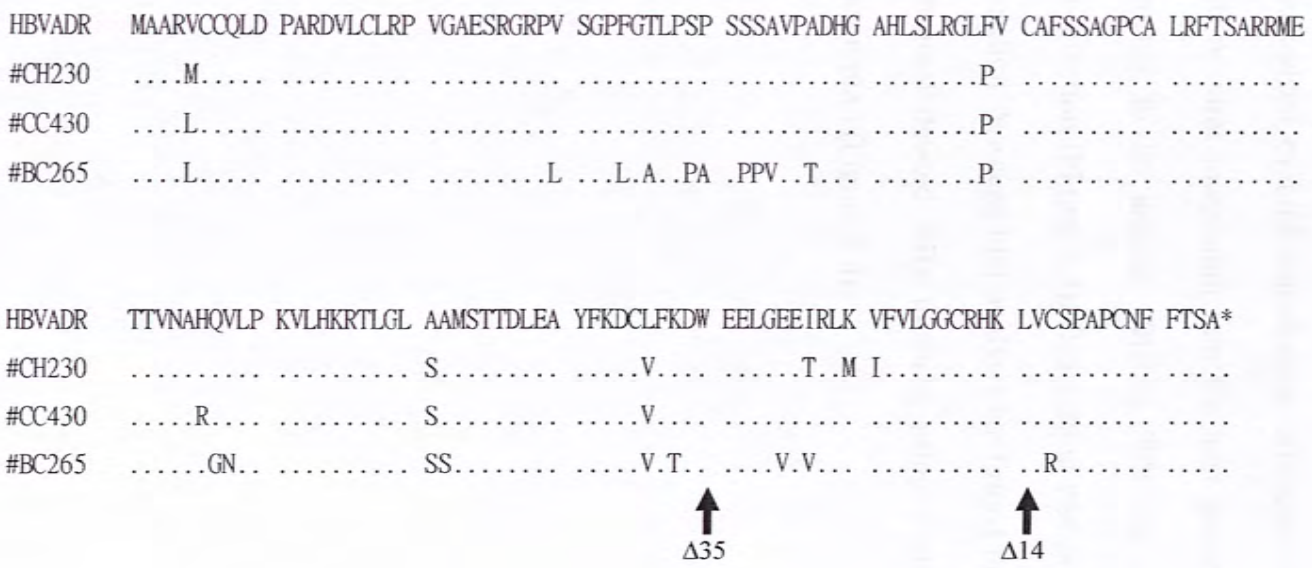

Figure 3.6 Alignment of four hepatitis B virus X protein amino acid sequences. The whole viral genome sequence of CH230, CC430 and BC265 was retrieved from our previous HBV genotype study (Sung *et al.*, 2007). HBVADR, described in Araki *et al.*, 1990 (X01587), was taken as a reference sequence. Multiple sequence alignment was carried out by ClustalX (1.83) (Thompson *et al.*, 1997). Classification of HBV genotype and subgenotype was based on the phylogenic analysis of the complete viral sequences. HBV subgenotype Ce: HBVADR and CH230; HBV subgenotype Cs: CC430; and HBV genotype B: BC265. Truncation sites of the COOH-terminal deleted HBx constructs (HBxΔ14 and HBxΔ35) were indicated by arrows.

3.4.2 Generation of Various HBx-expressing Hepatocyte Cell Lines

The biological effects of various versions of HBx were investigated by transducing an immortalized, non-tumorigenic hepatocyte cell line, MIHA, with Lenti-X, Lenti-XΔ14, Lenti-XΔ35 and a mock-control. Lentiviral infection was characterized by high transduction efficiency and stable transgene expression as a result of viral integration into the host genome. The transduction efficiency was estimated to be around 70% to 90% by a fluorescent microscope at day 3 post-infection (Figure 3.7). Cell sorting was performed to enrich the EGFP-positive population. Western blot analysis confirmed the expression of full-length HBx and C-terminal deleted HBx mutants, using a mouse monoclonal anti-HBx antibody (Abcam plc.) (Figure 3.8).

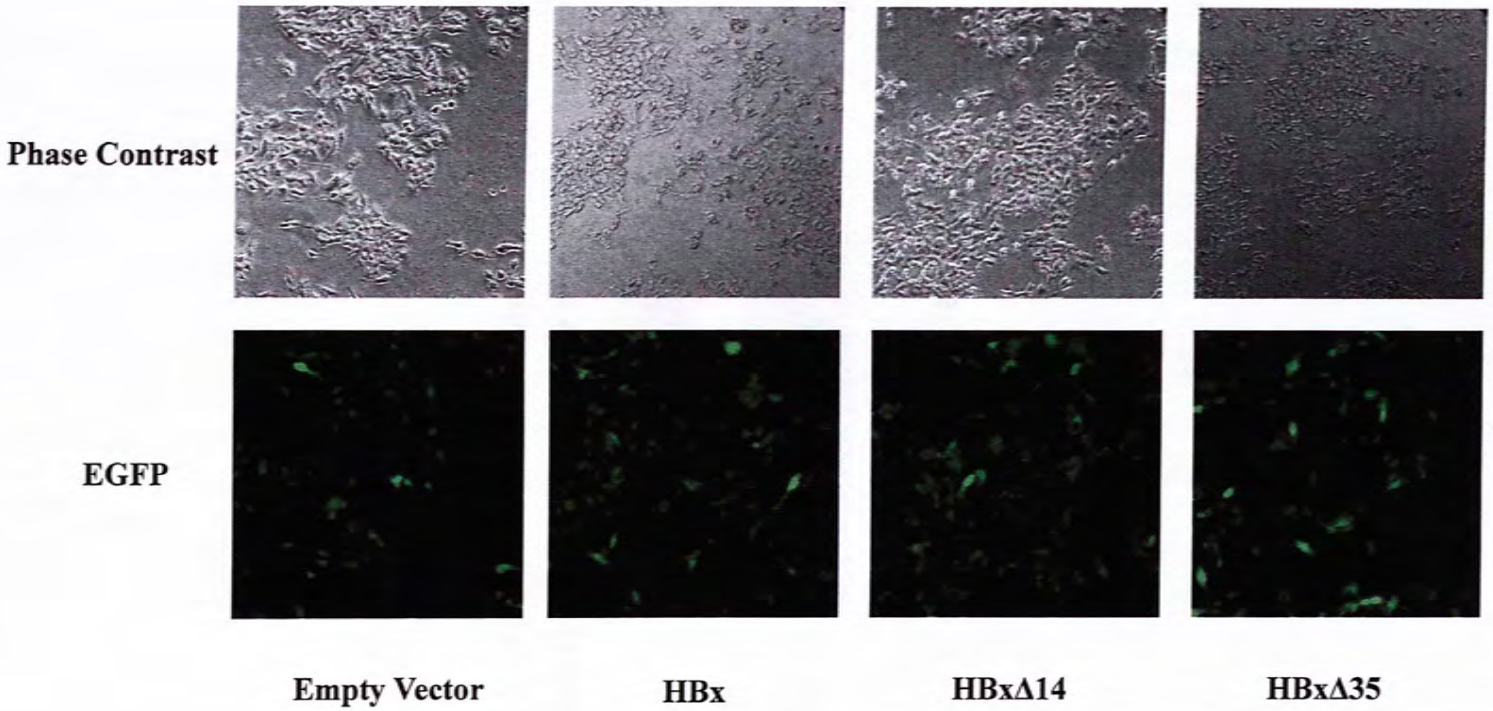

Figure 3.7 Microscopic examination of MIHA cell line infected by lentivirus

A non-tumorigenic hepatocyte cell line, MIHA, was transduced by various HBx-expressing lentiviruses or mock-control virus. The transduction efficiency was estimated by the percentage of EGFP-positive cells under a fluorescent microscope. Photos were taken at day 3 post-infection.

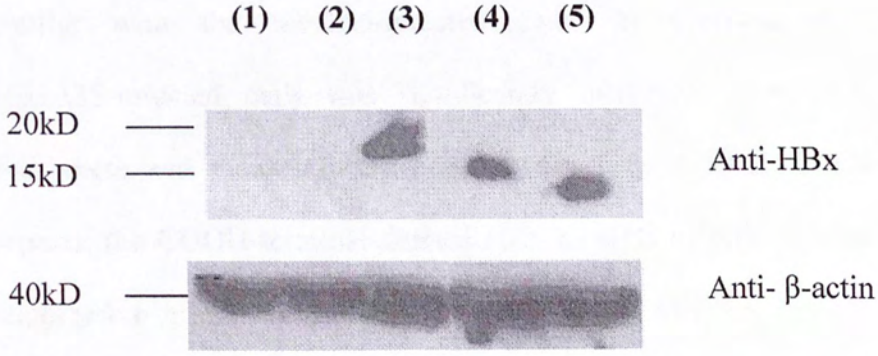

Figure 3.8 Western-blot of MIHA cell line transduced with various versions of HBx. (1) MIHA, (2) Empty vector, (3) Full-length HBx, (4) HBxΔ14 and (5) HBxΔ35.

3.4.3 Effect of Full-length and COOH-terminal Truncated HBx on Cell Proliferation

To investigate whether various forms of HBx affected cell growth, a colorimetric method was used to measure the viability of lentiviral-infected MIHA cells expressing HBx, HBxΔ14 and HBxΔ35, and mock-infected control for 5 consecutive days (Figure 3.9).

The growth of full-length HBx-infected cells was significantly decreased when compared with mock-infected cells ($p < 0.05$) on day 4 and remained slower on day 5. Throughout the period of investigation, the growth of HBxΔ14-infected cells was similar with the mocked-infected cells. In contrast, the proliferation of HBxΔ35-infected cells was significantly increased when compared with both full-length and mock-infected cells on day 5 ($p < 0.05$). Consistent to previous reports, the COOH-terminal deleted HBx mutants effectively abrogated the growth suppressive effect induced by full-length HBx, and the 35-aa deleted HBx even promoted cell proliferation.

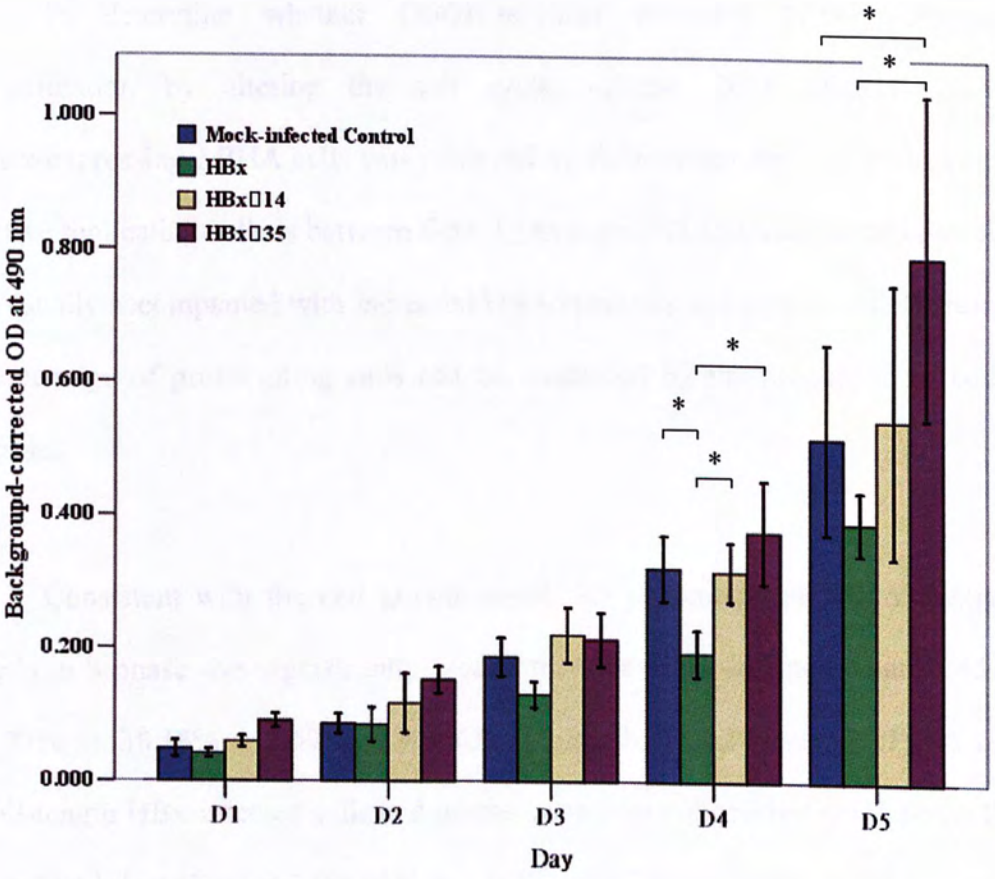

Figure 3.9 Cell viability of MIHA cells induced by various forms of HBx for 5 days. A background-corrected absorbance at 490 nm was shown. At least six replicates were included in each experiment. Results represented the mean and SD of 2 independent experiments. "*" indicated $p < 0.05$.

3.4.4 Effect of Full-length and COOH-terminal Truncated HBx on Cell Cycle

To determine whether COOH-terminal truncated HBx promoted cell proliferation by altering the cell cycle, cellular DNA content of various HBx-expressing MIHA cells was analyzed by flow cytometry. The DNA content of active replicating cells is between G0/G1 phase and G2/M phase, as cell proliferation is usually accompanied with increased DNA synthesis and replication. Therefore, the percentage of proliferating cells can be quantified by the proportion of cells in S phase.

Consistent with the cell growth result, the percentage of HBxΔ35-expressing cells in S phase was significantly greater than the mock-infected control (45.37% ± 2.77% vs 38.18% ± 2.69%, $p < 0.05$) (Figure 3.10 and Figure 3.11). In contrast, full-length HBx-infected cells had greater proportion of cell in G0/G1 phase than the mocked-infected control (58.01% ± 2.14% vs 44.73% ± 5.69%, $p < 0.05$), while the percentage of S phase cells was lower than its truncated mutants and the mock-infected control ($p < 0.05$). Overall, COOH-truncated HBx might stimulate cell growth by promoting cells to the S phase, whereas the full-length HBx might inhibit cell proliferation by causing G0/G1 arrest.

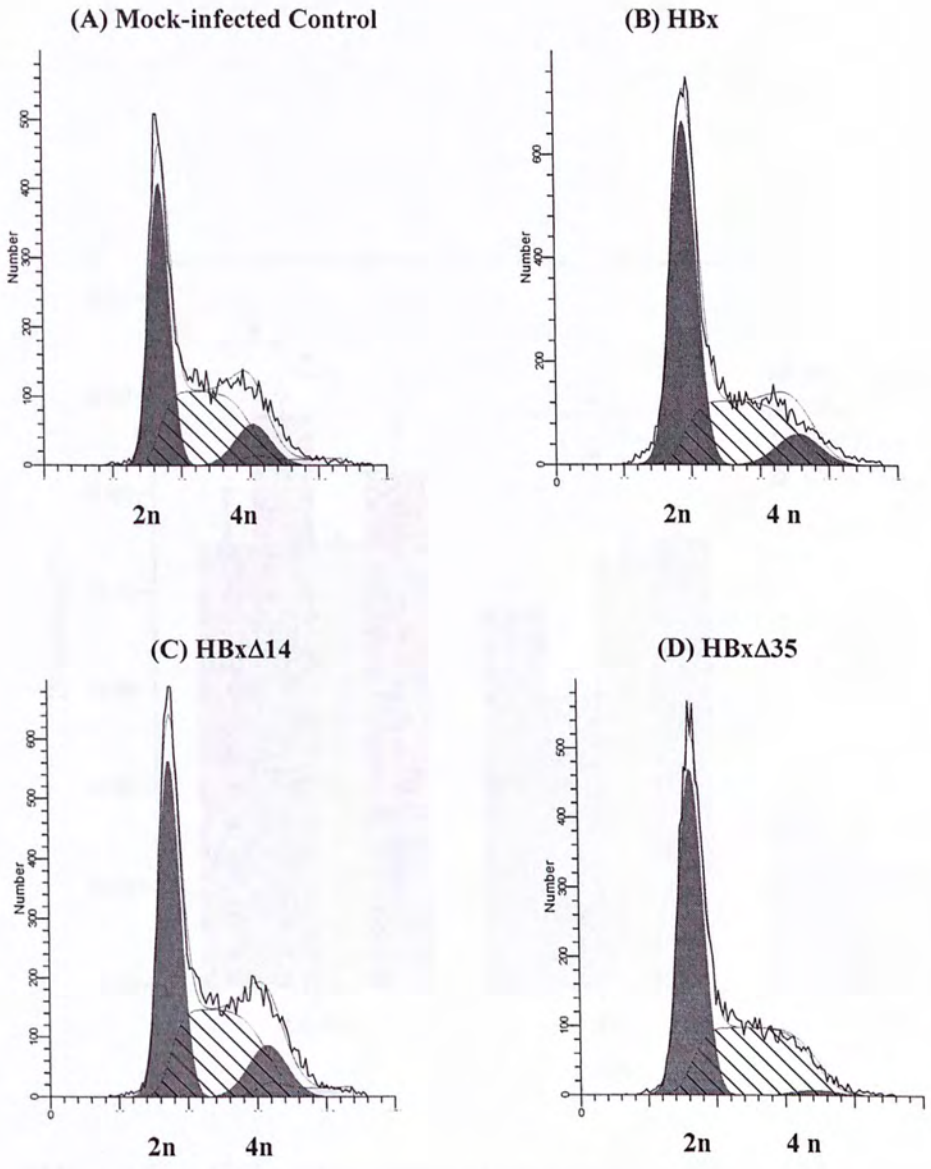

Figure 3.10 DNA histograms of various versions of HBx expressing MIHA. Shown here were the representative figures of a set of experiment. EGFP-positive cells were gated for analysis. The histogram modeling was performed by Modfit LT (Verity Software House). The G0/G1 phase and the G2/M phase were indicated by 2n and 4n respectively, whereas the S phase region was shaded. The proportion of cells in G0/G1 phase, S phase and G2/M phase were shown in Figure 3.9.

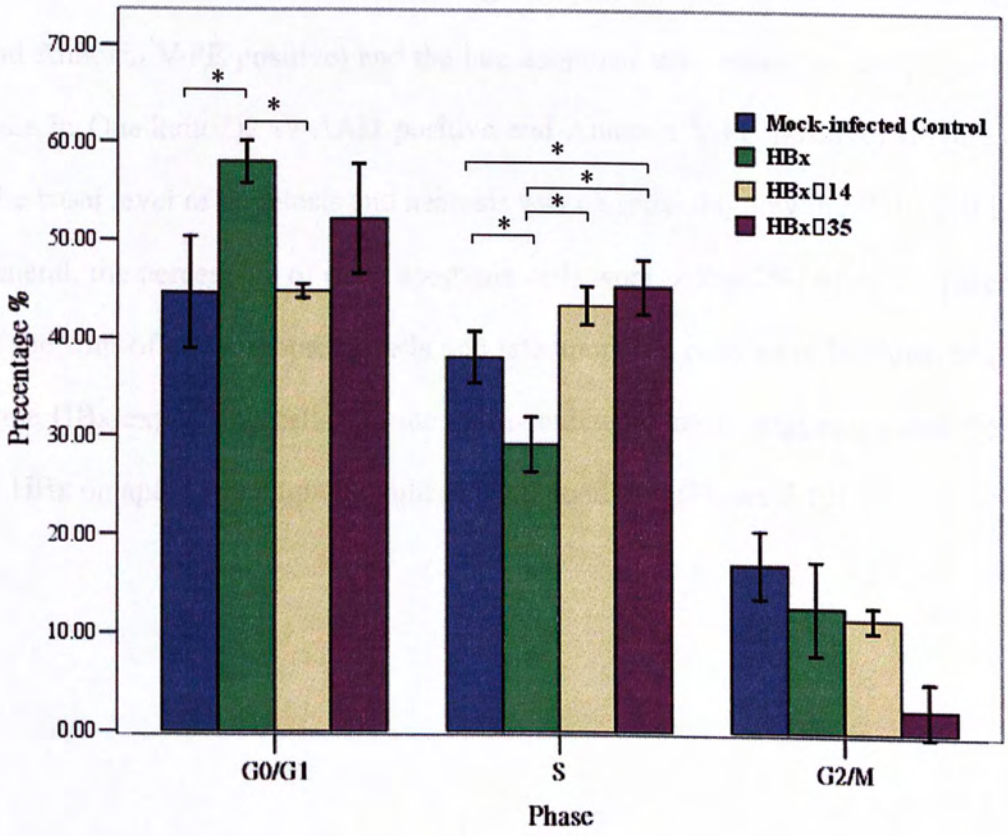

Figure 3.11 Cell cycle analysis of various HBx-infected MIHA cells. Shown here were the mean and SD of 3 independent experiments. "*" indicated $p < 0.05$.

3.4.5 Effect of Full-length HBx and COOH- terminal Truncated HBx on Apoptosis

To address whether various HBx-expressing cells promoted apoptotic cell death, flow cytometry was employed to detect apoptosis using Annexin V assay. The early apoptosis was defined as the percentage of cells in Quadrant Q4 (7-AAD negative and Annexin V-PE positive) and the late apoptosis was defined as the percentage of cells in Quadrant Q2 (7-AAD positive and Annexin V-PE positive) (Figure 4.12). The basal level of apoptosis and necrosis was considerably low in MIHA cell line. In general, the percentage of early apoptotic cells were below 2%, while the percentage of the sum of early apoptotic cells and late apoptotic cells were less than 5% in the three HBx-expressing cells and the mock-infected control, suggesting that the effect of HBx on apoptosis might be mild in basal condition (Figure 3.12).

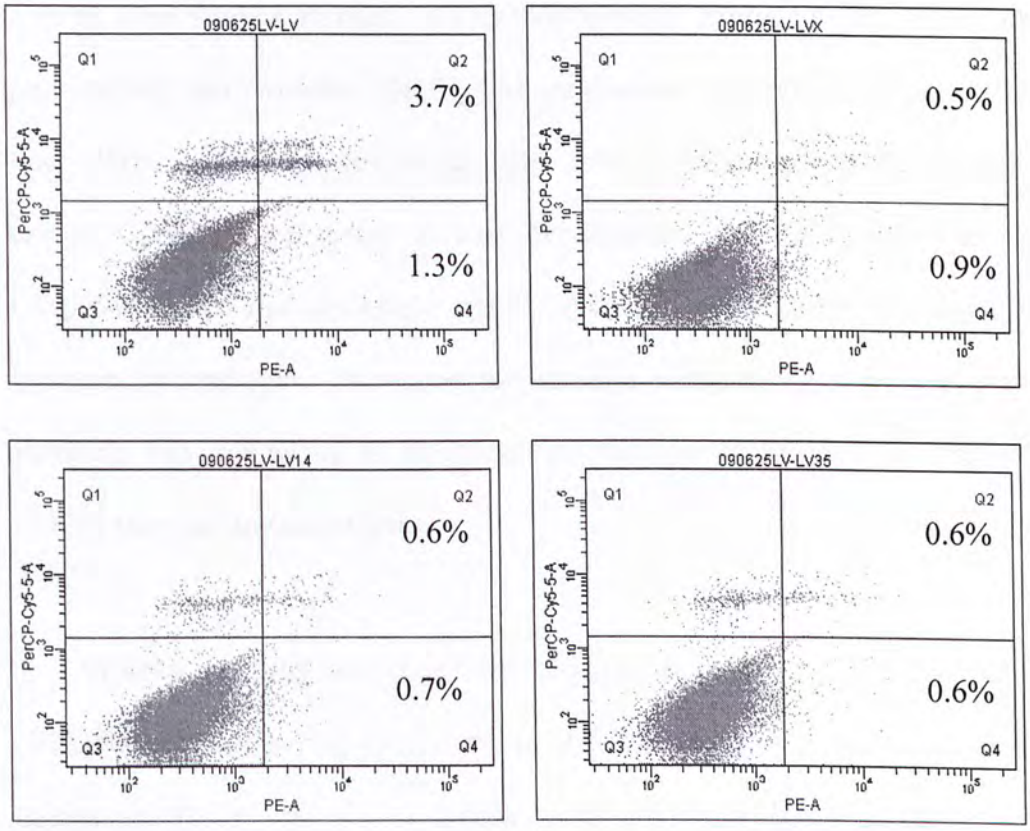

Figure 3.12 Assessment of eary stage apoptosis by Annexin V assay. Cell apoptosis was assayed using Annexin V by flow cytometry. An unstained control, a 7-AAD stained control and a Annexin V-PE stained control were set up to define quadrants corresponding to viable cells, apoptotic cells and necrotic cells. Quadrant Q2, late stage apoptotic cells or necrotic cells (7-AAD positive and PE-conjugated Annexin V positive); Quadrant Q3, viable cells (7-AAD negative and PE-conjugated Annexin V negative); Quadrant Q4, early apoptotic cells (7-AAD negative and PE-conjugated annexin V positive). EGFP-positive cells were gated for analysis of the percentage of apoptotic events.

3.5 MicroRNA Profiling of Various HBx-expressing Hepatocyte Cell Lines

3.5.1 Identification of Deregulated MicroRNAs by Microarray

In vitro studies showed that COOH-terminal truncated HBx stimulated cell proliferation and promoted the S phase progression of a non-tumorigenic liver cell line, MIHA. In contrast, full-length HBx- infected cells suppressed cell growth and caused G0/G1 phase arrest. It was hypothesized that full-length HBx and its COOH-truncated mutants might regulate different sets of genes, leading to distinct biological phenotypes. To address this issue, a comprehensive miRNA microarray profiling was conducted to compare the miRNAs deregulated by full-length or COOH-terminal truncated HBx.

MiRNA profiling was conducted using an Agilent human miRNA microarray (V2) platform, containing feature probes of 723 human and 76 viral miRNAs (Sanger database v. 10.1). Total RNA extracted from full-length HBx and HBxΔ35- infected MIHA cells were taken for the microarray profiling, and the profiles were compared with the mock-infected control. GeneSpring software (Agilent Technology Ltd.) was used to extract, normalize and analyze the microarray data. A list of miRNAs deregulated by full-length HBx and HBxΔ35 was shown in Table 3.5.

A total of 23 miRNAs were identified to be altered by full-length HBx and/ or HBxΔ35 by at least 2-fold. Fifteen miRNAs were up-regulated by full-length HBx while 5 miRNAs were down-regulated. For HBxΔ35- induced miRNAs, 1 miRNA was up-regulated while 5 miRNAs were down-regulated. MiR-19a and miR-19b were down-regulated while miR-23a was up-regulated by 2-fold or above by both

forms of HBx. These commonly deregulated miRNAs might be essential mediators of the functions of HBx.

In order to identify the essential miRNAs that contributed to distinct biological phenotypes of the full-length and COOH-terminal truncated HBx, we put our emphasis on miRNAs that differentially expressed between full-length HBx and truncated HBx- infected cells. As no miRNAs was differentially expressed in full-length HBx and HBxΔ35- expressing cells by more than 2-fold, the filtering stringency was reduced to 1.5-fold. A total of 6 miRNAs were identified to be up-regulated by HBx but down-regulated by HBxΔ35 (Table 3.6).

Table 3.5 A list of miRNAs deregulated by full-length HBx and HBxΔ35. The fold change was compared to the mocked-infected control. Cutoff: fold change ≥ 2 or ≤0.5.

MicroRNA	Fold Change	
	HBx/Vector	HBxΔ35/Vector
hsa-miR-122	3.47	1.47
hsa-miR-365	3.13	0.71
hsa-miR-125a-5p	2.65	1.16
hsa-miR-193b	2.63	0.63
hsa-let-7e	2.36	1.16
hsa-miR-23a	2.33	2.07
hsa-miR-222	2.27	1.06
hsa-miR-27a	2.25	1.84
hsa-miR-923	2.23	1.37
hsa-miR-99b	2.23	1.18
hsa-miR-768-3p	2.21	0.83
hsa-miR-23b	2.12	0.94
hsa-miR-186	2.11	0.75
hsa-miR-34b*	2.06	0.78
hsa-miR-29b-1*	2.01	1.5
hsa-miR-210	1.98	0.25
hsa-miR-30e	1.07	0.44
hsa-miR-301a	0.7	0.46
hsa-miR-18a	0.47	0.73
hsa-miR-7-1*	0.45	1.04
hsa-miR-19a	0.4	0.36
hsa-miR-19b	0.4	0.48
hsa-miR-19b-1*	0.17	0.71

Table 3.6 A list of miRNAs differentially expressed between full-length HBx and HBxΔ35 cells. The fold change was compared to the mocked-infected control. Cutoff: fold change ≥ 1.5 or ≤0.67.

	Fold Change		
MicroRNA	**HBx/Vector**	**HBxΔ35/Vector**	**HBxΔ35/HBx**
hsa-miR-146a	1.86	0.65	0.35
hsa-miR-210	1.98	0.25	0.13
hsa-miR-26a	1.63	0.67	0.41
hsa-miR-26b	1.55	0.62	0.40
hsa-miR-30d	1.86	0.64	0.34
hsa-miR-574-3p	1.63	0.56	0.34

3.5.2 Validation of Deregulated MiRNAs by Real-time PCR Analysis

The microarray results were further validated by real-time PCR using TaqMan MicroRNA Assays. Eleven miRNAs were chosen for validation based on different expression patterns between full-length and truncated HBx- infected cells: (A) 6 miRNAs with the same expression trend (miR-23a, miR-27a, miR-125a-5p and miR-99b were up-regulated by either full-length or COOH-terminal truncated HBx by at least two-fold; miR-19a and miR-19b were down-regulated by either full-length and COOH-terminal truncated HBx by at least two-fold); (B) 3 miRNAs with differential expression patterns, up-regulated by full-length HBx but down-regulated by COOH-terminal truncated HBx; (C) one miRNA undetectable by microarray (miR-190) and one was randomly chosen (miR-29c).

Our validation study showed that the real-time PCR were consistent with the microarray results in 7 out of 10 miRNAs (70%) (Figure 3.13). This included the 6 group A miRNAs, which had similar expression pattern between full-length HBx and truncated HBx, and 2 group B miRNAs, which showed opposite expression pattern between the two forms of HBx. For the remaining miRNAs, miR-29c, miR-193b and miR-365, opposite expression patterns were detected by real-time-PCR and microarray in full-length HBx or HBxΔ35- expressing cells, but the degree of disparity was relatively low. Besides, the expression of miR-190, which could not be detected by microarray, was detected by real-time PCR. This data suggested that the detection sensitivity of real-time PCR might be higher than those of microarray. In general, the microarray results could be validated by the real-time PCR, supporting the accuracy of the data (Figure 3.13). These miRNAs might represent some of the regulators causing the different biological effects of the two forms of HBx.

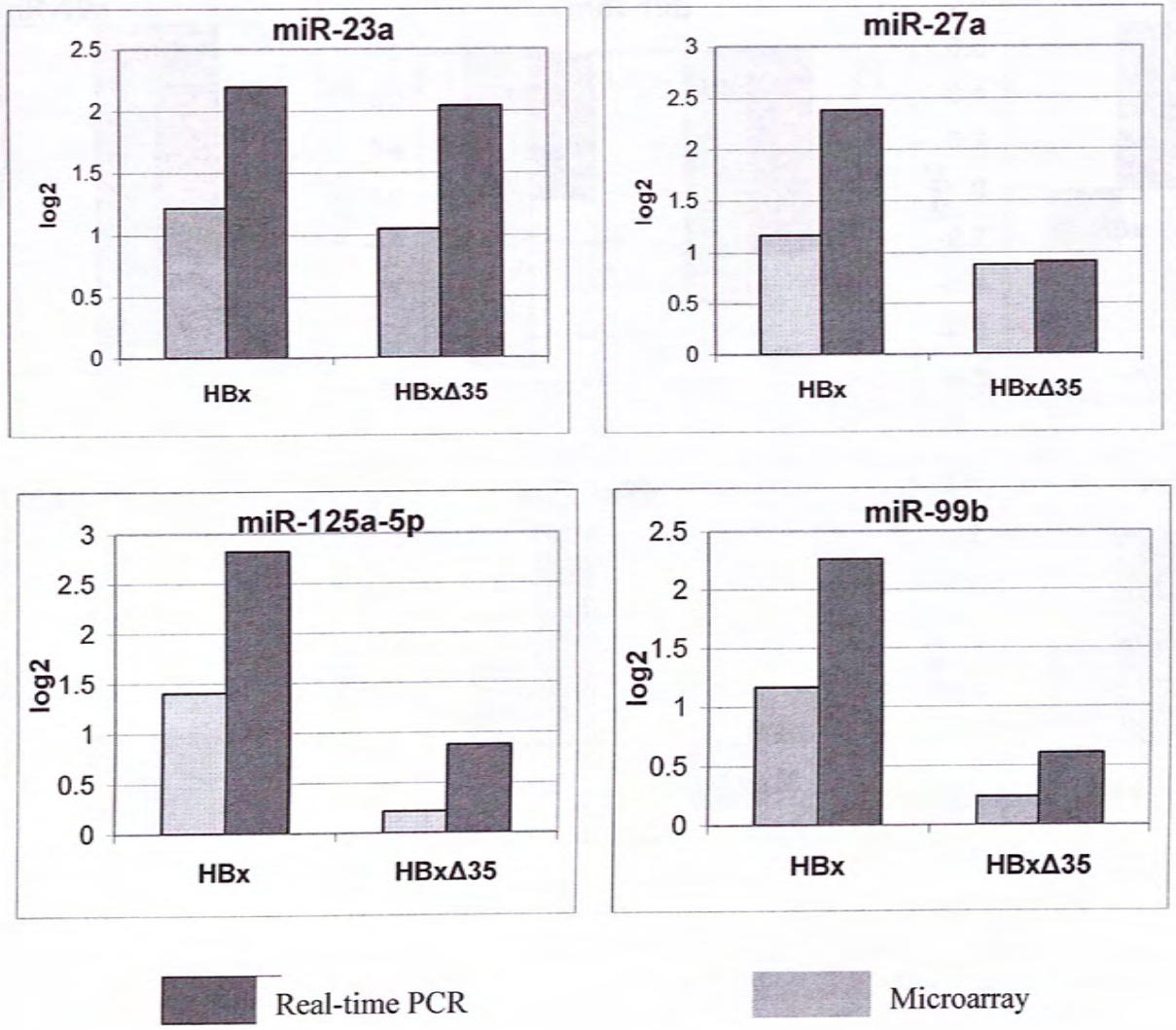
miR-23a
log2
2.5
2
1.5
1
0.5
0
HBx
HBxΔ35
miR-27a
log2
3
2.5
2
1.5
1
0.5
0
HBx
HBxΔ35
miR-125a-5p
log2
3
2.5
2
1.5
1
0.5
0
HBx
HBxΔ35
miR-99b
log2
2.5
2
1.5
1
0.5
0
HBx
HBxΔ35
Real-time PCR
Microarray

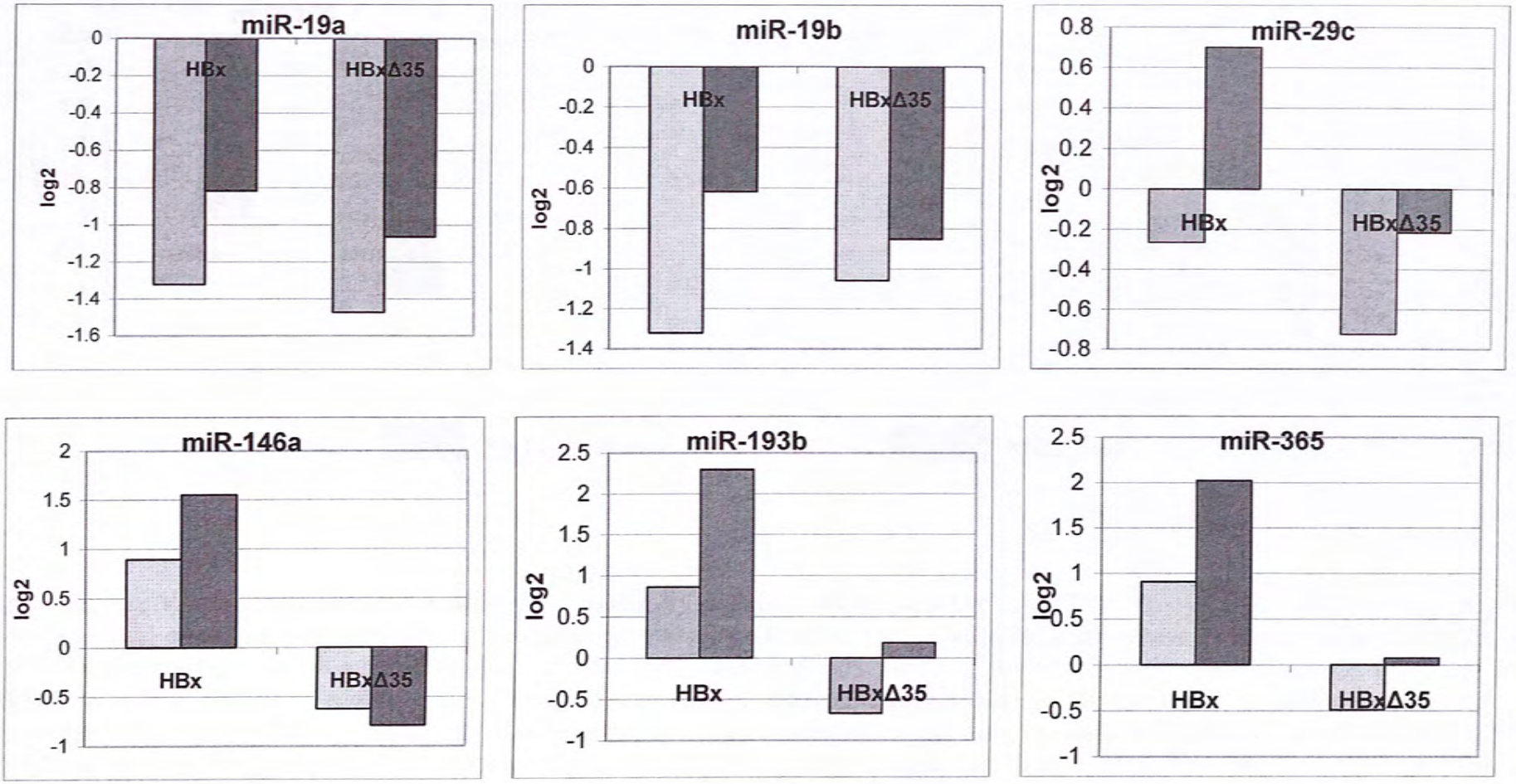
miR-19a
log2
0
-0.2
-0.4
-0.6
-0.8
-1
-1.2
-1.4
-1.6
HBx
HBxΔ35
miR-19b
log2
0
-0.2
-0.4
-0.6
-0.8
-1
-1.2
-1.4
HBx
HBxΔ35
miR-29c
log2
0.8
0.6
0.4
0.2
0
-0.2
-0.4
-0.6
-0.8
HBx
HBxΔ35
miR-146a
log2
2
1.5
1
0.5
0
-0.5
-1
HBx
HBxΔ35
miR-193b
log2
2.5
2
1.5
1
0.5
0
-0.5
-1
HBx
HBxΔ35
miR-365
log2
2.5
2
1.5
1
0.5
0
-0.5
-1
HBx
HBxΔ35
Real-time PCR
Microarray

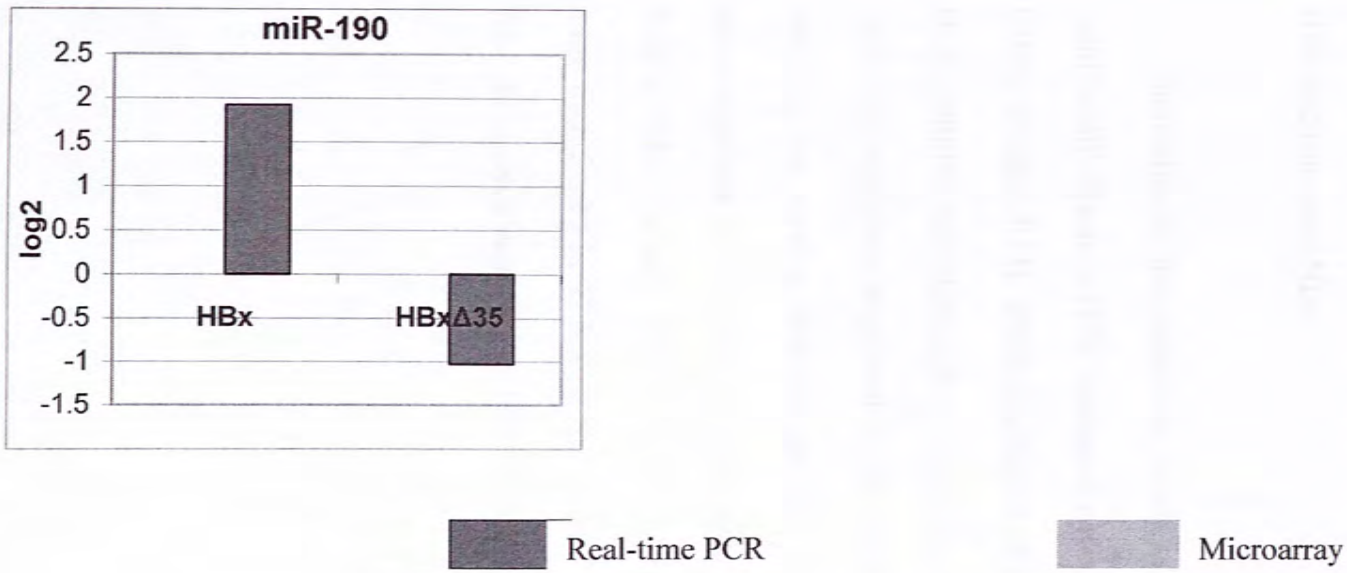

Figure 3.13 Validation of miRNA microarray results by real-time PCR. TaqMan MicroRNA Assays were used for validating the expression level of cellular miRNAs induced by full-length HBx and HBxΔ35. Eleven miRNAs were chosen for validation based on different expression patterns between full-length HBx and truncated HBx- expressed cells. Group A, similar expression pattern between full-length HBx and HBxΔ35 (down-regulation: miR-19a, miR-19b; up-regulation: miR-23a, miR-27a, miR-125a-5p and miR-99b); group B, different expression pattern (up-regulated by full-length HBx, but down-regulated by HBxΔ35, miR193b, miR-146a and miR-365); group C, an miRNA undetectable by microarray (miR-190) and miR-29c was randomly chosen.The Ct value was normalized with a small RNA molecule, RNU6B. The fold change was compared with the mock-infected control, and presented in log2 scale.

3.5.3 Confirmation of Deregulated MiRNAs in HCC and Adjacent Non-tumor Tissues

To test whether these deregulated miRNAs have functional relevance in human tumors, we measured their expression levels in 16 pairs of HCC and their matched adjacent non-tumor tissues. MiR-29c, miR-146a and miR-190 were selected for real-time PCR confirmation because they were differentially regulated by full-length HBx and truncated HBx.

Interestingly, the expression levels of miR-29c, miR-146a and miR-190 were significantly lower in HCC compared to the adjacent non-tumor tissues ($p < 0.001$ to 0.028) (Figure 3.14). Down-regulation of miR-146a was observed in 14 out of 16 HCC samples, and among the 14 samples, the median fold change was 0.36 ± 0.19. MiR-190 was down-regulated in 11 out of 16 HCC samples, and among the 11 samples, the median fold change was 0.29 ± 0.14. Furthermore, miR-29c was down-regulated in 12 out of 16 liver tumor samples and the median fold change was 0.40 ± 0.35. Overall, miR-29c, miR-146a and miR-190 were down-regulated by more than 2-fold in 37.5 – 62.5% of HCC samples, suggesting that these miRNAs were down-regulated by COOH-terminal truncated HBx of the HCC tissues.

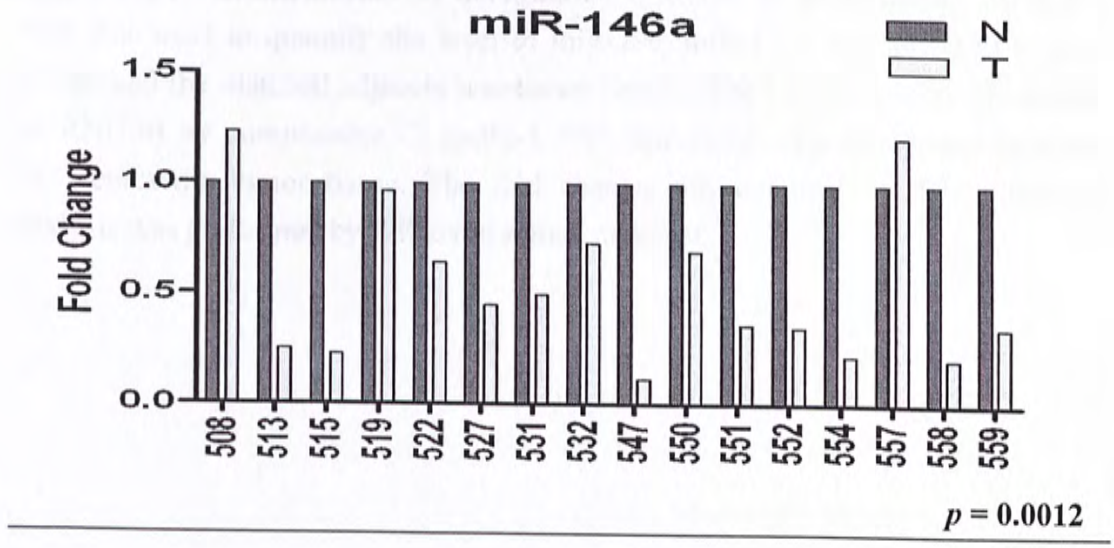

$p = 0.0012$

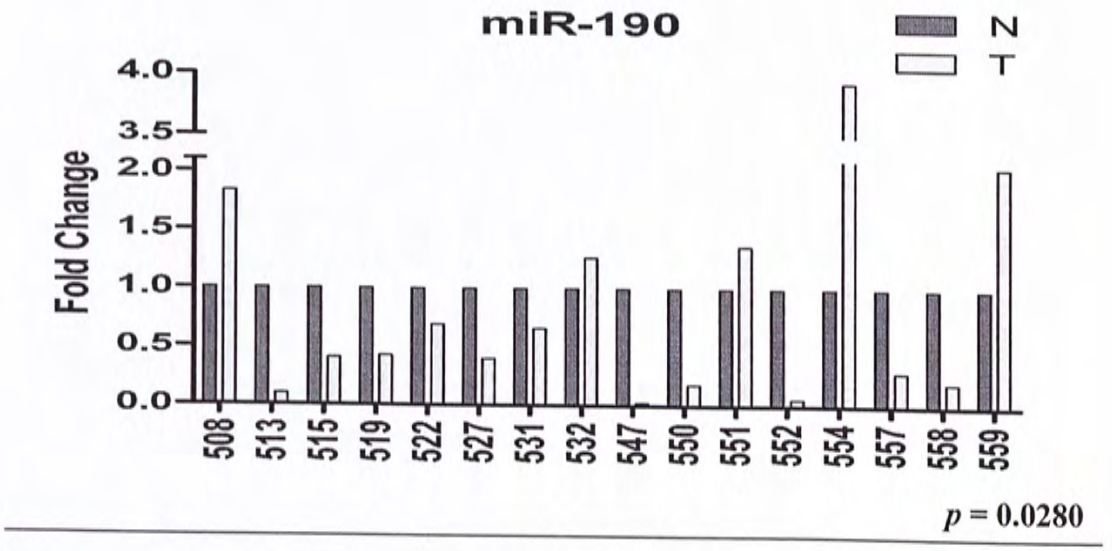

$p = 0.0280$

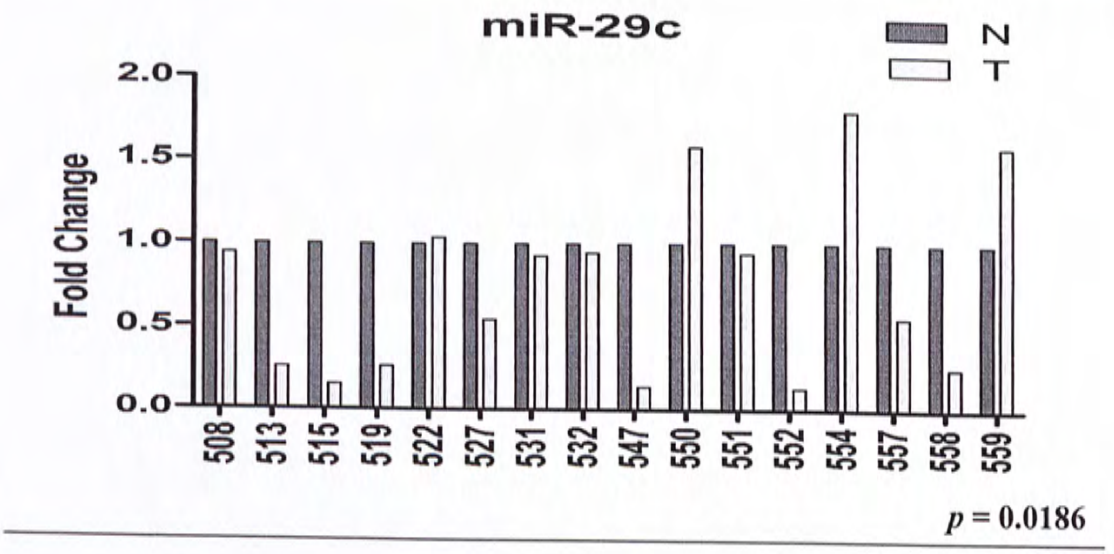

$p = 0.0186$

Figure 3.14 Confirmation of deregulated miRNAs in liver tissues. Real-time PCR was used to quantify the level of miR-29c, miR-146a and miR-190 in HCC tissues and the matched adjacent non-tumor tissues. The Ct values were normalized by RNU6B by comparative Ct method. "N" represents adjacent non-tumor tissue; "T" represents tumor tissue. The fold change was obtained by T/N. Statistical analysis was performed by Wilcoxon signed rank test.

3.5.4 Potential Downstream Targets of the HBx-deregulated MiRNAs

To further explore the possible downstream targets, we employed two miRNA target prediction algorithms, TargetScan http://www.targetscan.org/ (Lewis *et al.*, 2005) and PicTar http://pictar.mdc-berlin.de/ (Chen *et al.*, 2006). An overlapping feature shared by these two algorithms was constructed by miRGen http://www.diana.pcbi.upenn.edu/miRGen/v3/miRGen.html (Megraw *et al.*, 2006). Gene ontology of miR-146a was assisted by UniProt http://www.uniprot.org/. For miR-146a, we found that 157 target genes were predicted by TargetScan and 130 genes were predicted by PicTar. Among them, 34 genes are in common between the two algorithms and 4 of them are related to cell growth and cell cycle, including SMAD4, NF2, PSMD3 and EIF5A2 (Figure 3.15a). For miR-190, 128 target genes were predicted by TargetScan while 86 genes were predicted by PicTar, and 68 genes are in common (Figure 3.15b). Among the 68 genes in common, PTCH, CDKN1B and HECA are involved in cell proliferation and cell cycle. Besides, 729 and 602 target genes were predicted by PicTar and TargetScan respectively to be modulated by miR-29c (Figure 3.15c). A total of 448 predicted genes are shared by these two algorithms. Among them, 33 genes are taken part in cell proliferation and cell cycle, including CDK6, PTEN, CCND2, TGFB3, E2F7, etc.

Quite a large number of genes regulated by miR-29c, miR-146a and miR-190 were predicted to be involved in cell cycle and cell proliferation (Table 3.7). By validating the predicted miRNA targets, it might explain the distinct biological effects in full-length HBx and COOH-terminal-truncated HBx- expressing cells.

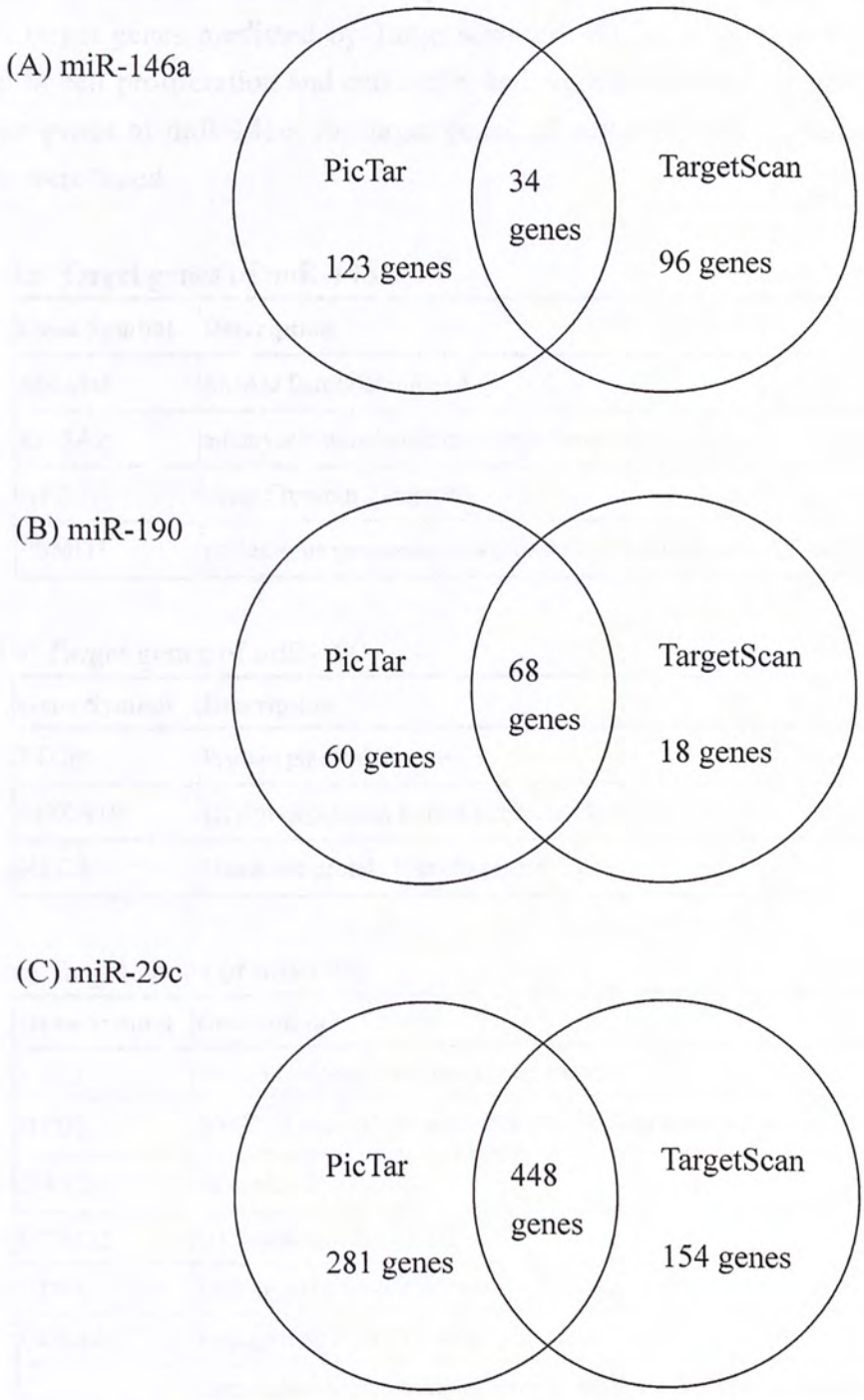

Figure 3.15 MiRNA targets predicted by PicTar and TargetScan. MiR-146a, miR-190 and miR-29c were taken for miRNA target prediction using 2 different algorithms. An intersection of these two pools of genes was identified by miRGen. Cell cycle and cell proliferation related genes were identified by gene ontology.

Table 3.7 Genes involved in cell proliferation and cell cycle. Among the common target genes predicted by TargetScan and PicTar, a number of them were involved in cell proliferation and cell cycle, and were determined by gene ontology. (a) Target genes of miR-146a; (b) target genes of miR-190; and (c) target genes of miR-29c were listed.

(a) Target genes of miR-146a

Gene Symbol	Description
SMAD4	SMAD family member 4
EIF5A2	eukaryotic translation initiation factor 5A2
NF2	neurofibromin 2 (merlin)
PSMD3	proteasome (prosome, macropain) 26S subunit, non-ATPase, 3

(b) Target genes of miR-190

Gene Symbol	Description
PTCH	Protein patched homolog 1
CDKN1B	Cyclin-dependent kinase inhibitor 1B
HECA	Headcase protein homolog (hHDC)

(c) Target genes of miR-29c

Gene Symbol	Description
ABL1	Proto-oncogene tyrosine-protein kinase
BTG2	BTG2 protein (NGF-inducible anti-proliferative protein PC3)
CAV2	Caveolin-2.
CCND2	G1/S-specific cyclin-D2
CDK6	Cell division protein kinase 6
COL4A3	Collagen alpha-3(IV) chain precursor
CTNNBIP1	Beta-catenin-interacting protein 1 (Inhibitor of beta-catenin and Tcf- 4)
DBC1	Protein FAM5A precursor
E2F7	E2F transcription factor 7
EMP1	Epithelial membrane protein 1
FGA	Fibrinogen alpha chain precursor
GAB1	GRB2-associated-binding protein 1
GAS7	Growth-arrest-specific protein 7

HBP1	HMG box-containing protein 1
HDAC4	Histone deacetylase 4
INSIG1	Insulin-induced gene 1 protein
KLF4	Krueppel-like factor 4
LAMC1	Laminin gamma-1 chain precursor
MAP2K6	Dual specificity mitogen-activated protein kinase kinase 6
MLLT7	Fork head domain transcription factor
MXI1	MAX-interacting protein 1
MYBL2	Myb-related protein B
PCTK1	Serine/threonine-protein kinase
PDGFB	Platelet-derived growth factor B chain precursor
PDGFC	platelet-derived growth factor C precursor
PMP22	Peripheral myelin protein 22
PPM1D	Protein phosphatase 2C isoform delta
PPP1R13B	Apoptosis-stimulating of p53 protein 1 (Protein phosphatase 1 regulatory subunit 13B)
PRKRA	Interferon-inducible double stranded RNA-dependent protein kinase activator A
PTEN	Phosphatidylinositol-3,4,5-trisphosphate 3-phosphatase and dual-specificity protein phosphatase PTEN
PTP4A1	Protein tyrosine phosphatase type IVA protein 1
SMPD3	Sphingomyelin phosphodiesterase 3
TGFB3	Transforming growth factor beta-3 precursor

Chapter 4 DISCUSSION

4.1 The Impact of COOH-terminal Truncated HBx in HCC

Extensive research has been conducted on HCC, but the molecular mechanism is still poorly understood. One of the examples is the ambiguous role of full-length HBx on apoptosis. On one hand, full-length HBx was reported to induce apoptosis or sensitize cells to proapoptotic stimuli (Su *et al.*, 1997; Kim *et al.*, 1998; Bergametti *et al.*, 1999; Liang *et al.*, 2007). On the other hand, the X protein was found to prevent apoptosis or had no effect on apoptosis (Gottlob *et al.*, 1998; Kim *et al.*, 2001; Hodgson *et al.*, 2008; Cheng *et al.*, 2008). Besides, HBx-mediated apoptosis might depend on the balance between cellular c-Myc and members of the NFκB transcription factor family (Su *et al.*, 2001). Some researchers attempted to explain the growth suppressive effect of full-length HBx as a positive contributor to carcinogenesis. For instance, cell growth retarded by full-length HBx facilitated viral replication (Ozer *et al.*, 1996). Furthermore, full-length HBx could also inhibit DNA repair, enhancing its susceptibility to carcinogens (Prost *et al.*, 1998; Jia *et al.*, 1999).

In our study, HBx expression was examined in 20 pairs of HCC tissues and the matched adjacent non-tumor tissues by immunostaning. The immunostaining scores suggested that the expression of HBx, including full-length and various forms of truncated HBx mutants, was lower in HCC than in adjacent non-tumor tissues. This was consistent with the immunostaining results by another group of investigators (Wang *et al.*, 1991). It was found that HBV replication occurred only in adjacent non-tumor tissues but not in HCC tissues (Wang *et al.*, 1991). In contrast, integrated HBV was more frequently observed in HCC than in adjacent non-tumor tissues (Lai

et al., 1988). As a result, it was suggested that the HBx expression in HCC might be contributed mainly by the integrated HBV, which had much lower copy number than the free HBV form (Wang *et al.*, 1991). This finding may explain the low HBx expression in HCC than in adjacent non-tumor tissues.

Previous reports suggested that full-length HBx was strongly associated with HCC development, but its controversial effects on tumorigenesis, including growth retardation and apoptosis, causing one to doubt its role in HBV-related HCC (Unsal *et al*, 1994). Moreover, we detected the COOH-terminal truncated versions, instead of full-length HBx, in 50% of HCC specimens, implying that the truncated forms of HBx are more relevant in HBV-associated HCC. Our results confirmed that full-length and COOH-terminal truncated HBx demonstrated distinct biological effects on a non-tumorgenic liver cell line. While full-length HBx suppressed cell proliferation and induced G0/G1 arrest, COOH-terminal truncated HBx abrogated the growth suppressive effect induced by full-length HBx. A certain form of the truncated mutants stimulated cells proliferation and promoted S phase progression.

The difference in the biological phenotypes between full-length and COOH-terminal truncated HBx might be contributed by their subcellular localization in liver cells determined by immunofluoresence. One reported showed that full-length HBx was localized in the cytoplasm, whereas HBx mutants with 7-aa to 65-aa delected from the C-terminus were mainly localized in the nucleus (Bock *et al.*, 2008). As a result, the effect of COOH-terminal truncated HBx on the activation of certain signal transduction pathway, including Ras-Raf-MAPK, would be diminished (Doria *et al.*, 1995). In constrast, the transcriptional regulation mediated by truncated HBx might be enhanced due to its nuclear localization. These findings provided

biological insight into the mechanism of action of COOH-terminal truncated HBx. As a whole, COOH-terminal truncated HBx might play a direct role in HCC.

.

4.2 The Biological Significance of COOH-terminal Truncated HBx Induced MiRNAs

MiRNAs have been implicated in the development of various cancers, including liver, breast and lung cancer (Dalmay and Edwards, 2009). Certain tumor suppressor genes or oncogenes were deregulated by these small RNA molecules by post-transcriptional regulation. To better understand how miRNA mediates its effects on tumorigenesis, it is essential to find the downstream targets.

We found that certain miRNAs were deregulated in cells expressing COOH-terminal truncated HBx and in HCC specimens, including miR-29c, miR-146a and miR-190, but their roles in HCC are not currently understood. Individual reports suggested that down-regulation of miR-29 was strong associated with HCC and NPC (Su *et al.*, 2009; Sengupta *et al.*, 2008). As an antiproliferative and pro-apoptoic miRNA, it was confirmed to regulate the expression of a transcription factor, YY1 (Wang *et al.*, 2008a), a DNA methyltransferase, DMNT3A (Fabbri *et al.*, 2007), and apoptosis regulators, Mcl-1 (Mott *et al.*, 2007), CDC2 and p85 alpha (Park *et al.*, 2009). Deregulation of miR-29 might have a strong impact on gene regulation and cell survival.

MiR-146a played a role in the regulation of immune response by targeting TRAF6 and IRAK1 (Taganov *et al.*, 2006). The oncoproteins of EBV and HTLV-1 were found to stimulate the level of cellular miR-146a, possibly through activating NFκB (Motsch *et al.*, 2007; Cameron *et al.*, 2008; Pichler *et al.*, 2008). Interestingly, HBx could also activate NFκB to promote cell survival (Su *et al.*, 1996; Yun *et al.*, 2002; Um *et al.*, 2007). It might suggest a possible linkage between HBx, NFκB and

miR-146a in HBx-induced HCC. Though functional polymorphism of miR-146a was associated with HCC, its effect on hepatocarcinogenesis was not being investigated (Xu *et al.*, 2008). Evidences suggested that miR-146a might be implicated in cell proliferation and cancer metastasis. For instance, up-regulation of miR-146a was found to suppress breast cancer metastasis (Hurst *et al.*, 2009). In leukemia cell lines, miR-146a retarded cell proliferation by inhibiting CXCR4 expression (Labbaye *et al.*, 2008).

MiR-190 was a member of the miRNA signature that differentiated HBV-infected livers from HCV-infected livers in a large scale miRNA profiling study (Ura *et al.*, 2009). In addition, it was reported to be deregulated in HCC mice, but the current information on this miRNA was limited (Kutay *et al.*, 2006).

In addition to their biological impacts, there is increasing concern on the diagnostic and prognostic value of miRNAs. Being detected in the blood plasma or serum, miRNAs displayed a great potential as non-invasive biomarkers (Gilad *et al.*, 2008; Chen *et al.*, 2008). Compared to mRNA, these tiny RNA molecules remained stable in the plasma or serum samples upon repeated freeze-and-flaw cycles or RNase treatment (Mitchell *et al.*, 2008).

Plasma miR-184 levels were significantly higher in patients diagnosed with squamous cell carcinoma of tongue compared with normal individuals (Wong *et al.*, 2008b). In addition, quantification of plasma miR-92 levels allowed one to differentiate patients diagnosed with colorectal cancer from normal individuals with high sensitivity and specificity (Ng *et al.*, 2009). Besides, circulating miRNAs were associated with pregnancy or certain disease states, including drug-induced liver

injury (Chim *et al.*, 2008; Wang *et al.*, 2009a). These studies suggested that miRNA might be a potential diagnostic marker of various cancers or disease states.

In addition to its diagnostic potential, miRNA profiling of cancer patients was also displayed encouraging prognostic benefits. Prognosis and progression of patients with chronic lymphocytic leukemia could be inferred by simply a 13-miRNA signature (Calin *et al.*, 2005). The prognostic efficacy of miRNAs was also suggested in lung cancers (Yanaihara *et al.*, 2006), colon adenocarcinoma (Schetter *et al.*, 2008) and esophageal squamous cell carcinoma (Guo *et al.*, 2008)

MiRNA may also be a potential therapeutic target. This hypothesis had been testified by re-introducing miR-26a, a frequently downregulated miRNA in liver tumor tissues, into HCC transgenic mice induced by myc oncoprotein using Adeno-associated virus AAV infection (Kota *et al.*, 2009). The apoptotic evenets mediated by miR-26a was observed in cancer cells, but not in nonmalignant heaptocytes. The tumor-selectivity demonstrated in this study strengthened our belief that miRNA might be a potential therapeutic option in cancer treatment.

4.3 Limitations of the Present Study

Detection of COOH-terminal truncated HBx was carried out by PCR amplification using 5 sets of primers. The results were interpreted by the presence or absence of PCR bands after gel electrophoresis. In this way, we could not quantify the amount of truncated HBx or even determine the exact truncation sites of HBx in tissues. By using this qualitative approach, the discriminating power was satisfactory when the form of HBx in clinical samples was homogenous. However, it might fail to detect truncated variants of HBx in tissue specimens when full-length HBx co-existed, leading to false-negative results.

This situation might be improved by immunohistochemical staining of liver sections using two different anti-HBx antibodies, one targeting on the N-terminal domain or the central region of HBx protein, and the other recognizing the C-terminal domain (Ma *et al.*, 2008). The present of truncated HBx might be justified by the staining pattern by the two antibodies. However, the COOH-targeting anti-HBx antibody is not commercially available and a time-consuming immunizing procedure is needed.

Nevertheless, the sensitivity of PCR and immunohistochemical staining is still a limiting factor for detecting the minority population of HBx mutants. To enhance the detection limit, a high-throughput massive-parallel sequencing technology, pyrosequencing, can be employed (Thomas *et al.*, 2006). By this technology, the presence of truncated HBx and the sites of truncation could be accurately determined and quantified in tissue specimens.

4.4 Future Studies

To better understand the molecular mechanism of HBV-related HCC, the differential miRNA expression induced by full-length HBx and COOH-terminal truncated HBx should be further studied. Investigation can be carried out to elucidate the upstream pathway that deregulated HBx-induced miRNA expression, and the downstream biological effects of the HBx-induced miRNAs. To characterize the biological significance of these miRNAs, proliferation assay or cell cycle analysis will be investigated. Over-expression of miRNAs in cells expressing COOH-terminal truncated HBx will be performed to restore the biological effects. In addition, downstream targets of the altered miRNAs may be identified by utilizing the gene expression microarray and the existing miRNA target prediction programs. The potential targets will be further confirmed by luciferase reporter assays and western blot analysis. By further our study, we may better understand the mechanism of HBx-induced HCC.

Chapter 5 CONCLUSION

COOH-terminal truncated HBx was detected and expressed in at least 50 % of HCC tissues, but not in the adjacent nontumor tissues. Distinct biological effects were observed in the two forms of HBx. For instance, COOH-terminal truncated HBx (HBxΔ35) stimulated cell proliferation possibly by promoting S phase progression, whereas full-length HBx inhibited cell growth via G0/G1 arrest. Furthermore, miRNA profiles showed that cells infected by HBx and HBxΔ35 showed differential expression of some miRNAs. Concordantly, miR-29c, miR146a and miR-190 were down-regulated in HCC tissues compared to the adjacent tissues, suggesting that these miRNAs might be implicated in HBV-related HCC.

In conclusion, our findings demonstrated the importance of COOH-terminal truncated HBx in HCC and explored the possible linkage between miRNAs and COOH-terminal truncated HBx- induced hepatocarcinogenesis. By understanding the biological effects and the downstream targets of the deregulated miRNAs, the mechanism of HBV-induced HCC will be more thoroughly dissected.

REFERENCES

Alter HJ, Purcell RH, Gerin JL, et al. (1977). Transmission of hepatitis B to chimpanzees by hepatitis B surface antigen-positive saliva and semen. Infect Immun. 16:928–33.

Araki K, Akagi K, Miyazaki J, Matsubara K, Yamamura K. (1990) Correlation of Tissue-specific Methylation with Gene Inactivity in Hepatitis B Virus Transgenic Mice. Jpn J Cancer Res. 81(12):1265-71

Arase Y, Ikeda K, Suzuki F, Suzuki Y, Saitoh S, Kobayashi M, Akuta N, Someya T, Hosaka T, Sezaki H, Kobayashi M, Kumada H. (2006). Long-term outcome after hepatitis B surface antigen seroclearance in patients with chronic hepatitis B. Am J Med. 71.e9-16.

Bancroft WH, Snitbhan R, Scott RM, et al. (1977). Transmission of hepatitis B virus to gibbons by exposure to human saliva containing hepatitis B surface antigen. J Infect Dis. 135:79–85.

Barry SC, Harder B, Brzezinski M, Flint LY, Seppen J, Osborne WR. (2001). Lentivirus vectors encoding both central polypurine tract and posttranscriptional regulatory element provide enhanced transduction and transgene expression. Hum Gene Ther. 12(9):1103-8.

Bartel DP. (2004). MicroRNAs: genomics, biogenesis, mechanism, and function. Cell. 116(2):281-97.

Beasley RP, Hwang LY, Lin CC, Chien CS. (1981). Hepatocellular carcinoma and hepatitis B virus. A prospective study of 22 707 men in Taiwan. Lancet. ii:1129–1133.

Benn J, Schneider, RJ. (1994). The hepatitis B virus HBx protein activates Ras±GTP complex formation and establishes a Ras, Raf, MAP kinase signalling cascade. Proc Natl Acad Sci. 91:10350-4.

Benn J, Su F, Doria M, Schneider RJ. (1996). Hepatitis B virus HBx protein induces transcription factor AP-1 by activation of extracellular signal-regulated and c-Jun N-terminal mitogen-activated protein kinases. J Virol. 70(8):4978-85.

Bergametti F, Prigent S, Luber B, Benoit A, Tiollais P, Sarasin A, Transy C. (1999). The proapoptotic effect of hepatitis B virus HBx protein correlates with its transactivation activity in stably transfected cell lines. Oncogene. 18(18):2860-71.

Bock CT, Toan NL, Koeberlein B, Song le H, Chin R, Zentgraf H, Kandolf R, Torresi J. (2008). Subcellular mislocalization of mutant hepatitis B X proteins contributes to modulation of STAT/SOCS signaling in hepatocellular carcinoma. Intervirology. 51(6):432-43.

Bond WW, Favero MS, Petersen NJ, Gravelle CR, Ebert JW, Maynard JE. (2006). Survival of hepatitis B virus after drying and storage for one week. Lancet. 1(8219):550–1.

Borchert GM, Lanier W, Davidson BL. (2006) RNA polymerase III transcribes human microRNAs. Nat Struct Mol Biol. 13(12):1097-101.

Bouchard MJ, Wang L, Schneider RJ. (2006). Activation of focal adhesion kinase by hepatitis B virus HBx protein: multiple functions in viral replication. J Virol. 80(9):4406-14.

Bouchard MJ, Wang LH, Schneider RJ. (2001). Calcium signaling by HBx protein in hepatitis B virus DNA replication. Science. 294(5550):2376-8.

Brown JJ, Parashar B, Moshage H, Tanaka KE, Engelhardt D, Rabbani E, Roy-Chowdhury N, Roy-Chowdhury J. (2000). A long-term hepatitis B viremia model generated by transplanting nontumorigenic immortalized human hepatocytes in Rag-2-deficient mice. Hepatology. 31(1):173-81.

Budhu A, Jia HL, Forgues M, Liu CG, Goldstein D, Lam A, Zanetti KA, Ye QH, Qin LX, Croce CM, Tang ZY, Wang XW. (2008). Identification of metastasis-related microRNAs in hepatocellular carcinoma. Hepatology. 47(3):897-907.

Bugianesi E, Leone N, Vanni E, Marchesini G, Brunello F, Carucci P, Musso A, De Paolis P, Capussotti L, Salizzoni M, Rizzetto M. (2002). Expanding the natural history of nonalcoholic steatohepatitis: from cryptogenic cirrhosis to hepatocellular carcinoma. Gastroenterology. 123(1):134-40.

Calin GA, Ferracin M, Cimmino A, Di Leva G, Shimizu M, Wojcik SE, Iorio MV, Visone R, Sever NI, Fabbri M, Iuliano R, Palumbo T, Pichiorrri F, Roldo C, Garzon

R, Sevignani C, Rassenti L, Alder H, Volinia S, Liu CG, Kipps TJ, Negrini M, Croce CM. (2005). A MicroRNA signature associated with prognosis and progression in chronic lymphocytic leukemia. N Engl J Med. 353(17):1793-801.

Cameron JE, Yin Q, Fewell C, Lacey M, McBride J, Wang X, Lin Z, Schaefer BC, Flemington EK. (2008). Epstein-Barr virus latent membrane protein 1 induces cellular MicroRNA miR-146a, a modulator of lymphocyte signaling pathways. J Virol. 82(4):1946-58.

Centers for Disease Control and Prevention (CDC):A comprehensive immunization strategy to eliminate transmission of hepatitis B virus infection in the UnitedStates: recommendations of the Advisory Committee onImmunization Practices (ACIP); part 2: immunization of adults. MMWR Morb Mortal Wkly Rep 2005, 55:1–33.

Chan HL, Hui AY, Wong ML, Tse AM, Hung LC, Wong VW, Sung JJ. (2004). Genotype C hepatitis B virus infection is associated with an increased risk of hepatocellular carcinoma. Gut. 53(10):1494-8.

Chan HL, Tse CH, Mo F, Koh J, Wong VW, Wong GL, Lam Chan S, Yeo W, Sung JJ, Mok TS. (2008). High viral load and hepatitis B virus subgenotype ce are associated with increased risk of hepatocellular carcinoma. J Clin Oncol. 26(2):177-82.

Chan HL, Tsui SK, Tse CH, Ng EY, Au TC, Yuen L, Bartholomeusz A, Leung KS, Lee KH, Locarnini S, Sung JJ. (2005). Epidemiological and virological characteristics of 2 subgroups of hepatitis B virus genotype C. J Infect Dis. 191(12):2022-32.

Chang C, Enders G, Sprengel R, Peters N, Varmus HE, Ganem D. (1987). Expression of the precore region of an avian hepatitis B virus is not required for viral replication. J Virol. 61:3322-3325.

Chang TT, Gish RG, de Man R, Gadano A, Sollano J, Chao YC, Lok AS, Han KH, Goodman Z, Zhu J, Cross A, DeHertogh D, Wilber R, Colonno R, Apelian D. (2006). BEHoLD AI463022 Study Group..A comparison of entecavir and lamivudine for HBeAg-positive chronic hepatitisB. N Engl J Med. 354:1001-10.

Chen K, Rajewsky N. (2006). Natural selection on human microRNA binding sites inferred from SNP data. Nat Genet. 38(12):1452-6

Chen MT, Billaud JN, Sällberg M, Guidotti LG, Chisari FV, Jones J, Hughes J, Milich DR. (2004). A function of the hepatitis B virus precore protein is to regulate the immune response to the core antigen. Proc Natl Acad Sci. 101(41):14913-8.

Chen X, Ba Y, Ma L, Cai X, Yin Y, Wang K, Guo J, Zhang Y, Chen J, Guo X, Li Q, Li X, Wang W, Zhang Y, Wang J, Jiang X, Xiang Y, Xu C, Zheng P, Zhang J, Li R, Zhang H, Shang X, Gong T, Ning G, Wang J, Zen K, Zhang J, Zhang CY. (2008). Characterization of microRNAs in serum: a novel class of biomarkers for diagnosis of cancer and other diseases. Cell Res. 18(10):997-1006.

Chen Y, Lin MC, Yao H, Wang H, Zhang AQ, Yu J, Hui CK, Lau GK, He ML, Sung J, Kung HF. (2007). Lentivirus-mediated RNA interference targeting enhancer of zeste homolog 2 inhibits hepatocellular carcinoma growth through down-regulation of stathmin. Hepatology. 46(1):200-8.

Cheng AS, Jin VX, Fan M, Smith LT, Liyanarachchi S, Yan PS, Leu YW, Chan MW, Plass C, Nephew KP, Davuluri RV, Huang TH. (2006). Combinatorial analysis of transcription factor partners reveals recruitment of c-MYC to estrogen receptor-alpha responsive promoters. Mol Cell. 21(3):393-404.

Cheng AS, Yu J, Lai PB, Chan HL, Sung JJ. (2008). COX-2 mediates hepatitis B virus X protein abrogation of p53-induced apoptosis. Biochem Biophys Res Commun. 374(2):175-80

Cheong JH, Yi M, Lin Y, Murakami S. (1995). Human RPB5, a subunit shared by eukaryotic nuclear RNA polymerases, binds human hepatitis B virus X protein and may play a role in X transactivation EMBO J. 14(1):143-50.

Chim SS, Shing TK, Hung EC, Leung TY, Lau TK, Chiu RW, Lo YM. (2008). Detection and characterization of placental microRNAs in maternal plasma Clin Chem. 54(3):482-90.

Chu CJ, Hussain M, Lok AS. (2002). Hepatitis B virus genotype B is associated with earlier HBeAg seroconversion compared with hepatitis B virus genotype C. Gastroenterology. 122:1756-1762.

Chung TW, Lee YC, Kim CH. (2004). Hepatitis B viral HBx induces matrix metalloproteinase-9 gene expression through activation of ERK and PI-3K/AKT pathways: involvement of invasive potential. FASEB J. 18(10):1123-5.

Cougot D, Wu Y, Cairo S, Caramel J, Renard CA, Lévy L, Buendia MA, Neuveut C. (2007). The hepatitis B virus X protein functionally interacts with CREB-binding protein/p300 in the regulation of CREB-mediated transcription. J Biol Chem. 282(7):4277-87.

Dalmay T, Edwards DR. MicroRNAs and the hallmarks of cancer. Oncogene. 2006 Oct 9;25(46):6170-5

Diao J, Khine AA, Sarangi F, Hsu E, Iorio C, Tibbles LA, Woodgett JR, Penninger J, Richardson CD. (2001). X protein of hepatitis B virus inhibits Fas-mediated apoptosis and is associated with up-regulation of the SAPK/JNK pathway. J Biol Chem. 276(11):8328-40.

Dienstag JL, Schiff ER, Wright TL, Perrillo RP, Hann HW, Goodman Z, Crowther L, Condreay LD, Woessner M, Rubin M, Brown NA. (1999). Lamivudine as initial treatment for chronic hepatitis B in the United States. N Engl J Med. 341(17):1256-63.

Donato F, Tagger A, Gelatti U, Parrinello G, Boffetta P, Albertini A, Decarli A, Trevisi P, Ribero ML, Martelli C, Porru S, Nardi G. (2002) Alcohol and hepatocellular carcinoma: the effect of lifetime intake and hepatitis virus infections in men and women. Am J Epidemiol. 155(4):323-31.

Doria M, Klein N, Lucito R, Schneider RJ. (1995). The hepatitis B virus HBx protein is a dual specificity cytoplasmic activator of Ras and nuclear activator of transcription factors. EMBO J. 14(19):4747-57.

Du J, Yang S, An D, Hu F, Yuan W, Zhai C, Zhu T. (2009). BMP-6 inhibits microRNA-21 expression in breast cancer through repressing deltaEF1 and AP-1. Cell Res. 19(4):487-96.

Fabbri M, Garzon R, Cimmino A, Liu Z, Zanesi N, Callegari E, Liu S, Alder H, Costinean S, Fernandez-Cymering C, Volinia S, Guler G, Morrison CD, Chan KK, Marcucci G, Calin GA, Huebner K, Croce CM. (2007). MicroRNA-29 family reverts aberrant methylation in lung cancer by targeting DNA methyltransferases 3A and 3B. Proc Natl Acad Sci USA. 104(40):15805-10.

Fan ST. (1999). Hepatectomy for hepatocellular carcinoma The surgeon's role in

long-term survival. Arch Surg. 134:1124-30.

Fasanaro P, D'Alessandra Y, Di Stefano V, Melchionna R, Romani S, Pompilio G, Capogrossi MC, Martelli F. (2008). MicroRNA-210 modulates endothelial cell response to hypoxia and inhibits the receptor tyrosine kinase ligand Ephrin-A3. J Biol Chem. 283(23):15878-83.

Felsenstein, J. (2009). PHYLIP (Phylogeny Inference Package) version 3.68. Distributed by the author. Department of Genetics, University of Washington, Seattle.

Fernette CT, Gish RG.. (2009). The new epidemiology of hepatitis B in the United States, Current Hepatitis Report. 8:3-9.

Fisicaro P, Valdatta C, Boni C, Massari M, Mori C, Zerbini A, Orlandini A, Sacchelli L, Missale G, Ferrari C. (2009). Early kinetics of innate and adaptive immune responses during hepatitis B virus infection. Gut. 58(7): 974 - 982.

Forman JJ, Legesse-Miller A, Coller HA. (2008). A search for conserved sequences in coding regions reveals that the let-7 microRNA targets Dicer within its coding sequence. Proc Natl Acad Sci USA. 105(39):14879-84.

Fornari F, Gramantieri L, Ferracin M, Veronese A, Sabbioni S, Calin GA, Grazi GL, Giovannini C, Croce CM, Bolondi L, Negrini M. (2008). MiR-221 controls CDKN1C/p57 and CDKN1B/p27 expression in human hepatocellular carcinoma. Oncogene. 27(43):5651-61.

Fujita S, Ito T, Mizutani T, Minoguchi S, Yamamichi N, Sakurai K, Iba H. (2008). miR-21 Gene expression triggered by AP-1 is sustained through a double-negative feedback mechanism. J Mol Biol. 378(3):492-504

Gatto G, Rossi A, Rossi D, Kroening S, Bonatti S, Mallardo M. (2008). Epstein-Barr virus latent membrane protein 1 trans-activates miR-155 transcription through the NF-kappaB pathway. Nucleic Acids Res. 36(20):6608-19.

Gerlich W, Robinson WS. (1980). Hepatitis B virus contains protein attached to the 5_ end of its complete strand. Cell. 21:801-811.

Gilad S, Meiri E, Yogev Y, Benjamin S, Lebanony D, Yerushalmi N, Benjamin H,

Kushnir M, Cholakh H, Melamed N, Bentwich Z, Hod M, Goren Y, Chajut A. (2008). Serum microRNAs are promising novel biomarkers. PLoS One. 3(9):e3148.

Gottlob K, Fulco M, Levrero M, Graessmann A. (1998). The hepatitis B virus HBx protein inhibits caspase 3 activity. J Biol Chem. 273(50):33347-53.

Griffiths-Jones S, Saini HK, van Dongen S, Enright AJ. (2008). miRBase: tools for microRNA genomics. Nucleic Acids Res. 36(Database issue):D154-8.

Guo Y, Chen Z, Zhang L, Zhou F, Shi S, Feng X, Li B, Meng X, Ma X, Luo M, Shrao K, Li N, Qiu B, Mitchelson K, Cheng J, He J. (2008). Distinctive microRNA profiles relating to patient survival in esophageal squamous cell carcinoma. Cancer Res. 68(1):26-33.

Haviv I, Vaizel D, Shaul Y. (1996). pX, the HBV-encoded coactivator interacts with components of the transcription machinery and stimulates transcription in a TAF-independent manner. EMBO J. 15:3413–3420.

Hellerbrand C, Pöppl A, Hartmann A, Schölmerich J, Lock G. (2003). HFE C282Y heterozygosity in hepatocellular carcinoma: evidence for an increased prevalence. Clin Gastroenterol Hepatol. 1(4):279-84.

Henkler F, Hoare J, Waseem N, Goldin RD, McGarvey MJ, Koshy R, King IA. (2001). Intracellular localization of the hepatitis B virus HBx protein. J Gen Virol. 82(Pt 4):871-82.

Hodgson AJ, Keasler VV, Slagle BL. (2008). Premature cell cycle entry induced by hepatitis B virus regulatory HBx protein during compensatory liver regeneration. Cancer Res. 68(24):10341-8.

Hurst DR, Edmonds MD, Scott GK, Benz CC, Vaidya KS, Welch DR. (2009). Breast cancer metastasis suppressor 1 up-regulates miR-146, which suppresses breast cancer metastasis. Cancer Res. 69(4):1279-83.

Jia L, Wang XW, Harris CC. (1999). Hepatitis B virus X protein inhibits nucleotide excision repair. Int J Cancer. 80(6):875-9.

Jiang J, Gusev Y, Aderca I, Mettler TA, Nagorney DM, Brackett DJ, Roberts LR, Schmittgen TD. (2008). Association of MicroRNA expression in hepatocellular

carcinomas with hepatitis infection, cirrhosis, and patient survival. Clin Cancer Res. 14(2):419-27.

Jindal S, Young RA. (1992). Vaccinia virus infection induces a stress response that leads to association of Hsp70 with viral proteins. J Virol. 66(9):5357-62.

Johnston IA, Lee HT, Macqueen DJ, Paranthaman K, Kawashima C, Anwar A, Kinghorn JR, Dalmay T. (2009). Embryonic temperature affects muscle fibre recruitment in adult zebrafish: genome-wide changes in gene and microRNA expression associated with the transition from hyperplastic to hypertrophic growth phenotypes. J Exp Biol. 212(Pt 12):1781-93.

Jung JK, Arora P, Pagano JS, Jang KL. (2007). Expression of DNA methyltransferase 1 is activated by hepatitis B virus X protein via a regulatory circuit involving the p16INK4a-cyclin D1-CDK 4/6-pRb-E2F1 pathway. Cancer Res. 67(12):5771-8.

Kao JH, Chen PJ, Lai MY, Chen DS. (2000). Hepatitis B genotypes correlate with clinical outcomes in patients with chronic hepatitis B. Gastroenterology. 118:554-559.

Kim CM, Koike K, Saito I, Miyamura T, Jay G. (1991). HBx gene of hepatitis B virus induces liver cancer in transgenic mice. Nature. 351(6324):317-20.

Kim H, Lee H, Yun Y. (1998). X-gene product of hepatitis B virus induces apoptosis in liver cells. J Biol Chem. 273(1):381-5.

Kim YC, Song KS, Yoon G, Nam MJ, Ryu WS. (2001). Activated ras oncogene collaborates with HBx gene of hepatitis B virus to transform cells by suppressing HBx-mediated apoptosis. Oncogene. 20(1):16-23.

Knappik A, Pluckthun A. (1994). An improved affinity tag based on the FLAG peptide for the detection and purification of recombinant antibody fragments. Biotechniques. 17(4):754-761.

Kota J, Chivukula RR, O'Donnell KA, Wentzel EA, Montgomery CL, Hwang HW, Chang TC, Vivekanandan P, Torbenson M, Clark KR, Mendell JR, Mendell JT. (2009). Therapeutic microRNA delivery suppresses tumorigenesis in a murine liver cancer model. Cell. 137(6):1005-17.

Kozak M. (1987). At least six nucleotides preceding the AUG initiator codon enhance translation in mammalian cells. J Mol Biol. 196(4):947-50.

Kutay H, Bai S, Datta J, Motiwala T, Pogribny I, Frankel W, Jacob ST, Ghoshal K. (2006). Downregulation of miR-122 in the rodent and human hepatocellular carcinomas. J Cell Biochem. 99(3):671-8.

Labbaye C, Spinello I, Quaranta MT, Pelosi E, Pasquini L, Petrucci E, Biffoni M, Nuzzolo ER, Billi M, Foà R, Brunetti E, Grignani F, Testa U, Peschle C. (2008). A three-step pathway comprising PLZF/miR-146a/CXCR4 controls megakaryopoiesis. Nat Cell Biol. 10(7):788-801.

Ladeiro Y, Couchy G, Balabaud C, Bioulac-Sage P, Pelletier L, Rebouissou S, Zucman-Rossi J. (2008). MicroRNA profiling in hepatocellular tumors is associated with clinical features and oncogene/tumor suppressor gene mutations. Hepatology. 47(6):1955-63.

Lai CL, Gane E, Liaw YF, Hsu CW, Thongsawat S, Wang Y, Chen Y, Heathcote EJ, Rasenack J, Bzowej N, Naoumov NV, Di Bisceglie AM, Zeuzem S, Moon YM, Goodman Z, Chao G, Constance BF, Brown NA. (2007). Globe Study Group Telbivudine versus lamivudine in patients with chronic hepatitis B., N Engl J Med. 357(25):2576-88.

Lai CL, Shouval D, Lok AS, Chang TT, Cheinquer H, Goodman Z, DeHertogh D, Wilber R, Zink RC, Cross A, Colonno R, Fernandes L (2006). BEHoLD AI463027 Study Group. Entecavir versus lamivudine for patients with HBeAg-negative chronic hepatitis B. N Engl J Med. 354(10):1011-20.

Lai MY, Chen DS, Chen PJ, Lee SC, Sheu JC, Huang GT, Wei TC, Lee CS, Yu SC, Hsu HC, Sung JL. (1988). Status of hepatitis B virus DNA in hepatocellular carcinoma: a study based on paired tumor and nontumor liver tissues. J Med Virol. 25(3):249-58

Lee RC, Feinbaum RL, Ambros V. (1993). The C. elegans heterochronic gene lin-4 encodes small RNAs with antisense complementarity to lin-14. Cell. 75(5):843-54.

Lee WM. (1997). Hepatitis B virus infection. N Engl J Med. 337(24):1733-45.

Lee Y, Kim M, Han J, Yeom KH, Lee S, Baek SH, Kim VN. (2004). MicroRNA

genes are transcribed by RNA polymerase II. EMBO J. 23(20):4051-60.

Lee YH, Yun Y. (1998). HBx protein of hepatitis B virus activates Jak1-STAT signaling. J Biol Chem. 273:25510-9.

Leistner CM, Gruen-Bernhard S, Glebe D. (2008). Role of glycosaminoglycans for binding and infection of hepatitis B virus. Cell Microbiol. 10(1):122-33.

Lewis BP, Burge CB, Bartel DP. (2005). Conserved seed pairing, often flanked by adenosines, indicates that thousands of human genes are microRNA targets. Cell. 120(1):15-20.

Li S, Fu H, Wang Y, Tie Y, Xing R, Zhu J, Sun Z, Wei L, Zheng X. (2009). MicroRNA-101 regulates expression of the v-fos FBJ murine osteosarcoma viral oncogene homolog (FOS) oncogene in human hepatocellular carcinoma. Hepatology. 49(4):1194-202.

Li SK, Ho SF, Tsui KW, Fung KP, Waye MY. (2008). Identification of functionally important amino acid residues in the mitochondria targeting sequence of hepatitis B virus X protein. Virology. 381(1):81-8.

Liang TJ. (2009). Hepatitis B: the virus and disease. 49(5 Suppl):S13-21.

Liang X, Liu Y, Zhang Q, Gao L, Han L, Ma C, Zhang L, Chen YH, Sun W. (2007). Hepatitis B virus sensitizes hepatocytes to TRAIL-induced apoptosis through Bax. J Immunol. 178(1):503-10.

Lin CJ, Gong HY, Tseng HC, Wang WL, Wu JL. (2008). miR-122 targets an anti-apoptotic gene, Bcl-w, in human hepatocellular carcinoma cell lines. Biochem Biophys Res Commun. 375(3):315-20.

Löffler D, Brocke-Heidrich K, Pfeifer G, Stocsits C, Hackermüller J, Kretzschmar AK, Burger R, Gramatzki M, Blumert C, Bauer K, Cvijic H, Ullmann AK, Stadler PF, Horn F. (2007). Interleukin-6 dependent survival of multiple myeloma cells involves the Stat3-mediated induction of microRNA-21 through a highly conserved enhancer. Blood. 110(4):1330-3.

Ma NF, Lau SH, Hu L, Xie D, Wu J, Yang J, Wang Y, Wu MC, Fung J, Bai X, Tzang CH. (2008). COOH-terminal truncated HBV X protein plays key role in

hepatocarcinogenesis. Clin Cancer Res. 14(16):5061-8.

Maheshwari S, Sarraj A, Kramer J, El-Serag HB. (2007). Oral contraception and the risk of hepatocellular carcinoma. J Hepatol. 47(4):506-13.

Majano P, Lara-Pezzi E, López-Cabrera M, Apolinario A, Moreno-Otero R, García-Monzón C. (2001). Hepatitis B virus X protein transactivates inducible nitric oxide synthase gene promoter through the proximal nuclear factor kappaB-binding site: evidence that cytoplasmic location of X protein is essential for gene transactivation. Hepatology. 34(6):1218-24.

Marcellin P, Heathcote EJ, Buti M, Gane E, de Man RA, Krastev Z, Germanidis G, Lee SS, Flisiak R, Kaita K, Manns M, Kotzev I, Tchernev K, Buggisch P, Weilert F, Kurdas OO, Shiffman ML, Trinh H, Washington MK, Sorbel J, Anderson J, Snow-Lampart A, Mondou E, Quinn J, Rousseau F. (2008). Tenofovir disoproxil fumarate versus adefovir dipivoxil for chronic hepatitis B. N Engl J Med. 359(23):2442-55.

Marrero JA, Fontana RJ, Fu S, Conjeevaram HS, Su GL, Lok AS. (2005). Alcohol, tobacco and obesity are synergistic risk factors for hepatocellular carcinoma. J Hepatol. 42(2):218-24.

Marshall HM, Ronen K, Berry C, Llano M, Sutherland H, Saenz D, Bickmore W, Poeschla E, Bushman FD. (2007). Role of PSIP1/LEDGF/p75 in lentiviral infectivity and integration targeting. PLoS One. 2(12):e1340.

Maruyama T, Iino S, Koike K, Yasuda K, Milich DR. (1993). Serology of acute exacerbation in chronic hepatitis B virus infection. Gastroenterology. 105(4):1141-51.

Mastrangelo G, Fedeli U, Fadda E, Valentini F, Agnesi R, Magarotto G, Marchì T, Buda A, Pinzani M, Martines D. (2004). Increased risk of hepatocellular carcinoma and liver cirrhosis in vinyl chloride workers: synergistic effect of occupational exposure with alcohol intake. Environ Health Perspect. 112(11):1188-92.

Megraw M, Sethupathy P, Corda B, Hatzigeorgiou AG. (2006). miRGen: A database for the study of animal microRNA genomic organization and function. Nucleic Acids Res. 35: D149-D155.

Meng F, Henson R, Wehbe-Janek H, Ghoshal K, Jacob ST, Patel T. (2007). MicroRNA-21 regulates expression of the PTEN tumor suppressor gene in human hepatocellular cancer. Gastroenterology. 133(2):647-58.

Merican I, Guan R, Amarapuka D, Alexander MJ, Chutaputti A, Chien RN, Hasnian SS, Leung N, Lesmana L, Phiet PH, Sjalfoellah Noer HM, Sollano J, Sun HS, Xu DZ. (2000). Chronic hepatitis B virus infection in Asian countries. J Gastroenterol Hepatol. 15:1356-1361.

Mitchell PS, Parkin RK, Kroh EM, Fritz BR, Wyman SK, Pogosova-Agadjanyan EL, Peterson A, Noteboom J, O'Briant KC, Allen A, Lin DW, Urban N, Drescher CW, Knudsen BS, Stirewalt DL, Gentleman R, Vessella RL, Nelson PS, Martin DB, Tewari M. (2008). Circulating microRNAs as stable blood-based markers for cancer detection. Proc Natl Acad Sci USA. 105(30):10513-8.

Motsch N, Pfuhl T, Mrazek J, Barth S, Grässer FA. (2007). Epstein-Barr virus-encoded latent membrane protein 1 (LMP1) induces the expression of the cellular microRNA miR-146a. RNA Biol. 4(3):131-7.

Mott JL, Kobayashi S, Bronk SF, Gores GJ. mir-29 regulates Mcl-1 protein expression and apoptosis. Oncogene. (2007). 26(42):6133-40.

Murakami Y, Saigo K, Takashima H, Minami M, Okanoue T, Bréchot C, Paterlini-Bréchot P. (2005). Large scaled analysis of hepatitis B virus (HBV) DNA integration in HBV related hepatocellular carcinomas. Gut. 54:1162–8.

Murakami Y, Yasuda T, Saigo K, Urashima T, Toyoda H, Okanoue T, Shimotohno K. (2006). Comprehensive analysis of microRNA expression patterns in hepatocellular carcinoma and non-tumorous tissues. Oncogene. 25(17):2537-45.

Nakagawa S, Niimura Y, Gojobori T, Tanaka H, Miura K. (2008). Diversity of preferred nucleotide sequences around the translation initiation codon in eukaryote genomes. Nucleic Acids Res. 36(3):861-71.

Naldini L, Blömer U, Gallay P, Ory D, Mulligan R, Gage FH, Verma IM, Trono D. (1996). In vivo gene delivery and stable transduction of nondividing cells by a lentiviral vector. Science. 272(5259):263-7.

Ng EK, Chong WW, Jin H, Lam EK, Shin VY, Yu J, Poon TC, Ng SS, Sung JJ.

(2009). Differential expression of microRNAs in plasma of colorectal cancer patients: A potential marker for colorectal cancer screening. Gut. (In press)

Norder H, Couroucé AM, Magnius LO. (1994). Complete genomes, phylogenetic relatedness, and structural proteins of six strains of the hepatitis B virus, four of which represent two new genotypes. Virology. 198(2):489-503.

Ozer A, Khaoustov VI, Mearns M, Lewis DE, Genta RM, Darlington GJ, Yoffe B. (1996). Effect of hepatocyte proliferation and cellular DNA synthesis on hepatitis B virus replication. Gastroenterology. 110(5):1519-28.

Ozsolak F, Poling LL, Wang Z, Liu H, Liu XS, Roeder RG, Zhang X, Song JS, Fisher DE. (2008). Chromatin structure analyses identify miRNA promoters. Genes Dev. 22(22):3172-83.

Park IY, Sohn BH, Yu E, Suh DJ, Chung YH, Lee JH, Surzycki SJ, Lee YI. (2007). Aberrant epigenetic modifications in hepatocarcinogenesis induced by hepatitis B virus X protein. Gastroenterology. 132(4):1476-94.

Park SY, Lee JH, Ha M, Nam JW, Kim VN. (2002). miR-29 miRNAs activate p53 by targeting p85 alpha and CDC42. Nat Struct Mol Biol. 16(1):23-9.

Parkin DM, Bray F, Ferlay J, Pisani P. (2005). Global Cancer Statistics. CA Cancer J Clin. 55:74-108.

Parkin DM. (2006). The Global Health Burden of Infection-associated Cancers in the Year 2002. Int J Cancer. 118:2020-44.

Parkin DM. (2002). Cancer Incidence in five continents. IARC scientific publications volume VIII[No. 155]. Lyon: IARCPress

Pichler K, Schneider G, Grassmann R. (2008). MicroRNA miR-146a and further oncogenesis-related cellular microRNAs are dysregulated in HTLV-1-transformed T lymphocytes. Retrovirology. 5:100.

Poovorawan Y, Chongsrisawat V, Theamboonlers A, Srinivasa K, Hutagalung Y, Bock HL, Hoet B. (2009). Long-Term Benefit of Hepatitis B Vaccination among Children in Thailand with Transient Hepatitis B Virus Infection Who Were Born to Hepatitis B Surface Antigen-Positive Mothers. J Infect Dis. 200(1):33-8.

Prost S, Ford JM, Taylor C, Doig J, Harrison DJ. (1998). Hepatitis B x protein inhibits p53-dependent DNA repair in primary mouse hepatocytes. J Biol Chem. 273(50):33327-32.

Qadri I, Maguire HF, Siddiqui A. (1995). Hepatitis B virus transactivator protein X interacts with the TATA-binding protein. Proc Natl Acad Sci USA. 92:1003–1007.

Regimbeau JM, Colombat M, Mognol P, Durand F, Abdalla E. (2004). Obesity and diabetes as a risk factor for hepatocellular carcinoma. Liver Transpl. 10(2 Suppl 1):S69-S73.

Schetter AJ, Leung SY, Sohn JJ, et al. (2008). MicroRNA expression profiles associated with prognosis and therapeutic outcome in colon adenocarcinoma. JAMA. 299:425–436.

Schetter AJ, Leung SY, Sohn JJ, Zanetti KA, Bowman ED, Yanaihara N, Yuen ST, Chan TL, Kwong DL, Au GK, Liu CG, Calin GA, Croce CM, Harris CC. (2008). MicroRNA expression profiles associated with prognosis and therapeutic outcome in colon adenocarcinoma. JAMA. 299(4):425-36.

Schulze A, Gripon P, Urban S. (2007). Hepatitis B virus infection initiates with a large surface protein-dependent binding to heparan sulfate proteoglycans, Hepatology. 46(6):1759-68.

Selbach M, Schwanhäusser B, Thierfelder N, Fang Z, Khanin R, Rajewsky N. (2008). Widespread changes in protein synthesis induced by microRNAs. Nature. 455(7209):58-63.

Sengupta S, den Boon JA, Chen IH, Newton MA, Stanhope SA, Cheng YJ, Chen CJ, Hildesheim A, Sugden B, Ahlquist P. (2008). MicroRNA 29c is down-regulated in nasopharyngeal carcinomas, up-regulating mRNAs encoding extracellular matrix proteins. Proc Natl Acad Sci U S A. 105(15):5874-8

Shafritz DA, Shouval D, Sherman HI, Hadziyannis SJ, Kew MC. (1981). Integration of hepatitis B virus DNA into the genome of liver cells in chronic liver disease and hepatocellular carcinoma. Studies in percutaneous liver biopsies and post-mortem tissue specimens. N Engl J Med. 305(18):1067-73.

Shon JK, Shon BH, Park IY, Lee SU, Fa L, Chang KY, Shin JH, Lee YI. (2009). Hepatitis B virus-X protein recruits histone deacetylase 1 to repress insulin-like growth factor binding protein 3 transcription. Virus Res. 139(1):14-21.

Soini Y, Chia SC, Bennett WP, Groopman JD, Wang JS, DeBenedetti VM, Cawley H, Welsh JA, Hansen C, Bergasa NV, Jones EA, DiBisceglie AM, Trivers GE, Sandoval CA, Calderon IE, Munoz Espinosa LE, Harris CC. (1996). An aflatoxin-associated mutational hotspot at codon 249 in the p53 tumor suppressor gene occurs in hepatocellular carcinomas from Mexico. Carcinogenesis. 17(5):1007-12.

Steve R and Helen JS (2000). Primer3 on the WWW for general users and for biologist programmers. In: Krawetz S, Misener S (eds) Bioinformatics Methods and Protocols: Methods in Molecular Biology. Humana Press, Totowa, NJ, pp 365-386

Su F, Schneider RJ. (1996). Hepatitis B virus HBx protein activates transcription factor NF-kappaB by acting on multiple cytoplasmic inhibitors of rel-related proteins. J Virol. 70(7):4558-66.

Su F, Schneider RJ. (1997). Hepatitis B virus HBx protein sensitizes cells to apoptotic killing by tumor necrosis factor alpha. Proc Natl Acad Sci USA. 94(16):8744-9.

Su F, Theodosis CN, Schneider RJ. (2001). Role of NF-kappaB and myc proteins in apoptosis induced by hepatitis B virus HBx protein. J Virol. 75(1):215-25.

Su H, Yang JR, Xu T, Huang J, Xu L, Yuan Y, Zhuang SM. (2009). MicroRNA-101, down-regulated in hepatocellular carcinoma, promotes apoptosis and suppresses tumorigenicity. Cancer Res. 69(3):1135-42.

Su JM, Lai XM, Lan KH, Li CP, Chao Y, Yen SH, Chang FY, Lee SD, Lee WP. (2007). X protein of hepatitis B virus functions as a transcriptional corepressor on the human telomerase promoter. Hepatology. 46(2):402-13.

Sung JJ, Tsui SK, Tse CH, Ng EY, Leung KS, Lee KH, Mok TS, Bartholomeusz A, Au TC, Tsoi KK, Locarnini S, Chan HL. (2008). Genotype-specific genomic markers associated with primary hepatomas, based on complete genomic sequencing of hepatitis B virus. J Virol. Apr;82(7):3604-11.

Sung WK, Lu Y, Lee CW, Zhang D, Ronaghi M, Lee CG. (2009) Deregulated direct

targets of the hepatitis B viral (HBV) protein, HBx, identified through chromatin immunoprecipitation and expression microarray profiling. J Biol Chem. 284(33):21941-54

Taganov KD, Boldin MP, Chang KJ, Baltimore D. (2006). NF-kappaB-dependent induction of microRNA miR-146, an inhibitor targeted to signaling proteins of innate immune responses. Proc Natl Acad Sci USA. 103(33):12481-6.

Takagi T, Iio A, Nakagawa Y, Naoe T, Tanigawa N, Akao Y. (2009). Decreased Expression of MicroRNA-143 and -145 in Human Gastric Cancers. Oncology. 77(1):12-21.

Tay Y, Zhang J, Thomson AM, Lim B, Rigoutsos I. (2008). MicroRNAs to Nanog, Oct4 and Sox2 coding regions modulate embryonic stem cell differentiation. Nature. 455(7216):1124-8.

Thomas RK, Nickerson E, Simons JF, Jänne PA, Tengs T, Yuza Y, Garraway LA, LaFramboise T, Lee JC, Shah K, O'Neill K, Sasaki H, Lindeman N, Wong KK, Borras AM, Gutmann EJ, Dragnev KH, DeBiasi R, Chen TH, Glatt KA, Greulich H, Desany B, Lubeski CK, Brockman W, Alvarez P, Hutchison SK, Leamon JH, Ronan MT, Turenchalk GS, Egholm M, Sellers WR, Rothberg JM, Meyerson M. (2006). Sensitive mutation detection in heterogeneous cancer specimens by massively parallel picoliter reactor sequencing. Nat Med. 12(7):852-5.

Thompson JD, Gibson TJ, Plewniak F, Jeanmougin F and Higgins DG.. (1997). The ClustalX windows interface: flexible strategies for multiple sequence alignment aided by quality analysis tools. Nucleic Acids Research. 25:4876-4882.

Tiscornia G, Singer O, Verma IM. (2006). Production and purification of lentiviral vectors. Nat Protoc. 1(1):241-5.

Tsai WC, Hsu PW, Lai TC, Chau GY, Lin CW, Chen CM, Lin CD, Liao YL, Wang JL, Chau YP, Hsu MT, Hsiao M, Huang HD, Tsou AP. (2009). MicroRNA-122, a tumor suppressor microRNA that regulates intrahepatic metastasis of hepatocellular carcinoma. Hepatology. 49(5):1571-82.

Tsai YH, Wu MF, Wu YH, Chang SJ, Lin SF, Sharp TV, Wang HW. (2008). The M type K15 protein of Kaposi's sarcoma-associated herpesvirus regulates microRNA expression via its SH2-binding motif to induce cell migration and invasion. J Virol.

83(2):622-32.

Tu H, Bonura C, Giannini C, Mouly H, Soussan P, Kew M, Paterlini-Bréchot P, Bréchot C, Kremsdorf D. (2001). Biological impact of natural COOH-terminal deletions of hepatitis B virus X protein in hepatocellular carcinoma tissues. Cancer Res. 61(21):7803-10.

Um HR, Lim WC, Chae SY, Park S, Park JH, Cho H. (2007). Raf-1 and protein kinase B regulate cell survival through the activation of NF-kappaB in hepatitis B virus X-expressing cells. Virus Res. 125(1):1-8.

Unsal H, Yarkicier C, Marçais C, Kerw M, Volkmann M, Zentgraf H, Isselbacher KJ, Ozturk M. (1994). Genetic heterogeneity of hepatocellular carcinoma. Proc Natl Acad. Sci USA. 91:822–826.

Ura S, Honda M, Yamashita T, Ueda T, Takatori H, Nishino R, Sunakozaka H, Sakai Y, Horimoto K, Kaneko S. (2009) Differential microRNA expression between hepatitis B and hepatitis C leading disease progression to hepatocellular carcinoma. Hepatology. 49(4):1098-112

Van Engeland M, Ramaekers FC, Schutte B, Reutelingsperger CP. (1996). A novel assay to measure loss of plasma membrane asymmetry during apoptosis of adherent cells in culture. Cytometry. 24(2):131-9.

Wai CT, Chu CJ, Hussain M, Lok AS. (2002). HBV genotype B is associated with better response to interferon therapy in HBeAg(+) chronic hepatitis than genotype C. Hepatology. 36:1425-1430.

Wang CL, Wang BB, Bartha G, Li L, Channa N, Klinger M, Killeen N, Wabl M. (2006). Activation of an oncogenic microRNA cistron by provirus integration. Proc Natl Acad Sci USA. 103(49):18680-4.

Wang H, Garzon R, Sun H, Ladner KJ, Singh R, Dahlman J, Cheng A, Hall BM, Qualman SJ, Chandler DS, Croce CM, Guttridge DC. (2008a). NF-kappaB-YY1-miR-29 regulatory circuitry in skeletal myogenesis and rhabdomyosarcoma. Cancer Cell. 14(5):369-81.

Wang K, Zhang S, Marzolf B, Troisch P, Brightman A, Hu Z, Hood LE, Galas DJ. (2009a). Circulating microRNAs, potential biomarkers for drug-induced liver injury.

Proc Natl Acad Sci USA. 106(11):4402-7.

Wang LL, Zhang Z, Li Q, Yang R, Pei X, Xu Y, Wang J, Zhou SF, Li Y. (2009b). Ethanol exposure induces differential microRNA and target gene expression and teratogenic effects which can be suppressed by folic acid supplementation. Hum Reprod. 24(3):562-79.

Wang WL, London WT, Feitelson MA. (1991). Hepatitis B x antigen in hepatitis B virus carrier patients with liver cancer. Cancer Res. 15;51(18):4971-7.

Wang X, Wang HK, McCoy JP, Banerjee NS, Rader JS, Broker TR, Meyers C, Chow LT, Zheng ZM. (2009c). Oncogenic HPV infection interrupts the expression of tumor-suppressive miR-34a through viral oncoprotein E6. RNA. 15:637-47.

Wang Y, Lee AT, Ma JZ, Wang J, Ren J, Yang Y, Tantoso E, Li KB, Ooi LL, Tan P, Lee CG. (2008b). Profiling microRNA expression in hepatocellular carcinoma reveals microRNA-224 up-regulation and apoptosis inhibitor-5 as a microRNA-224-specific target. J Biol Chem. 283(19):13205-15.

Wei Y, Etiemble J, Fourel G, Vitvitski-Trepo L, Buendia MA. (1995). Hepadna virus integration generates virus-cell cotranscripts carrying 3' truncated X genes in human and woodchuck liver tumors. J Med Virol. 45(1):82-90.

Wong QW, Lung RW, Law PT, Lai PB, Chan KY, To KF, Wong N. (2008a). MicroRNA-223 is commonly repressed in hepatocellular carcinoma and potentiates expression of Stathmin1.Gastroenterology. 135(1):257-69.

Wong TS, Liu XB, Wong BY, Ng RW, Yuen AP, Wei WI. (2008b). Mature miR-184 as Potential Oncogenic microRNA of Squamous Cell Carcinoma of Tongue. Clin Cancer Res. 14(9):2588-92.

Xu N, Papagiannakopoulos T, Pan G, Thomson JA, Kosik KS. (2009). MicroRNA-145 regulates OCT4, SOX2, and KLF4 and represses pluripotency in human embryonic stem cells. Cell. 137(4):647-58.

Xu R, Zhang X, Zhang W, Fang Y, Zheng S, Yu XF. (2007). Association of human APOBEC3 cytidine deaminases with the generation of hepatitis virus B x antigen mutants and hepatocellular carcinoma. Hepatology. 46(6):1810-20.

Xu T, Zhu Y, Wei QK, Yuan Y, Zhou F, Ge YY, Yang JR, Su H, Zhuang SM. (2008.) A functional polymorphism in the miR-146a gene is associated with the risk for hepatocellular carcinoma. Carcinogenesis. 29(11):2126-31.

Xu T, Zhu Y, Xiong Y, Ge YY, Yun JP, Zhuang SM. (2009). MicroRNA-195 suppresses tumorigenicity and regulates G(1)/S transition of human hepatocellular carcinoma cells. Hepatology. 50(1):113-21

Yanaihara N, Caplen N, Bowman E, Seike M, Kumamoto K, Yi M, Stephens RM, Okamoto A, Yokota J, Tanaka T, Calin GA, Liu CG, Croce CM, Harris CC. (2006). Unique microRNA molecular profiles in lung cancer diagnosis and prognosis. Cancer Cell. 9(3):189-98.

Yang BM, Kim CH, Kim JY. (2004). Cost of chronic hepatitis B infection in South Korea. J Clin Gastroenterol. 38(10 Suppl 3):S153-7.

Yuen MF, Wong DK, Fung J, Ip P, But D, Hung I, Lau K, Yuen JC, Lai CL. (2008). HBsAg Seroclearance in chronic hepatitis B in Asian patients: replicative level and risk of hepatocellular carcinoma. Gastroenterology. 135(4):1192-9.

Yeung ML, Yasunaga J, Bennasser Y, Dusetti N, Harris D, Ahmad N, Matsuoka M, Jeang KT. (2008). Roles for microRNAs, miR-93 and miR-130b, and tumor protein 53-induced nuclear protein 1 tumor suppressor in cell growth dysregulation by human T-cell lymphotrophic virus 1. Cancer Res. 68(21):8976-85.

Yun C, Um HR, Jin YH, Wang JH, Lee MO, Park S, Lee JH, Cho H. (2002). NF-kappaB activation by hepatitis B virus X (HBx) protein shifts the cellular fate toward survival. Cancer Lett. 184(1):97-104.

Zhang G, Gurtu V, Kain SR, Yan G. (1997). Early detection of apoptosis using a fluorescent conjugate of annexin V. Biotechniques. 23(3):525-31.

Zhang H, Shan CL, Li N, Zhang X, Zhang XZ, Xu FQ, Zhang S, Qiu LY, Ye LH, Zhang XD. (2008). Identification of a natural mutant of HBV X protein truncated 27 amino acids at the COOH terminal and its effect on liver cell proliferation. Acta Pharmacol Sin. 29(4):473-80.

Zhang X, Liu S, Hu T, Liu S, He Y, Sun S. (2009). Up-regulated microRNA-143 transcribed by nuclear factor kappa B enhances hepatocarcinoma metastasis by

repressing fibronectin expression. Hepatology. 50(2):490-9

Zheng DL, Zhang L, Cheng N, Xu X, Deng Q, Teng XM, Wang KS, Zhang X, Huang J, Han ZG. (2009). Epigenetic modification induced by hepatitis B virus X protein via interaction with de novo DNA methyltransferase DNMT3A. J Hepatol. 50(2):377-87.

Zhiqiang G, Zhaohui D, Qinhuan W, Dexian C, Yunyun F, Hongtao L, Iloeje UH. (2004). Cost of chronic hepatitis B infection in China. J Clin Gastroenterol. 38(10 Suppl 3):S175-8.

Zhu AX. (2006). Systemic therapy of advanced hepatocellular carcinoma: How hopeful should we be? Oncologist. 11:790-800.